Novel Convergence Results in Nonlinear Filtering

Jennifer Lynn Bonniwell
Marquette University

NOVEL CONVERGENCE RESULTS IN NONLINEAR FILTERING

by

Jennifer L. Bonniwell, B.S., M.S

A Dissertation submitted to the Faculty of the Graduate School,
Marquette University,
in Partial Fulfillment of the Requirements for
the Degree of Doctor of Philosophy

Milwaukee, Wisconsin

May 2016

ABSTRACT
NOVEL CONVERGENCE RESULTS
IN NONLINEAR FILTERING

Jennifer L. Bonniwell, B.S., M.S

Marquette University, 2016

In this dissertation, the discrete-time extended Kalman filter is analyzed for its ability to attenuate finite-energy disturbances, known as the H_∞-property. Though the extended Kalman filter is designed to be a locally optimal minimum variance estimator, this dissertation proves that it has additional properties, such as H_∞. This analysis is performed with the extended Kalman filter in direct form. Since this form reduces assumptions placed on the system in previous works on convergence and H_2-properties of the extended Kalman filter, the extended Kalman filter used as a nonlinear observer for noise-free models is revisited using the direct form to demonstrate these properties.

Additionally, two representations for the discrete-time uncertain measurement model with finite-energy disturbances are considered: 1) each sensor in the measurement can fail independently with different failure rates and 2) all of the sensors in the measurement fail at the same time. The discrete-time extended Kalman filters designed for such models are analyzed for general convergence, the H_2-property, and the H_∞-property.

As an extension of this work, the continuous-time extended Kalman filter is applied to systems with finite-energy disturbances. This continuous-time extended Kalman filter is shown to inherently have the H_∞-property. Simulation studies have been performed on all of the extended Kalman filters in this dissertation. These simulation studies demonstrate that when the extended Kalman filters converge, they will also exhibit the H_2 and H_∞ properties. The bounds developed on these properties are affected by the same constraints that affect convergence, i.e. magnitudes of the initial estimation error and the disturbance as well as the severity of the nonlinearities in the model.

ACKNOWLEDGMENTS

Jennifer L. Bonniwell, B.S., M.S

The work in this dissertation would not have been possible without the guidance and support from my advisors, Dr. Edwin Yaz and Dr. Susan Schneider. I am grateful for the time and effort they invested in helping me grow academically as well as personally.

Furthermore, I would like to thank my dissertation committee members: Dr. James Heinen, Dr. Henry Medeiros, and Dr. Michael Wenzel. Their time, feedback, and suggestions were crucial to the completion of this dissertation.

Finally, I would like to thank my parents, David A. and Joanne Riffer, my brother and sister, Jamie Tumbrink and David L. Riffer, my husband, Joe Bonniwell, and the rest of my family for all of their support in everything that I do.

TABLE OF CONTENTS

LIST OF TABLES

LIST OF FIGURES

CHAPTER 1

INTRODUCTION

In this dissertation, the discrete-time extended Kalman filter is analyzed for its ability to attenuate finite-energy disturbances, known as the H_∞-property. Though the extended Kalman filter is designed to be a locally optimal minimum variance estimator, this dissertation proves that it has additional properties, such as H_∞. This analysis is performed with the extended Kalman filter in direct form, which reduces assumptions placed on the system in previous works on convergence and H_2-properties of the extended Kalman filter. In addition to the basic nonlinear model with finite-energy disturbances, two representations for the discrete-time uncertain measurement model with finite-energy disturbances are considered: 1) each sensor in the measurement can fail independently with different failure rates and 2) all of the sensors in the measurement fail at the same time. The discrete-time extended Kalman filters designed for such models are analyzed for general convergence, the H_2-property, and the H_∞-property. As an extension of this work, the continuous-time extended Kalman filter is applied to systems with finite-energy disturbances. This continuous-time extended Kalman filter is shown to inherently have the H_∞-property.

1.1 Filter Properties

Why do we need filters and estimation techniques? Consider a signal being sent from a satellite to a ground station. The signal begins as a ”clean” signal (without noise) at the satellite, but as this signal travels through space and then through the Earth’s atmosphere, noise is added to the signal. When the ground station receives the signal, one of the tasks it has to perform is to filter the

noise from the signal, which implies estimating the original signal sent from the satellite. The error signal resulting from the difference between the ”clean” signal and the estimate is the central point for generating an accurate estimate. For this reason, properties relating to the error signal are essential to know when choosing a filter for use in the design of an estimation system. This work focuses on the analysis of the estimation error resulting from variations of the extended Kalman filter (EKF). There are three specific properties that are of interest: (1) convergence of the error; (2) H_∞, the effect of disturbances on the energy of the error; and (3) H_2, the effect of initial conditions on the energy of the error.

1.1.1 Convergence

Convergence of the error describes if the error reaches the desired value of zero, or if the error is moving away, or diverging, from zero. There are various methods used in convergence analysis; in this work, Lyapunov methods are used. In Lyapunov convergence analysis of the estimation error, a Lyapunov energy function candidate, V, is defined, which is a positive function of the error signal and must equal zero when the initial error is zero. If this Lyapunov energy function candidate accurately represents the energy of the system, the energy will decrease over time for a converging system. This is the reason that the time evolution and time derivative of the Lyapunov energy function candidate is analyzed to determine if it is negative as shown here for discrete- and continuous-time, respectively

$$V_{k+1} - V_k < 0 \tag{1.1}$$

$$\dot{V}(t) < 0 \tag{1.2}$$

If the inequality holds, then the filter exhibits convergence.

1.1.2 H_∞- and H_2-Properties

If the filter is known to converge, then further analysis can lead to values for the H_∞- and H_2-properties. One of the main contributions of this dissertation is the analysis of the H_∞-property of several variations of the EKF. There are two types of disturbances considered in the analysis, both with finite energy. In the discrete-time analysis, a disturbance, w_k that is an element of stochastic ℓ_2, defined in Section 1.5, is a random disturbance with bounded estimated energy defined in discrete-time as

$$\sum_{k=0}^{\infty} \overline{\|w_k\|^2} < \infty \tag{1.3}$$

Similarly in the continuous-time analysis, a disturbance, $w(t)$, that is an element of $\mathcal{L}_2$, defined in Section 1.5, is a deterministic disturbance with bounded energy defined in continuous-time as

$$\int_0^{\infty} \|w(t)\|^2 dt < \infty \tag{1.4}$$

If a system contains one of these bounded energy (or finite-energy) disturbances and has the H_∞-property, then the energy of the estimation error in discrete-time, e_k, and continuous-time, $e(t)$, respectively, are guaranteed to be bounded as

$$\sum_{k=0}^{\infty} \|e_k\|^2 \leq \alpha_d \sum_{k=0}^{\infty} \|w_k\|^2 \tag{1.5}$$

$$\int_0^{\infty} \|e(t)\|^2 dt \leq \alpha_c \int_0^{\infty} \|w(t)\|^2 dt \tag{1.6}$$

where α_d and α_c are the H_∞-gains.

Similarly, the H_2-property gives insight into the effect of the initial conditions on the energy of the estimation error. If a term that is a function of the

initial error is bounded, such as the discrete- and continuous-time Lyapunov function candidates $V(e_0)$ and $V(e(0))$, then the energy of the estimation error in discrete- and continuous-time, respectively, are bounded as

$$\sum_{k=0}^{\infty} \|e_k\|^2 \leq \beta_d V(e_0) \tag{1.7}$$

$$\int_0^{\infty} \|e(t)\|^2 dt \leq \beta_c V(e(0)) \tag{1.8}$$

where β_d and β_c are the H_2-gains.

Additionally, the EKFs designed for the two discrete-time models for uncertain measurements only have the H_∞- and H_2-properties for a finite period of time. One example of a system that would have a finite-time property would be a tracking system for highly maneuverable targets as the target is only in the sensing range for a short period of time. These finite-time H_∞- and H_2-properties are defined similarly to their infinite-horizon counterparts as follows

$$\sum_{k=0}^{T} \|e_k\|^2 \leq \alpha_d \sum_{k=0}^{T} \|w_k\|^2 \tag{1.9}$$

$$\sum_{k=0}^{T} \|e_k\|^2 \leq \beta_d V(e_0) \tag{1.10}$$

for some integer $0 < T < \infty$, where the finite window of time is usually quite limited, e.g. $0 < T < 100$.

1.2 Nonlinear Filtering

This section highlights various works that have been completed to date on the topics of convergence, H_2, and H_∞ properties of the EKF. The Kalman filter [1] is the minimum variance state estimator for linear systems. Furthmore, a model with unknown parameters can be rewritten such that the parameter is one of the

state variables, allowing the Kalman filter to also be the minimum variance parameter estimator for linear systems. The design of the Kalman filter has been extended to be a locally optimal minimum variance estimator for nonlinear systems through linearization about the current estimate as presented in [2] and [3], among others; this design is well known as the extended Kalman filter (EKF). The EKF is used in thousands of applications, e.g. in estimation of vehicle velocities in [4] and for system identification in [5]. In addition to applications of the EKF, various performance properties of the EKF have been analyzed in previous works. Convergence studies have been performed to show under what conditions the EKF will work in both continuous [6], [7], [8], [9], [10] and discrete-time [11], [12], [13], [14].

1.2.1 Two Forms of the Discrete-Time Extended Kalman Filter

The analysis of the discrete-time extended Kalman filter to date has focused on the "predict-update" form. This form has two steps: 1) use the past estimate to predict the current estimate and 2) use the current measurement to update the predicted estimate. For the system

$$x_{k+1} = f(x_k) + F_k w_k \tag{1.11}$$

$$y_k = h(x_k) + H_k w_k \tag{1.12}$$

with Jacobians

$$A_{k|k-1} = \left.\frac{\partial f(x_{k-1})}{\partial x_{k-1}}\right|_{x_{k-1}=\hat{x}_{k|k-1}} \tag{1.13}$$

$$C_{k|k-1} = \left.\frac{\partial h(x_{k-1})}{\partial x_{k-1}}\right|_{x_{k-1}=\hat{x}_{k|k-1}} \tag{1.14}$$

where $x_k \in \Re^n$ is the state, $y_k \in \Re^p$ is the measurement, $w_k \in \Re^l$ is white noise with zero mean and identity covariance, $f(x_k) \in \Re^n$ and $h(x_k) \in \Re^p$ are analytic vector functions, and F_k and H_k are the noise coefficient matrices. Note, the

subscript $\hat{x}_{k|k-1}$ represents the current estimate based on the previous measurement and $\hat{x}_{k|k}$ represents the current estimate based on the current measurement. The algorithm is as follows [15]

- State prediction

$$\hat{x}_{k|k-1} = f(\hat{x}_{k-1|k-1}) \tag{1.15}$$

- Covariance prediction

$$P_{k|k-1} = A_{k|k-1} P_{k-1|k-1} A_{k|k-1}^T + F_{k-1} F_{k-1}^T \tag{1.16}$$

- Innovation

$$e_k = y_k - h(\hat{x}_{k|k-1}) \tag{1.17}$$

- Innovation covariance

$$R_k^{ee} = C_{k|k-1} P_{k|k-1} C_{k|k-1}^T + H_k H_k^T \tag{1.18}$$

- Gain

$$K_k = P_{k|k-1} C_{k|k-1}^T \left(R_k^{ee}\right)^{-1} \tag{1.19}$$

- State update

$$\hat{x}_{k|k} = \hat{x}_{k|k-1} + K_k e_k \tag{1.20}$$

- Covariance update

$$P_{k|k} = (I_n - K_k C_{k|k-1}) P_{k|k-1} \tag{1.21}$$

Alternatively, there is the ”direct” form of the EKF, which performs prediction and update in one step, that has not been widely used in analysis. The algorithm for this form is as follows

- State estimate

$$\hat{x}_{k+1} = f(\hat{x}_k) + K_k(y_k - h(\hat{x}_k)) \tag{1.22}$$

- Kalman Gain

$$K_k = (A_k P_k C_k^T + F_k H_k^T)(C_k P_k C_k^T + H_k H_k^T)^{-1} \tag{1.23}$$

- Riccati Difference Equation

$$P_{k+1} = (A_k - K_k C_k) P_k (A_k - K_k C_k)^T + (F_k - K_k H_k)(F_k - K_k H_k)^T \tag{1.24}$$

- Jacobians

$$A_k = \left.\frac{\partial f(x_k)}{\partial x_k}\right|_{x_k = \hat{x}_k} \tag{1.25}$$

$$C_k = \left.\frac{\partial h(x_k)}{\partial x_k}\right|_{x_k = \hat{x}_k} \tag{1.26}$$

One of the main contributions of this work is to use the direct form of the EKF in the analysis which lends itself to be used with the Schur complement, defined below in Section 1.6 Lemma 4.

1.2.2 Current State of Analysis of the Extended Kalman Filter

In [6], Ljung considers the continuous-time EKF used as a parameter estimator for linear systems by treating the parameter as another state. From this formulation of the problem, Ljung is able to show convergence properties for the EKF used as a parameter estimator. Following a similar procedure as Ljung, Ursin made a small change in the derivation that leads to improved convergence results [7]. Verification of these results was performed in [8], in which Campbell and Wiberg show that when the EKF used as a parameter estimator converges, it always converges to the expected parameters and never to a "spurious" point.

Reif et al. analyze the EKF as a state estimator for continuous-time nonlinear stochastic systems. Through the use of Itō calculus, they show under

what conditions the EKF maintains stochastic stability [9]. In [10], Bonnabel and Slotine investigate an EKF for deterministic continuous-time nonlinear systems and use contraction theory to perform the convergence analysis. The form of their results leads to additional analysis on the robustness of the EKF.

In [11], Reif et al. consider an EKF for stochastic discrete-time nonlinear systems. Using the "predict-update" form of the EKF, they derive the convergence conditions for the estimation error of an EKF for noisy systems through the use of Lyapunov analysis. To obtain their result, they assume that the system Jacobian, A_k, is invertible, which reduces the systems that this analysis is valid for. In [12], Boutayeb et al. study the convergence of the EKF for deterministic discrete-time nonlinear systems using Lyapunov analysis and include the residues from the first order Taylor Series approximations of the nonlinear system in their formulation. In [13], Reif and Unbehauen show through Lyapunov analysis that the EKF can be modified to work as an exponential observer for deterministic discrete-time nonlinear systems. Similarly in [14], Song and Grizzle show that the EKF can also be used as a local asymptotic observer for deterministic discrete-time nonlinear systems.

Variations of the EKF have been developed for various models over the years; one that is focused on as part of this dissertation is the uncertain measurement model. There are two common definitions for uncertain measurements: the measurement data is provided via a communication network with occasional packet loss that results in a measurement signal of zero (referred to in this work as intermittent measurements); and the measurement data always contains noise but the data signal is sparse in nature or exhibits signs of sensor degradation and failure (referred to in this work as uncertain measurements). To emphasize the differences, consider a sinusoidal measurement as shown in Figure 1.1. When additive noise is introduced to the measurement, it becomes Figure 1.2.

Now consider examples for the two definitions above, both are the sinusoidal

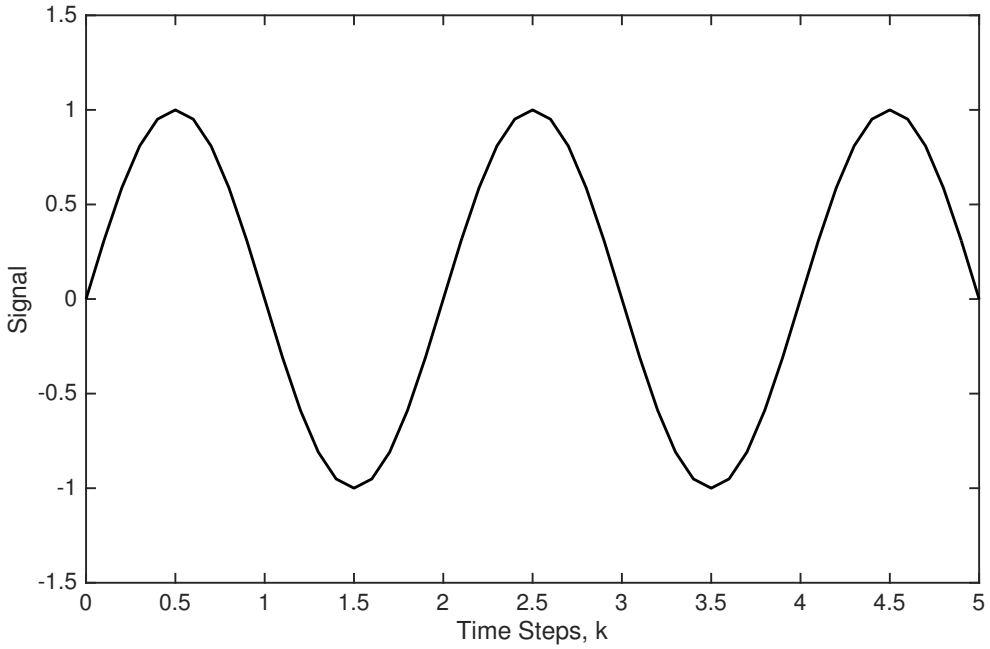

Figure 1.1: Example of a sinusoidal measurement

measurement with noise but Figure 1.3 contains an intermittent measurement and Figure 1.4 shows an uncertain measurement. The circles denote the same region in both plots, highlighting the differences in the model. The intermittent model is exactly zero when packets are dropped, while the uncertain measurement is sending noise from the sensor to the estimation system.

Many researchers have provided work on Kalman filtering for the intermittent measurement model. Sinopoli et al. [16] derive the Kalman filter for discrete-time systems with intermittent measurements and this EKF is analyzed in [17], [18], [19], [20], [21], [22]. On the other hand, Wang and Yaz derive an EKF for the discrete-time uncertain measurement model in [23] and there is yet to be progress regarding additional analysis of this EKF.

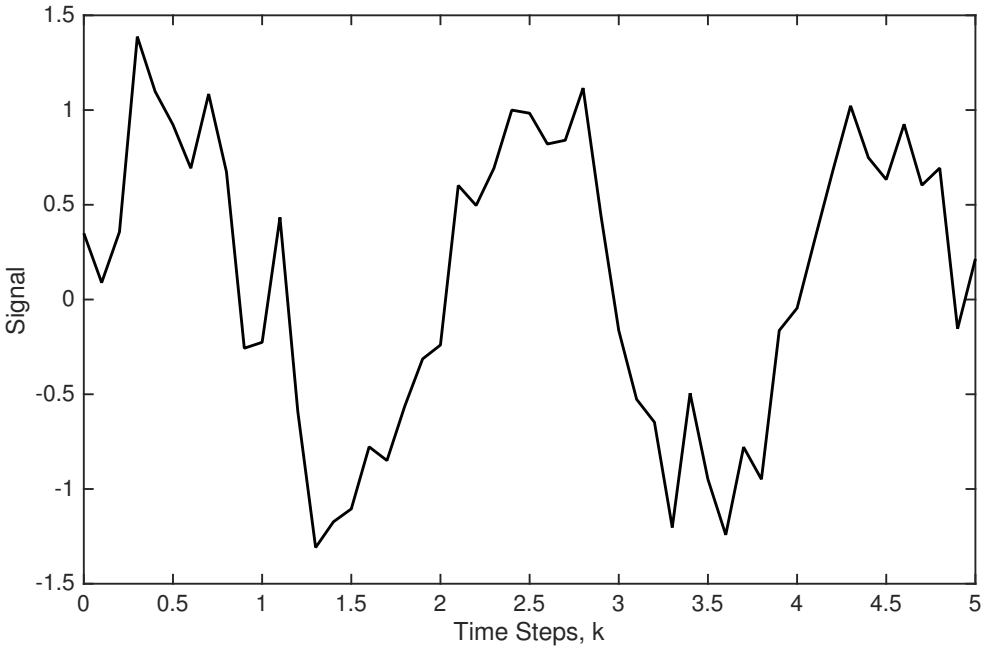

Figure 1.2: Example of a sinusoidal measurement with additive noise

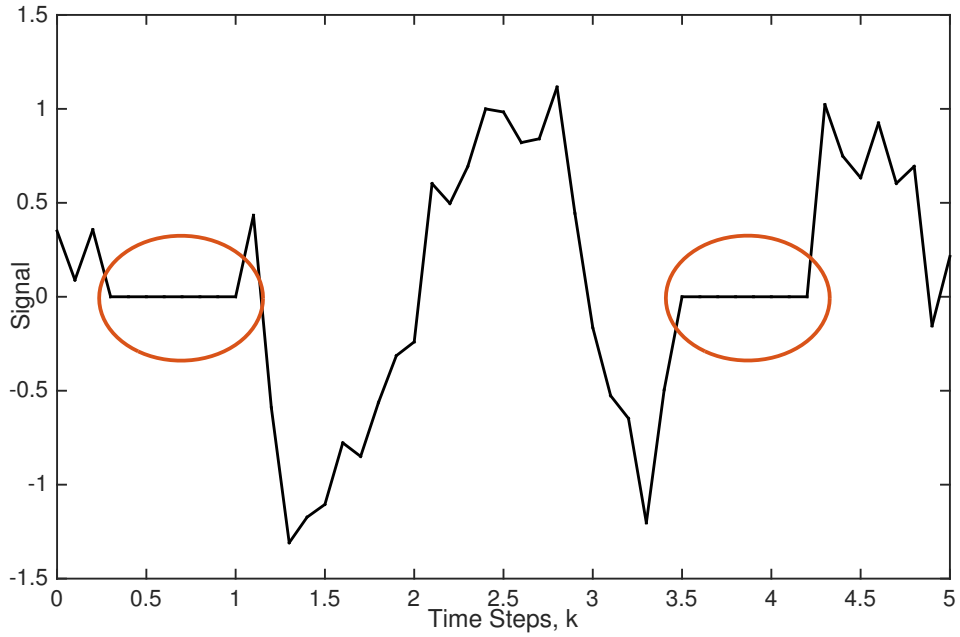

Figure 1.3: Example of an intermittent measurement

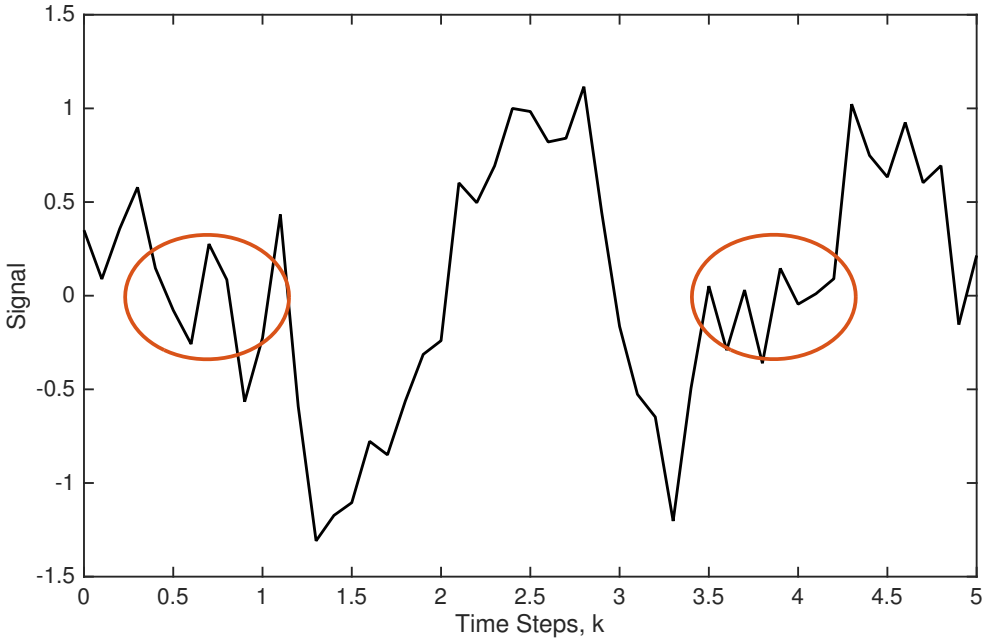

Figure 1.4: Example of an uncertain measurement

1.3 Main Contributions

The ubiquitous discrete- and continuous-time extended Kalman filters are applied to systems with finite-energy disturbances and are analyzed for convergence, H_∞- and H_2-properties. The following are the main contributions of this work.

- Convergence and error energy analysis are performed on the discrete-time EKF in the direct form applied to system models that are noise-free as well as models with stochastic finite-energy noise.
  - By analyzing the EKF in the direct form, the assumptions on the system are reduced, such as not having to invoke the assumption that A_k is invertible as in [11].
  - Much has been studied regarding the convergence of these filters, but little in regards to the H_∞- and H_2-properties, which are provided in

this work.

- Novel results on general convergence, H_∞-, and H_2-properties of two variations of the discrete-time extended Kalman filter designed for systems with uncertain measurements are provided.
  - The two uncertain measurement models used are: 1) measurement sensors fail independently and 2) all sensors fail simultaneously.
- Through similar analysis performed in discrete-time, the continuous-time EKF is also shown to inherently have the H_∞- and H_2-properties.

1.4 Dissertation Organization

This dissertation contains seven chapters. Chapter 1 consists of an introduction to filter analysis and the H_∞- and H_2-properties as well as notation and lemmata used throughout the dissertation. Chapter 2 contains the analysis of the discrete-time extended Kalman filter applied to noise-free systems to show an alternative method in obtaining convergence and H_2-property results as well as simulation studies. Chapter 3 contains the analysis of the discrete-time extended Kalman filter applied to systems with disturbances taken as an element of stochastic ℓ_2 accompanied with simulation studies. Chapter 4 includes the analysis of the discrete-time extended Kalman filter designed for systems with uncertain measurements with each sensor in the system having an individual failure rate, i.e. the sensors fail independently from each other. Chapter 5 contains a special case of Chapter 4, the analysis of the discrete-time extended Kalman filter designed for systems with uncertain measurements with one failure rate for all of the sensors, i.e. all sensors fail at the same time. Chapter 6 is an extension of the discrete-time analysis to the continuous-time extended Kalman filter applied to systems with deterministic finite-energy disturbances. Chapter 7 will conclude the dissertation summarizing the work and introducing future work ideas.

1.5 Notation

The following notation is used throughout this dissertation:

- $x \in \Re^n$ is an n-dimensional vector with real elements
- x^T represents the transpose of vector x
- $A \in \Re^{m \times n}$ is an $m \times n$ matrix with real elements
- I_n is the $n \times n$ identity matrix
- $A > 0$ ($A \geq 0$) is a positive definite (semi-definite) matrix
- $\circ$ denotes the Hadamard product, given below in Section 1.6 Lemma 7
- $\| \cdot \|$ denotes the Euclidean norm of real vectors
- $\| A \|_i$ represents the induced 2-norm (the spectral norm) of the matrix A
- $\lambda_{min}(A)$ and $\lambda_{max}(A)$ are the minimum and maximum eigenvalues of the symmetric matrix A
- A_k denotes a time-varying matrix, that is, a matrix that changes with the discrete-time index $k = 0, 1, 2, \ldots$
- A_t denotes a time-varying matrix, that is, a matrix that changes with the continuous-time $t \geq 0$
- $\dot{A}_t$ is the time derivative of the matrix A_t
- $E\{x\} = \overline{x}$ is the expected value of the random variable x
- $E\{x|y\}$ is the expected value of x conditional on y
- Stochastic ℓ_2 is the space of bounded energy sequences that are zero mean and uncorrelated in time, i.e. $x_k \in \ell_2$ implies $\sum_{k=0}^{\infty} \overline{\|x_k\|^2} < \infty$, $\overline{x_k} = 0$, $\overline{x_k^T x_{k-1}} = 0$
- $\mathcal{L}_2$ is the space of square integrable (finite-energy) vector functions, for $x \in \mathcal{L}_2$, $\int_0^{\infty} \|x(t)\|^2 dt < \infty$

1.6 Lemmata

Lemma 1 (Minimization by Completion of Squares)**.** *[24] For $A = A^T > 0$, $X = -B^T A^{-1}$ is the minimum solution of $D = C + B^T X^T + XB + XAX^T$*

Proof. To minimize

$$D_1 = C + B^T X^T + XB + XAX^T \tag{1.27}$$

over X, the equation is written in a quadratic form

$$D_2 = C + (X - Y)A(X - Y)^T - YAY^T \tag{1.28}$$

where YAY^T has been added and subtracted. For (1.27) and (1.28) to be equivalent, like terms can be identified by expanding (1.28) as

$$\begin{aligned} D_2 &= C + XAX^T - YAX^T - XAY^T + YAY^T - YAY^T \\ &= C - YAX^T - XAY^T + XAX^T \end{aligned} \tag{1.29}$$

where it can be seen that

$$B^T X^T = -YAX^T \tag{1.30}$$

or

$$B^T = -YA \tag{1.31}$$

$$Y = -B^T A^{-1} \tag{1.32}$$

which must be true for (1.27) and (1.28) to be equivalent.

In (1.28), the only free variable is X, resulting in $(X - Y)A(X - Y)^T$ as the term to minimize. This term can be minimized by setting X equal to Y, yielding the zero matrix. Therefore (1.27) can be minimized by choosing $X = Y = -B^T A^{-1}$.

■

Lemma 2. *[2] If the pair (A_k, C_k) is uniformly observable, with $\|A_k\|_i \leq \bar{a}$, $\|C_k\|_i \leq \bar{c}$, $\|F_k\|_i \leq \bar{f}$, and $\|H_k\|_i \leq \bar{h}$ uniformly bounded in time, then the solution of the Riccati difference equation and the Kalman gain are uniformly bounded both above and below as $0 < \underline{p} I_n \leq P_k \leq \bar{p} I_n < \infty$ and $0 < \underline{k} I_n \leq K_k \leq \bar{k} I_n < \infty$, respectively, for $k = 1, 2, \ldots$.*

Lemma 3 (Rayleigh's inequality). *[25] For $Q = Q^T$,*
$\lambda_{min}(Q)\|x\|^2 \leq x^T Q x \leq \lambda_{max}(Q)\|x\|^2$

Lemma 4 (The Schur Complement). *[25] For matrices A, B, and C, the following conditions are equivalent:*
a) $\begin{bmatrix} A & B^T \\ B & C \end{bmatrix} \geq 0$
b) $C > 0$ *and* $A - B^T C^{-1} B \geq 0$
c) $A > 0$ *and* $C - B A^{-1} B^T \geq 0$

Lemma 5 (Smoothing property of expectations). *[26]* $E\{E\{x|y\}\} = E\{x\}$

Lemma 6. *[2] If the pair (A_k, C_k) is uniformly observable, with $\|A_k\|_i \leq \bar{a}$, $\|C_k\|_i \leq \bar{c}$, $\|F_k\|_i \leq \bar{f}$, $\|H_k\|_i \leq \bar{h}$, and $\|h(x_k)\| \leq \alpha_h$ uniformly bounded in time, then the solution of the Riccati difference equation and the Kalman gain are uniformly bounded both above and below as $0 < \underline{p} I_n \leq P_k \leq \bar{p} I_n < \infty$ and $0 < \underline{k} I_n \leq K_k \leq \bar{k} I_n < \infty$, respectively, for $k = 1, 2, \ldots$.*

Lemma 7 (Hadamard Product). *[25] For matrices A, $B \in \Re^{p \times p}$,*
$[A \circ B]_{i,j} = [A]_{i,j}[B]_{i,j}$

Corollary 7.1. *[25] For matrices satisfying Lemma 7 and $B = diag\{b_1, b_2, \ldots, b_p\}$ consisting of random elements, $E\{BAB^T\} = E\{BB^T\} \circ A$*

Lemma 8 (Time derivative of the inverse of a time-varying matrix). *[25]*
$\frac{d(A_t^{-1})}{dt} = -A_t^{-1} \dot{A}_t A_t^{-1}$

Lemma 9. *[2] If the pair (A_t, C_t) is uniformly observable, with $\|A_t\|_i \leq \bar{a}$, $\|C_t\|_i \leq \bar{c}$, $\|F_t\|_i \leq \bar{f}$, and $\|H_t\|_i \leq \bar{h}$ uniformly bounded in time, then the solution of the Riccati differential equation and the Kalman gain are uniformly bounded both above and below as $0 < \underline{p} I_n \leq P_t \leq \bar{p} I_n < \infty$ and $0 < \underline{k} I_n \leq K_t \leq \bar{k} I_n < \infty$, respectively, for $t \geq 0$*

Lemma 10 (Matrix Cross-Term Bound)**.** *[25] For appropriately sized vectors, e and w, and matrix M, where $\beta > 0$ is an arbitrary constant:*
$e^T M w + w^T M^T e \leq \beta e^T e + \beta^{-1} w^T M^T M w$

Lemma 11. *[27] Let X and Y be $n \times n$ Hermitian matrices where the subscript denotes the eigenvalue order, and the subscript n is the index of the minimum eigenvalue:*
$\lambda_{i+j-n}(XY) \geq \lambda_i(X)\lambda_j(Y)$, *for $i + j \geq n + 1$.*

CHAPTER 2

H_2-PROPERTY OF THE DISCRETE-TIME EXTENDED KALMAN FILTER APPLIED TO NOISE FREE SYSTEMS

The discrete-time EKF designed for systems with zero mean, white noise and correlation between the process and measurement noise is the focus of this chapter. The development of the direct form of this EKF is provided. This EKF is then analyzed using Lyapunov techniques for noise free systems showing both convergence and the H_2-property. Simulations are provided that study the effect of the initial conditions for three different types of nonlinearities. These simulations give insight into the validity and conservativeness of the results herein.

2.1 EKF Formulation

The discrete-time extended Kalman filter for systems with correlation between the process and measurement noise in direct form is derived in this section based on [24]. Consider the nonlinear discrete-time system in (2.1) and (2.2):

$$x_{k+1} = f(x_k) + F_k w_k \tag{2.1}$$

$$y_k = h(x_k) + H_k w_k \tag{2.2}$$

where $x_k \in \Re^n$ is the state, $y_k \in \Re^p$ is the measurement, $w_k \in \Re^l$ is zero mean, ($\overline{w_k} = 0$), white noise ($\overline{w_k w_{k-1}^T} = 0$), with identity covariance ($\overline{w_k w_k^T} = I_l$), F_k and H_k are the noise coefficient matrices resulting in the process noise covariance, $F_k F_k^T > 0$, the measurement noise covariance, $H_k H_k^T > 0$, and the correlation between the process and measurement noise, $F_k H_k^T$.

The state estimate dynamics are calculated using known information: the form of the nonlinearites, the current measurement, and the current estimate as

$$\hat{x}_{k+1} = f(\hat{x}_k) + K_k(y_k - h(\hat{x}_k)) \tag{2.3}$$

where $K_k \in \Re^{n \times p}$ will be the Kalman gain. The nonlinearities are approximated using a Taylor Series Expansion about the current estimate yielding

$$f(x_k) \cong f(\hat{x}_k) + A_k(x_k - \hat{x}_k) \tag{2.4}$$

$$h(x_k) \cong h(\hat{x}_k) + C_k(x_k - \hat{x}_k) \tag{2.5}$$

with the Jacobians defined as

$$A_k = \left.\frac{\partial f(x_k)}{\partial x_k}\right|_{x_k = \hat{x}_k} \tag{2.6}$$

$$C_k = \left.\frac{\partial h(x_k)}{\partial x_k}\right|_{x_k = \hat{x}_k} \tag{2.7}$$

The nonlinear observer error defined as the difference between the current state and the estimate,

$$e_k = x_k - \hat{x}_k \tag{2.8}$$

has the following dynamics

$$e_{k+1} = f(x_k) + F_k w_k - f(\hat{x}_k) - K_k(h(x_k) + H_k w_k - h(\hat{x}_k)) \tag{2.9}$$

which, when combined with the approximations in (2.4) and (2.5), yield

$$e_{k+1} \cong (A_k - K_k C_k)e_k + (F_k - K_k H_k)w_k \tag{2.10}$$

The goal of the EKF is to minimize the error covariance,

$$P_k = E\left\{e_k e_k^T\right\} \tag{2.11}$$

which is done through analysis of the error covariance dynamics,

$$\begin{aligned} P_{k+1} &= E\left\{e_{k+1}e_{k+1}^T\right\} \\ &\cong E\left\{((A_k - K_kC_k)e_k + (F_k - K_kH_k)w_k)((A_k - K_kC_k)e_k + (F_k - K_kH_k)w_k)^T\right\} \\ &= E\left\{\begin{array}{l}(A_k - K_kC_k)e_ke_k^T(A_k - K_kC_k)^T + (A_k - K_kC_k)e_kw_k^T(F_k - K_kH_k)^T \\ \quad +(F_k - K_kH_k)w_ke_k^T(A_k - K_kC_k)^T + (F_k - K_kH_k)w_kw_k^T(F_k - K_kH_k)^T\end{array}\right\} \end{aligned} \tag{2.12}$$

Since the expectation operator is linear, it can be applied separately to each term while also removing known terms from the expectation operation

$$\begin{aligned} P_{k+1} \cong &(A_k - K_kC_k)\overline{e_ke_k^T}(A_k - K_kC_k)^T + (A_k - K_kC_k)\overline{e_kw_k^T}(F_k - K_kH_k)^T \\ &+ (F_k - K_kH_k)\overline{w_ke_k^T}(A_k - K_kC_k)^T + (F_k - K_kH_k)\overline{w_kw_k^T}(F_k - K_kH_k)^T \end{aligned} \tag{2.13}$$

In (2.10), it is seen that the current observer error, e_k, is a function of the past noise, w_{k-1}. When the noise is white, w_k and w_{k-1} are uncorrelated, implying that w_k and e_k are uncorrelated, simplifying (2.13) to

$$\begin{aligned} P_{k+1} \cong &(A_k - K_kC_k)\overline{e_ke_k^T}(A_k - K_kC_k)^T + (A_k - K_kC_k)(\overline{e_k})\overline{w_k}^T(F_k - K_kH_k)^T \\ &+ (F_k - K_kH_k)(\overline{w_k})\overline{e_k}^T(A_k - K_kC_k)^T + (F_k - K_kH_k)\overline{w_kw_k^T}(F_k - K_kH_k)^T \end{aligned} \tag{2.14}$$

Using the error covariance definition in (2.11), and known statistics of the noise, zero mean and identity covariance, reduces (2.14) to

$$P_{k+1} \cong (A_k - K_kC_k)P_k(A_k - K_kC_k)^T + (F_k - K_kH_k)(F_k - K_kH_k)^T \tag{2.15}$$

To minimize the error covariance over the gain, K_k, (2.15) is expanded to obtain the form for use with Lemma 1

$$\begin{aligned} P_{k+1} \cong &A_kP_kA_k^T - A_kP_kC_k^TK_k^T - K_kC_kP_kA_k^T + K_kC_kP_kC_k^TK_k^T \\ &+ F_kF_k^T - F_kH_k^TK_k^T - K_kH_kF_k^T + K_kH_kH_k^TK_k^T \end{aligned} \tag{2.16}$$

followed by grouping terms with respect to K_k which leads to

$$\begin{aligned} P_{k+1} \cong & A_k P_k A_k^T + F_k F_k^T - (A_k P_k C_k^T + F_k H_k^T) K_k^T \\ & - K_k (C_k P_k A_k^T + H_k F_k^T) + K_k (C_k P_k C_k^T + H_k H_k^T) K_k^T \end{aligned} \tag{2.17}$$

Recognizing that (2.17) is now of the form in Lemma 1 where the corresponding terms are

$$A = C_k P_k C_k^T + H_k H_k^T \tag{2.18}$$

$$B = -(C_k P_k A_k^T + H_k F_k^T) \tag{2.19}$$

$$C = A_k P_k A_k^T + F_k F_k^T \tag{2.20}$$

$$D = P_{k+1} \tag{2.21}$$

$$X = K_k \tag{2.22}$$

applying Lemma 1 to (2.17) results in the locally optimal gain that minimizes (2.17)

$$K_k = (A_k P_k C_k^T + F_k H_k^T)(C_k P_k C_k^T + H_k H_k^T)^{-1} \tag{2.23}$$

Therefore, the extended Kalman filter for the system in (2.1) and (2.2) is defined by the following equations

- State estimate

$$\hat{x}_{k+1} = f(\hat{x}_k) + K_k (y_k - h(\hat{x}_k)) \tag{2.24}$$

- Kalman Gain

$$K_k = (A_k P_k C_k^T + F_k H_k^T)(C_k P_k C_k^T + H_k H_k^T)^{-1} \tag{2.25}$$

- Riccati Difference Equation

$$P_{k+1} = \mathcal{A}_k P_k \mathcal{A}_k^T + \mathcal{F}_k \mathcal{F}_k^T \tag{2.26}$$

where

$$\mathcal{A}_k = A_k - K_k C_k \tag{2.27}$$

$$\mathcal{F}_k = F_k - K_k H_k \tag{2.28}$$

with

$$\mathcal{F}_k \mathcal{F}_k^T > 0 \tag{2.29}$$

and A_k and C_k in (2.6) and (2.7), respectively.

2.2 Convergence Analysis of EKF Used on Noise-Free Systems

Now, consider the noise-free deterministic nonlinear discrete-time system in (2.30) and (2.31):

$$x_{k+1} = f(x_k) \tag{2.30}$$

$$y_k = h(x_k) \tag{2.31}$$

which has the following error dynamics, with error defined in (2.8),

$$e_{k+1} = f(x_k) - f(\hat{x}_k) - K_k(h(x_k) - h(\hat{x}_k)) \tag{2.32}$$

which, when combined with the approximations in (2.4) and (2.5), yield

$$e_{k+1} \cong \mathcal{A}_k e_k \tag{2.33}$$

Assumption 2.1. *The pair (A_k, C_k) is uniformly observable, with $\|A_k\|_i \leq \bar{a}$, $\|C_k\|_i \leq \bar{c}$, $\|F_k\|_i \leq \bar{f}$, and $\|H_k\|_i \leq \bar{h}$ uniformly bounded in time.*

Theorem 2.1. *Consider the deterministic nonlinear system* (2.30) *and measurement equation* (2.31) *with noise taken as $w_k = 0$ for any integer $k > 0$. Let the state be estimated using an extended Kalman filter with the gain from* (2.25)*, which was designed for systems with zero mean, white noise with identity covariance. With Assumption 2.1 on A_k, C_k, F_k, and H_k, Lemma 2 holds. With these conditions, the observer error is*

guaranteed to be asymptotically stable. Furthermore, the observer error energy is bounded as

$$\sum_{k=0}^{\infty} \|e_k\|^2 \leq \frac{1}{\varphi} e_0^T P_0^{-1} e_0 \tag{2.34}$$

for any integer $T > 0$ *where*

$$\varphi \triangleq \inf_k (\lambda_{min}(P_k^{-1} - \mathcal{A}_k^T P_{k+1}^{-1} \mathcal{A}_k)) \tag{2.35}$$

with $\mathcal{A}_k$ *in* (2.27)

Proof. This proof has two main sections, convergence analysis and H_2-analysis. With Assumption 2.1, Lemma 2 states that the solution to the Riccati equation, P_k, and the Kalman gain, K_k, are uniformly upper and lower bounded, which is essential throughout the proof. The Lyapunov energy function candidate

$$V_k = e_k^T P_k^{-1} e_k \tag{2.36}$$

and the asymptotic stability condition,

$$V_k - V_{k+1} > 0 \tag{2.37}$$

are used as the basis of this study. Substituting directly from (2.36), (2.37) becomes

$$e_k^T P_k^{-1} e_k - e_{k+1}^T P_{k+1}^{-1} e_{k+1} > 0 \tag{2.38}$$

Substituting from (2.10) and combining like terms, (2.38) simplifies to

$$e_k^T P_k^{-1} e_k - e_k^T \mathcal{A}_k^T P_{k+1}^{-1} \mathcal{A}_k e_k = e_k^T (P_k^{-1} - \mathcal{A}_k^T P_{k+1}^{-1} \mathcal{A}_k) e_k > 0 \tag{2.39}$$

With (2.39) positive and in quadtratic form, Lemma 3 is used to lower bound (2.39) as

$$V_k - V_{k+1} \geq \varphi e_k^T e_k > 0 \tag{2.40}$$

with φ in (2.35). Such a $\varphi > 0$ always exists if

$$P_k^{-1} - \mathcal{A}_k^T P_{k+1}^{-1} \mathcal{A}_k > 0 \tag{2.41}$$

The inverse of P_{k+1} makes it unclear if (2.41) is true; however, P_k is a positive definite matrix, allowing for Lemma 4 to be used. After substituting P_{k+1} with (2.26), the following conditions are equivalent to that in (2.41)

$$\begin{bmatrix} P_k^{-1} & \mathcal{A}_k^T \\ \mathcal{A}_k & \mathcal{A}_k P_k \mathcal{A}_k^T + \mathcal{F}_k \mathcal{F}_k^T \end{bmatrix} > 0 \tag{2.42}$$

$$\mathcal{A}_k P_k \mathcal{A}_k^T + \mathcal{F}_k \mathcal{F}_k^T - \mathcal{A}_k P_k \mathcal{A}_k^T > 0 \tag{2.43}$$

$$\mathcal{F}_k \mathcal{F}_k^T > 0 \tag{2.44}$$

With $\mathcal{F}_k \mathcal{F}_k^T > 0$ in (2.29), it is seen from (2.44) that the inequality is true, proving (2.41) and showing that the discrete-time EKF will converge asymptotically for noise-free systems with Assumption 2.1.

For H_2-analysis, the effect of initial conditions, $V_0 = e_0^T P_0^{-1} e_0$, on the observer error energy is considered by taking the summation of (2.40) from 0 to T, for any integer $T > 0$

$$V_0 - V_T \geq \varphi \sum_{k=0}^{T} \|e_k\|^2 \tag{2.45}$$

and for any $V_T > 0$, (2.45) is simplified as

$$\sum_{k=0}^{T} \|e_k\|^2 \leq \frac{1}{\varphi} V_0 \tag{2.46}$$

The inequality in (2.46) shows a bound on the H_2-gain of the EKF to be $1/\varphi$, with φ in (2.35). ■

2.3 Significance

When the discrete-time EKF is used as a nonlinear observer for noise-free systems that meet the specified conditions, the results show that the observer error converges asymptotically. In there derivation to show convergence, fewer assumptions imposed compared to previous works resulting in a more general

condition. In addition, it has been shown for the first time that the EKF has an H_2-property which says for bounded initial error, $e_0 < \infty$, the energy of the observer error is also bounded, $\sum_{k=0}^{\infty} \|e_k\|^2 < \infty$.

2.4 Simulations

Three simulation cases are provided to show convergence of the observer error and the validity of the H_2-bound. The first case study is a system with a sinusoidal nonlinearity, the second case study is a system with a quadratic nonlinearity, and the third case study has a cubic nonlinearity. The effect of initial error on the H_2-gain and bound is analyzed for each case showing that more "severe" nonlinearities may be more sensitive to large initial errors.

Three nonlinear systems of the form

$$\ddot{y} = -f(y) \tag{2.47}$$

which, when converted to state-space representation, become

$$\dot{x} = \begin{bmatrix} 0 & 1 \\ 0 & 0 \end{bmatrix} x + \begin{bmatrix} 0 \\ -f(x_1) \end{bmatrix} \tag{2.48}$$

$$y = \begin{bmatrix} 1 & 0 \end{bmatrix} x \tag{2.49}$$

In each case, the systems are discretized using a first-order Euler approximation

$$\frac{x_{k+1} - x_k}{\tau} = \begin{bmatrix} 0 & 1 \\ 0 & 0 \end{bmatrix} x_k + \begin{bmatrix} 0 \\ -f(x_{1,k}) \end{bmatrix} \tag{2.50}$$

$$y_k = \begin{bmatrix} 1 & 0 \end{bmatrix} x_k \tag{2.51}$$

which, after rearrangement, becomes

$$x_{k+1} = \begin{bmatrix} 1 & \tau \\ 0 & 1 \end{bmatrix} x_k + \begin{bmatrix} 0 \\ -\tau f(x_{1,k}) \end{bmatrix} \tag{2.52}$$

$$y_k = \begin{bmatrix} 1 & 0 \end{bmatrix} x_k \tag{2.53}$$

2.4.1 Sinusoidal Nonlinearity

Consider the continuous-time system in (2.54) which has a "mild" nonlinearity

$$\ddot{y} = -sin(y) \tag{2.54}$$

which is discretized following the steps provided in the introduction of this section as

$$x_{k+1} = \begin{bmatrix} 1 & \tau \\ 0 & 1 \end{bmatrix} x_k + \begin{bmatrix} 0 \\ -\tau sin(x_{1,k}) \end{bmatrix} \tag{2.55}$$

$$y_k = \begin{bmatrix} 1 & 0 \end{bmatrix} x_k \tag{2.56}$$

An EKF used as a nonlinear observer for the deterministic system in (2.55) and (2.56) with $F_k F_k^T = I_2$, $F_k H_k^T = 0$, and $H_k H_k^T = 1$ and sampling time $\tau = 0.1s$ has been analyzed to show convergence and compare the H_2-gain from simulation to the theoretical bound.

The initial observer error is considered in polar form:

$$e_0^T = \|e_0\| \begin{bmatrix} cos(\theta) & sin(\theta) \end{bmatrix}^T \tag{2.57}$$

To show convergence of the observer, the magnitude of the initial observer error is kept as $\|e_0\| = 5$ while the angle is swept through 360° in 45° increments. Figures 2.1 and 2.2 show the time responses of $e_k = [e_{1,k}, e_{2,k}]^T$ for the initial conditions given above. In all of the cases, the estimation error converges to zero.

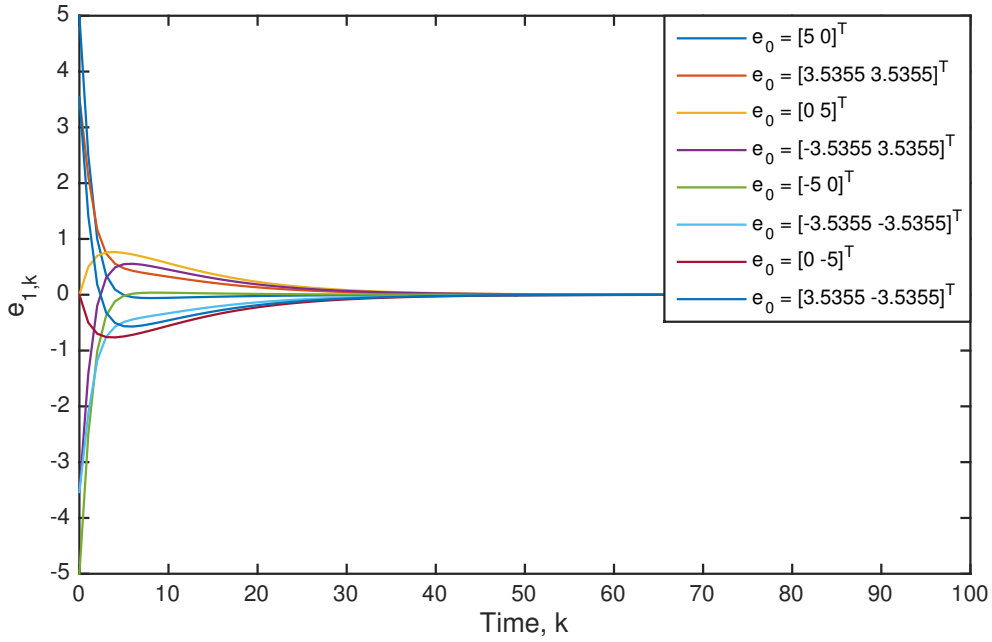

Figure 2.1: Time response of $e_{1,k}$

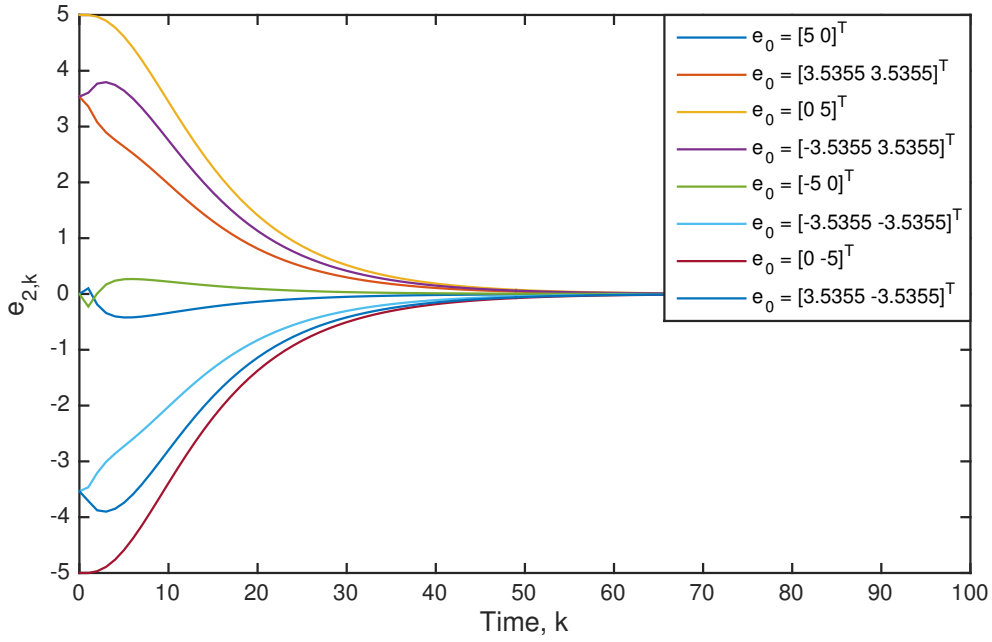

Figure 2.2: Time response of $e_{2,k}$

To analyze the H_2-gain, θ is swept through 360° in 1° increments and three values for the magnitude are used, $\|e_0\| = \{5, 25, 50\}$. The H_2-gain is calculated using results from the simulation and is compared to the theoretical H_2-bound by solving (2.46) as

$$\frac{\sum_{k=0}^{1} 00\|e_k\|^2}{e_0^T P_0^{-1} e_0} \leq \frac{1}{\varphi} \tag{2.58}$$

The left hand side of (2.58) is evaluated by calculating the 2-norm of the error at each instant in time, squaring each of those values and then summing them; this is then divided by the initial Lyapunov function, $e_0^T P_0 e_0$. The right hand side of (2.58) is evaluated by finding $\lambda_{min}(P_k^{-1} - \mathcal{A}_k^T P_{k+1}^{-1} \mathcal{A}_k)$ at each instant in time and then taking the minimum of these minimums to obtain φ. The ratio of observer error energy to V_0 should be less than the theoretical bound, $1/\varphi$. With this relationship between the H_2-gain from simulation and the theoretical bound, the ratio of these two values has certain properties: 1) the ratio should be greater than zero and less than one and 2) the closer the ratio is to one, the tighter the bound.

While keeping the magnitude of the initial observer error constant at $\|e_0\| = 5$ and sweeping the angle through 360°, the black dashed line in Figure 2.3 shows the values of the simulation to theoretical ratio at each 1° increment. Likewise, the blue dash-dot and red solid lines represent the simulation to theoretical ratio at each 1° increment for $\|e_0\| = 25$ and $\|e_0\| = 50$, respectively. Figure 2.3 shows that the magnitude of the initial error has little effect on the ratio. On the other hand, the angle component has a noticeable effect on this simulation to theoretical ratio, with the minimum approximately along the 30° line and the maximum approximately along the 120° line.

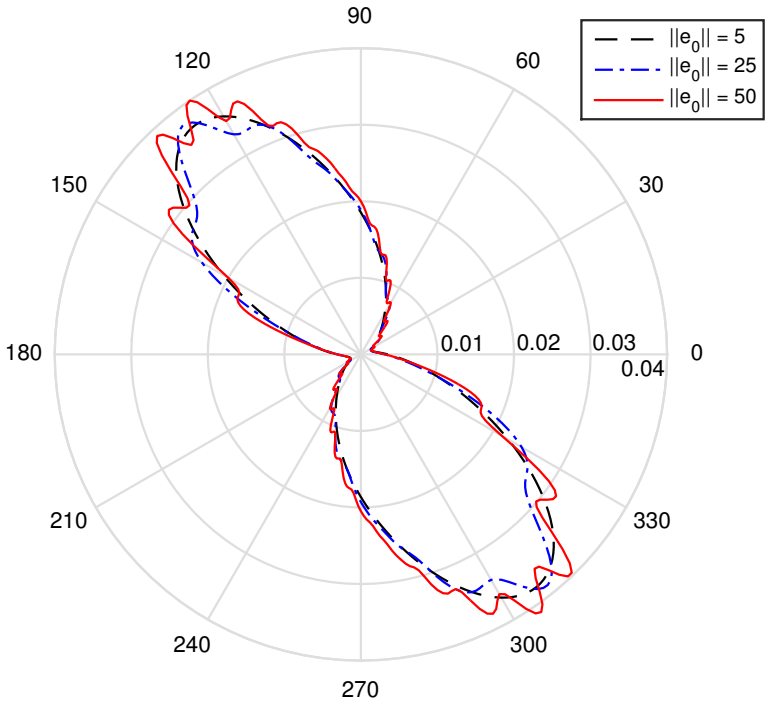

Figure 2.3: Sinusoidal nonlinearity - Ratio of H_2-gain from simulation to theoretical H_2

2.4.2 Quadratic Nonlinearity

The EKF is now used as a nonlinear observer for the deterministic system

$$\ddot{y} = -y^2 \tag{2.59}$$

which has a more "severe" nonlinearity and is discretized and converted to state space representation as (2.60) and (2.61) with $F_k F_k^T = I_2$, $F_k H_k^T = 0$ and $H_k H_k^T = 1$ and sampling time $\tau = 0.1s$.

$$x_{k+1} = \begin{bmatrix} 1 & \tau \\ 0 & 1 \end{bmatrix} x_k + \begin{bmatrix} 0 \\ -\tau x_{1,k}^2 \end{bmatrix} \tag{2.60}$$

$$y_k = \begin{bmatrix} 1 & 0 \end{bmatrix} x_k \tag{2.61}$$

With the knowledge that the existence of an H_2-gain implies that the error has finite energy, for the following two case studies, only the ratio between the H_2-gain from simulation and theoretical H_2-bound will be analyzed. The procedure is the same as before, θ is swept through 360° in 1° increments and three values for the magnitude are used, $\|e_0\| = \{5, 25, 50\}$.

While keeping the magnitude of the initial observer error constant at $\|e_0\| = 5$ and sweeping the angle through 360°, the black dashed line in Figure 2.4 shows the values of the simulation to theoretical ratio at each 1° increment. Likewise, the blue dash-dot and red solid lines represent the simulation to theoretical ratio at each 1° increment for $\|e_0\| = 25$ and $\|e_0\| = 50$, respectively. Figure 2.4 shows that for the system in (2.60) and (2.61), the magnitude and the angle of the initial error both have affect on the result.

2.4.3 Cubic Nonlinearity

Similar to the previous two case studies, the EKF is used as a nonlinear observer for the deterministic system

$$\ddot{y} = -y^3 \tag{2.62}$$

which has the most "severe" nonlinearity considered and is discretized and converted to state space representation in (2.63) and (2.64) with $F_k F_k^T = I_2$, $F_k H_k^T = 0$ and $H_k H_k^T = 1$ and sampling time $\tau = 0.1s$.

$$x_{k+1} = \begin{bmatrix} 1 & \tau \\ 0 & 1 \end{bmatrix} x_k + \begin{bmatrix} 0 \\ -\tau x_{1,k}^3 \end{bmatrix} \tag{2.63}$$

$$y_k = \begin{bmatrix} 1 & 0 \end{bmatrix} x_k \tag{2.64}$$

The procedure to compare the H_2-gain from simulation to theoretical H_2 bound is the same as before, θ is swept through 360° in 1° increments and three values for

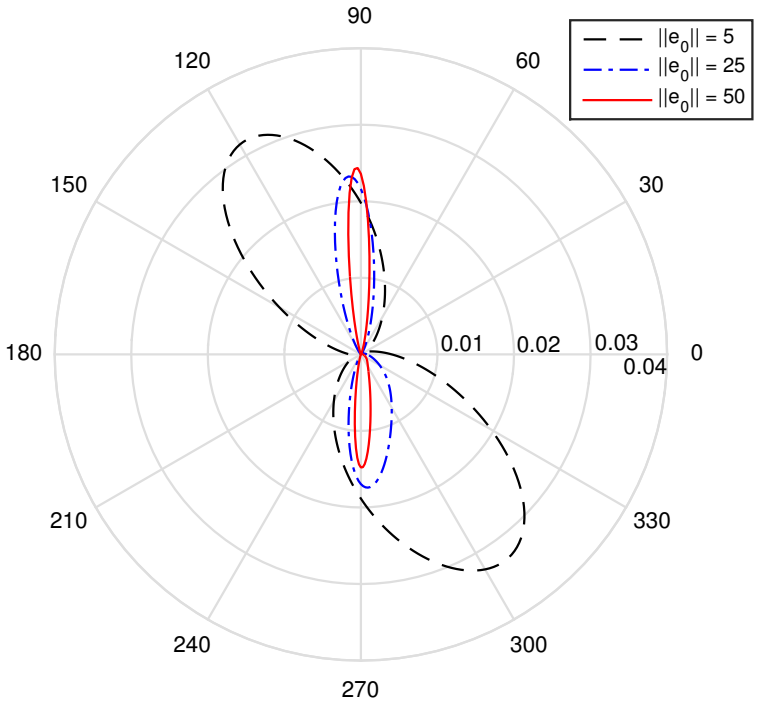

Figure 2.4: Quadratic nonlinearity - Ratio of H_2-gain from simulation to theoretical H_2

the magnitude are used, $\|e_0\| = \{2.5, 5, 7.5\}$. Notice that the range in error magnitude is smaller in this set of simulations. Due to the larger or more "severe" nonlinearity of $x_{1,k}^3$, the system Jacobian, A_k, grows unbounded with larger initial errors, which goes against Assumption 2.1. For this reason, the range has been reduced to look at the three different magnitudes given above.

While keeping the magnitude of the initial observer error constant at $\|e_0\| = 2.5$ and sweeping the angle through 360°, the black dashed line in Figure 2.5 shows the values of the simulation to theoretical ratio at each 1° increment. Likewise, the blue dash-dot and red solid lines represent the simulation to theoretical ratio at each 1° increment for $\|e_0\| = 4$ and $\|e_0\| = 8$, respectively.

Figure 2.5 shows that for the system in (2.60) and (2.61) the magnitude and the angle of the initial error both have an effect on the result. Also, the deformation of the shape's curvature in both the $\|e_0\| = 5$ and $\|e_0\| = 7.5$ cases signals that the initial error might be getting too large, nearly causing the assumptions to fail, which is indeed seen when $\|e_0\| = 10$.

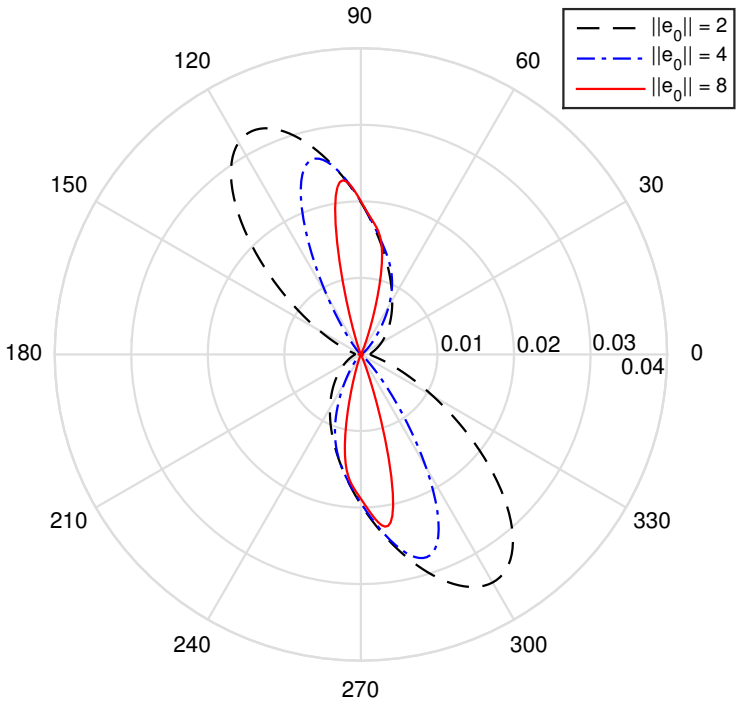

Figure 2.5: Cubic nonlinearity - Ratio of H_2-gain from simulation to theoretical H_2

2.5 Summary

Convergence of the discrete-time extended Kalman filter used as a nonlinear observer for noise-free deterministic systems was shown using Lyapunov analysis. Additionally, a bound on the H_2-gain was derived. Three

simulation studies were provided to show convergence of the observer error and the validity of the H_2-bound. The first case study was a system with a sinusoidal nonlinearity and was the "mildest" nonlinearity considered. For this system, the initial error magnitude had a lesser effect on the H_2-gain compared to the angle of the initial error. The second case study was a system with a quadratic nonlinearity, which is a more "severe" nonlinearity. The ratio between the H_2-gain from simulation and theoretical H_2-bound varied for the three initial error magnitudes, becoming more conservative as the magnitude of the initial error increased. The third case study had a cubic nonlinearity and was the most "severe" nonlinearity in the study. Unlike the system with the quadratic nonlinearity, where the overall shape of the three responses in Figure 2.4 stayed relatively similar but the size varied, in this case study, as the magnitude of the initial error increased, the general response of the ratio began having a deformed shape and became more conservative as the magnitude of the initial error increased. It was discussed that this deformation was due to the initial error nearing its maximum before the observer error might diverge. Next, this EKF will be further analyzed when applied to systems with finite-energy noise.

CHAPTER 3

H_∞-PROPERTY OF THE DISCRETE-TIME EXTENDED KALMAN FILTER APPLIED TO SYSTEMS WITH STOCHASTIC ℓ_2 DISTURBANCES

In Chapter 2, the EKF designed for systems with zero mean, white noise and correlation between the process and measurement was analyzed for noise-free systems. This chapter will extend that work to the same EKF being applied to systems that have stochastic ℓ_2 type disturbances in both the process and measurement. Lyapunov analysis will be completed to obtain general convergence as well as the H_∞-property. Simulations are provided to show the effect that the magnitude of the disturbance and the initial error have on convergence. Additional simulations provide analysis on the validity of the result by comparing the H_∞-gain calculated from simulation to the theoretical H_∞-bound.

3.1 EKF Formulation

For convenience, the main equations for the discrete-time extended Kalman filter for systems with correlation between process and measurement noise given in Chapter 2 are presented again here. Consider the nonlinear discrete-time system in (3.1) and (3.2):

$$x_{k+1} = f(x_k) + F_k w_k \tag{3.1}$$

$$y_k = h(x_k) + H_k w_k \tag{3.2}$$

where $x_k \in \Re^n$ is the state, $y_k \in \Re^p$ is the measurement, $w_k \in \Re^l$ is zero mean, ($\overline{w_k} = 0$), white noise ($\overline{w_k w_{k-1}^T} = 0$), with identity covariance ($\overline{w_k w_k^T} = I_l$), F_k and H_k are the noise coefficient matrices resulting in the process noise covariance, $F_k F_k^T$, the measurement noise covariance, $H_k H_k^T$, and the correlation between the process and measurement noise, $F_k H_k^T$.

The resulting extended Kalman filter for the system in (3.1) and (3.2) was shown in Chapter 2 to be defined by the following

- State estimate

$$\hat{x}_{k+1} = f(\hat{x}_k) + K_k(y_k - h(\hat{x}_k)) \tag{3.3}$$

- Kalman Gain

$$K_k = (A_k P_k C_k^T + F_k H_k^T)(C_k P_k C_k^T + H_k H_k^T)^{-1} \tag{3.4}$$

- Riccati Difference Equation

$$P_{k+1} = \mathcal{A}_k P_k \mathcal{A}_k^T + \mathcal{F}_k \mathcal{F}_k^T \tag{3.5}$$

  where

$$\mathcal{A}_k = A_k - K_k C_k \tag{3.6}$$

$$\mathcal{F}_k = F_k - K_k H_k \tag{3.7}$$

  with $\mathcal{F}_k \mathcal{F}_k^T > 0$ and A_k and C_k in (2.6) and (2.7), respectively.

3.2 Convergence Analysis of EKF Used on Systems with Finite-Energy Noise

Consider the nonlinear discrete-time system and measurement equations,

$$x_{k+1} = f(x_k) + F_k w_k \tag{3.8}$$

$$y_k = h(x_k) + H_k w_k \tag{3.9}$$

where the disturbance $w_k \in \ell_2$ is now zero mean, identity covariance, uncorrelated in time, and finite-energy. With the error defined as

$$e_k = x_k - \hat{x}_k \tag{3.10}$$

the error dynamics are

$$\begin{aligned} e_{k+1} &\cong x_{k+1} - \hat{x}_{k+1} \\ &= f(x_k) + F_k w_k - f(\hat{x}_k) - K_k(y_k - h(\hat{x}_k)) \end{aligned} \tag{3.11}$$

which, when combined with the Taylor series approximations (2.4) and (2.5) leads to

$$e_{k+1} \cong \mathcal{A}_k e_k + \mathcal{F}_k w_k \tag{3.12}$$

with $\mathcal{A}_k$ and $\mathcal{F}_k$ in (3.6) and (3.7). Note that in Chapter 2, the second term in (3.12) was not present because the disturbance, w_k, was zero.

Theorem 3.1. *Consider the nonlinear system* (3.8) *and measurement equation* (3.9)*, with the noise taken as an element of stochastic* ℓ_2 *and* $\mathcal{F}_k \mathcal{F}_k^T > 0$ *with* $\mathcal{F}_k$ *in* (3.7)*. Let the state be estimated using an extended Kalman filter, which was designed for white noise with zero mean and unit covariance, with gain* K_k *from* (3.4)*. With the conditions on* A_k*,* C_k*,* F_k*, and* H_k *in Assumption 2.1, Lemma 2 holds. With these conditions, the energy of the estimation error is bounded as follows*

$$\sum_{k=0}^{\infty} \overline{\|e_k\|^2} < \frac{1}{\varphi_1} \left(\overline{e_0^T P_0^{-1} e_0} + \varphi_2 \sum_{k=0}^{\infty} \overline{\|w_k\|^2} \right) \tag{3.13}$$

where

$$\varphi_1 \triangleq \inf_k (\lambda_{min}(P_k^{-1} - \overline{\mathcal{A}_k^T P_{k+1}^{-1} \mathcal{A}_k})) \tag{3.14}$$

$$\varphi_2 \triangleq \sup_k (\lambda_{max}(\overline{\mathcal{F}_k^T P_{k+1}^{-1} \mathcal{F}_k})) \tag{3.15}$$

with $\mathcal{A}_k$ *and* $\mathcal{F}_k$ *in* (3.6) *and* (3.7)

Proof. With Assumption 2.1, Lemma 2 states that the solution to the Riccati equation, P_k, and the Kalman gain, K_k, are uniformly upper and lower bounded, which is essential throughout the proof. Stochastic Lyapunov analysis is used to determine the stability of the estimation error and obtain the H_∞-gain. The Lyapunov function candidate,

$$V_k = e_k^T P_k^{-1} e_k \tag{3.16}$$

is analyzed along the dynamics of the error (3.12) to verify that the average energy decreases over time. To this end, consider the following stochastic Lyapunov difference

$$\begin{aligned} &E\{V_{k+1}|e_k, e_{k-1}, \dots\} - V_k \\ &= E\{e_{k+1}^T P_{k+1}^{-1} e_{k+1}|e_k, e_{k-1}, \dots\} - e_k^T P_k^{-1} e_k < 0 \end{aligned} \tag{3.17}$$

The inequality in (3.17) is rewritten by substitution from (3.12) as,

$$\begin{aligned} &E\{(\mathcal{A}_k e_k + \mathcal{F}_k w_k)^T P_{k+1}^{-1} (\mathcal{A}_k e_k + \mathcal{F}_k w_k)|e_k, e_{k-1}, \dots\} \\ &- e_k^T P_k^{-1} e_k < 0 \end{aligned} \tag{3.18}$$

which, when expanded, results in

$$-e_k^T \left(P_k^{-1} - \overline{\mathcal{A}_k^T P_{k+1}^{-1} \mathcal{A}_k}\right) e_k + 2\overline{w_k^T \mathcal{F}_k^T P_{k+1}^{-1} \mathcal{A}_k} e_k + \overline{w_k^T \mathcal{F}_k^T P_{k+1}^{-1} \mathcal{F}_k w_k} < 0 \tag{3.19}$$

Because $\mathcal{A}_k$, $\mathcal{F}_k$, $\hat{x}_k$, and therefore e_k, P_k and K_k are functions of w_{k-1} and since w_k is uncorrelated in time with zero mean, the second term in (3.19) can be rewritten so that the inequality becomes

$$\begin{aligned} &-e_k^T \left(P_k^{-1} - \overline{\mathcal{A}_k^T P_{k+1}^{-1} \mathcal{A}_k}\right) e_k + 2\left(\overline{w_k^T}\right)\left(\overline{\mathcal{F}_k^T P_{k+1}^{-1} \mathcal{A}_k}\right) e_k \\ &+ \overline{w_k^T \mathcal{F}_k^T P_{k+1}^{-1} \mathcal{F}_k w_k} < 0 \end{aligned} \tag{3.20}$$

leading to

$$-e_k^T \left(P_k^{-1} - \overline{\mathcal{A}_k^T P_{k+1}^{-1} \mathcal{A}_k}\right) e_k + \overline{w_k^T \mathcal{F}_k^T P_{k+1}^{-1} \mathcal{F}_k w_k} < 0 \tag{3.21}$$

To ensure (3.21) is negative, the development for an upper bound is provided next. The first term is lower bounded using Lemma 3

$$-\varphi_1 e_k^T e_k + \overline{w_k^T \mathcal{F}_k^T P_{k+1}^{-1} \mathcal{F}_k w_k} < 0 \tag{3.22}$$

with φ_1 defined in (3.14). Such a φ_1 always exists, if for any integer $k > 0$

$$P_k^{-1} - \mathcal{A}_k^T P_{k+1}^{-1} \mathcal{A}_k > 0 \tag{3.23}$$

This is shown by substituting P_{k+1} from (3.5) and using Lemma 4 twice resulting in the following equivalent matrix inequality conditions

$$\begin{bmatrix} P_k^{-1} & \mathcal{A}_k^T \\ \mathcal{A}_k & \mathcal{A}_k P_k \mathcal{A}_k^T + \mathcal{F}_k \mathcal{F}_k^T \end{bmatrix} > 0 \tag{3.24}$$

$$\mathcal{A}_k P_k \mathcal{A}_k^T + \mathcal{F}_k \mathcal{F}_k^T - \mathcal{A}_k P_k \mathcal{A}_k^T > 0 \tag{3.25}$$

and $\mathcal{F}_k \mathcal{F}_k^T > 0$ is true, therefore, for any integer $k > 0$

$$P_k^{-1} - \overline{\mathcal{A}_k^T P_{k+1}^{-1} \mathcal{A}_k} > 0 \tag{3.26}$$

To obtain an upper bound on the second term in (3.22), it is shown that for any integer $k > 0$

$$\mathcal{F}_k^T P_{k+1}^{-1} \mathcal{F}_k \leq I_l \tag{3.27}$$

When P_{k+1} is substituted from (3.5) and Lemma 4 is applied twice, the following matrix inequality conditions are equivalent

$$\begin{bmatrix} I_l & \mathcal{F}_k^T \\ \mathcal{F}_k & \mathcal{A}_k P_k \mathcal{A}_k^T + \mathcal{F}_k \mathcal{F}_k^T \end{bmatrix} \geq 0 \tag{3.28}$$

$$\mathcal{A}_k P_k \mathcal{A}_k^T + \mathcal{F}_k \mathcal{F}_k^T - \mathcal{F}_k \mathcal{F}_k^T \geq 0 \tag{3.29}$$

which agrees with $\mathcal{A}_k P_k \mathcal{A}_k^T \geq 0$. Therefore, it has been shown that I_l is a valid upper bound as shown in (3.27) and Lemma 3 can be applied to the second term in (3.22), resulting in φ_2 in (3.15) which is guaranteed to be bounded. These bounds result in

$$E\{V_{k+1} | e_k, e_{k-1}, \dots\} - V_k < -\varphi_1 e_k^T e_k + \varphi_2 \overline{w_k^T w_k} < 0 \tag{3.30}$$

Lastly, taking the expected value of (3.30) and using Lemma 5 results in

$$\overline{V_{k+1}} - \overline{V_k} < -\varphi_1 \overline{e_k^T e_k} + \varphi_2 \overline{w_k^T w_k} < 0 \tag{3.31}$$

To analyze the H_∞-property, the ratio of the estimation error energy to the disturbance energy is analyzed. To obtain terms that are representative of the

estimation error energy and the disturbance energy, the summation of (3.31) is taken from $k = 0$ to $k = T$ (for any integer $T > 0$) giving

$$\overline{V_T} - \overline{V_0} < -\varphi_1 \sum_{k=0}^{T} \overline{\|e_k\|^2} + \varphi_2 \sum_{k=0}^{T} \overline{\|w_k\|^2} \tag{3.32}$$

and for $\overline{V_T} \geq 0$,

$$-\overline{V_0} < -\varphi_1 \sum_{k=0}^{T} \overline{\|e_k\|^2} + \varphi_2 \sum_{k=0}^{T} \overline{\|w_k\|^2} \tag{3.33}$$

which is rearranged as

$$\sum_{k=0}^{T} \overline{\|e_k\|^2} < \frac{1}{\varphi_1} \left(\overline{e_0^T P_0^{-1} e_0} + \varphi_2 \sum_{k=0}^{T} \overline{\|w_k\|^2} \right) \tag{3.34}$$

This result indicates that the energy of the estimation error has an upper bound proportional to the initial estimation error and the disturbance energy, $\overline{e_0^T P_0^{-1} e_0}$ and $\sum_{k=0}^{T} \overline{\|w_k\|^2}$, where the proportionality constants φ_1 and φ_2 are defined in (3.14) and (3.15). ■

3.3 Significance

If the initial estimate has zero error, the result (3.34) is the H_∞-property resulting in the H_∞-gain defined below,

$$\frac{\sum_{k=0}^{\infty} \overline{\|e_k\|^2}}{\sum_{k=0}^{\infty} \overline{\|w_k\|^2}} < \frac{\varphi_2}{\varphi_1} \tag{3.35}$$

where φ_1 and φ_2 are defined in (3.14) and (3.15).

On the other hand, if there is no noise in the system for $k = 0, 1, 2, \ldots$, then (3.34) results in a special case that presents a bound on the estimation error energy in terms of the initial conditions, $\overline{e_0^T P_0^{-1} e_0}$, i.e. the H_2-property of the EKF

$$\sum_{k=0}^{\infty} \overline{\|e_k\|^2} < \frac{1}{\varphi_1} \overline{e_0^T P_0^{-1} e_0} \tag{3.36}$$

3.4 Simulations

Simulations are presented that demonstrate the two properties described in Section 3.3. For sufficiently small error in the initial estimate and disturbances with sufficiently small energy, the estimation error converges and the assumptions are met resulting in an attenuation of the effect of the disturbances. Then with the same initial estimate, the simulations show that for a stable system with sufficiently large disturbances, the assumptions for the H_∞-property are no longer met and the estimation error diverges. Finally, when the magnitude of the disturbance is the same as in the first case while the error in the initial estimate is increased, the simulations show that the assumptions for the H_∞-property are no longer met and, as expected, the estimation error diverges. A second system is studied where the estimation error is zero and a value for the H_∞-gain can be calculated for the system and compared to the theoretical bound. A multiplier on the noise terms is varied and the H_∞-gain from simulation is compared to the theoretical bound of the H_∞-gain. Lastly, the H_∞-gain from simulation is compared to the H_∞ theoretical bound for the systems given in Section 2.4 with sinusoidal, quadratic, and cubic nonlinearities. This will show how nonlinearities with different severities affect the H_∞-gain from simulation to theoretical bound ratio.

3.4.1 Effect of Initial Conditions and Disturbance Energy

Consider the nonlinear system based on reference [11] given by

$$x_{1,k+1} = x_{1,k} + \tau x_{2,k} + F_{11} w_k \tag{3.37}$$

$$x_{2,k+1} = x_{2,k} + \tau \left(-x_{1,k} + \left(x_{1,k}^2 + x_{2,k}^2 - 1 \right) x_{2,k} \right) \tag{3.38}$$

$$y_k = x_{1,k} + H_k w_k \tag{3.39}$$

$$x_0 = \begin{bmatrix} 0.8 & 0.2 \end{bmatrix}^T \tag{3.40}$$

where $\tau = 0.01s$ is the sampling period, $w_k \in \ell_2$ and F_{11} and H_{12} are elements of F and H, which are constant weighting matrices of the form

$$F = \begin{bmatrix} F_{11} & 0 \\ 0 & 0 \end{bmatrix} \tag{3.41}$$

$$H = \begin{bmatrix} 0 & H_{12} \end{bmatrix} \tag{3.42}$$

These matrices will be varied for the following simulation cases as provided in Table 3.1.

Following the procedure for the EKF, the nonlinearities of the system and measurement equations are linearized via a Taylor Series expansion around the state estimate

$$A_k = \begin{bmatrix} 1 & \tau \\ \tau \left(-1 + 2\hat{x}_{1,k}\hat{x}_{2,k} \right) & 1 + \tau \left(\hat{x}_{1,k}^2 + 3\hat{x}_{2,k}^2 - 1 \right) \end{bmatrix} \tag{3.43}$$

$$C_k = \begin{bmatrix} 1 & 0 \end{bmatrix} \tag{3.44}$$

These time varying matrices are used to calculate the solution to the Riccati difference equation (3.5) and the Kalman gain (3.4) at each time step. Three different cases are simulated, shown in Table 3.1, along with a qualitative stability analysis and H_∞-gain calculations. Each case is discussed in further detail below.

Table 3.1: Effect of initial values and constant weighting matrices

	Case 1	Case 2	Case 3
$\hat{x}_0$	$[0.5\ ,\ 0.5]^T$	$[0.5\ ,\ 0.5]^T$	$[1.5\ ,\ 1.2]^T$
F_{11}	10^{-3}	10^{-2}	10^{-3}
H_{12}	$0.1\sqrt{10}$	$\sqrt{10}$	$0.1\sqrt{10}$
Error Stability	Stable	Unstable	Unstable
H_∞-Gain	0.0185	—	—
Figures	3.1, 3.2, 3.3	3.4, 3.5, 3.6	3.7, 3.8, 3.9

Case 1 consists of a small error in the initial state estimate as well as small magnitudes for the elements of the weighting matrices. This produces results that meet the assumption of $\mathcal{F}_k\mathcal{F}_k^T > 0$ for $k = 0, 1, \ldots, N$. Figures 3.1 and 3.2 show that for this stable system, the estimates of the states are stable resulting in the same performance for the error, Figure 3.3.

Case 2 has the same initial error, with larger magnitudes in the weighting matrices. Figures 3.4 and 3.5 show that with larger noise, while the system is stable, the state estimate, and the error in Figure 3.6, becomes unbounded and does not demonstrate an H_∞-property. In this case, the assumption of $\mathcal{F}_k\mathcal{F}_k^T > 0$ does not hold, therefore it would be expected that this example does not have an H_∞-property.

Case 3 has large initial error but small magnitudes in the weighting matrices. Figures 3.7 and 3.8 show that the system response is stable but the estimate is unbounded and Figure 3.9 shows that this naturally leads to instability in the error. When checking the assumption of $\mathcal{F}_k\mathcal{F}_k^T > 0$, this assumption does not hold and explains why this case does not have an H_∞-property.

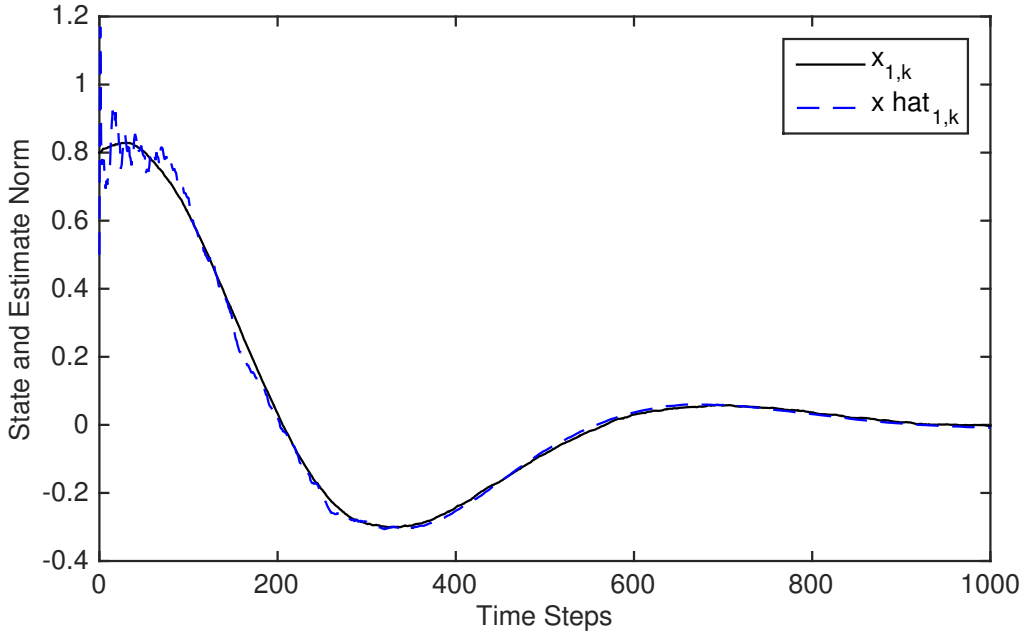

Figure 3.1: Second order system, Case 1 - State, $x_{1,k}$, and estimate, $\hat{x}_{1,k}$

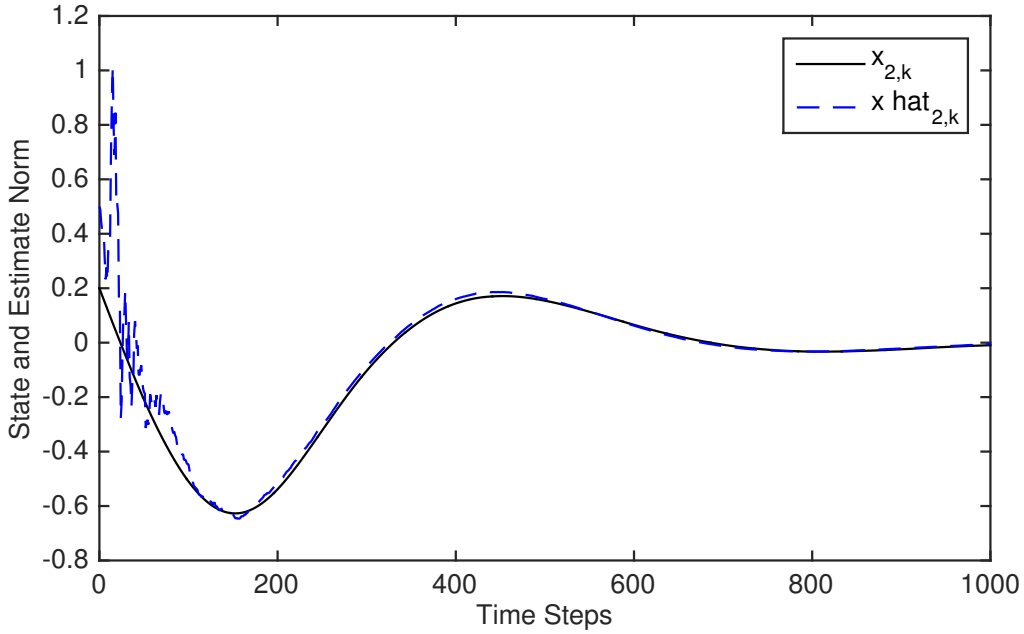

Figure 3.2: Second order system, Case 1 - State, $x_{2,k}$, and estimate, $\hat{x}_{2,k}$

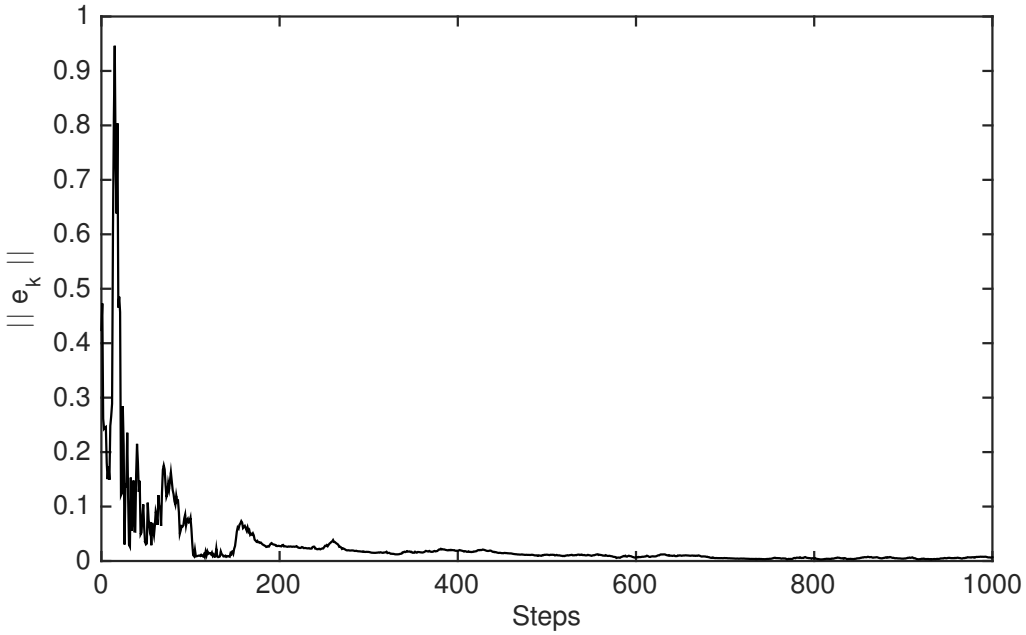

Figure 3.3: Second order system, Case 1 - Norm of the estimation error

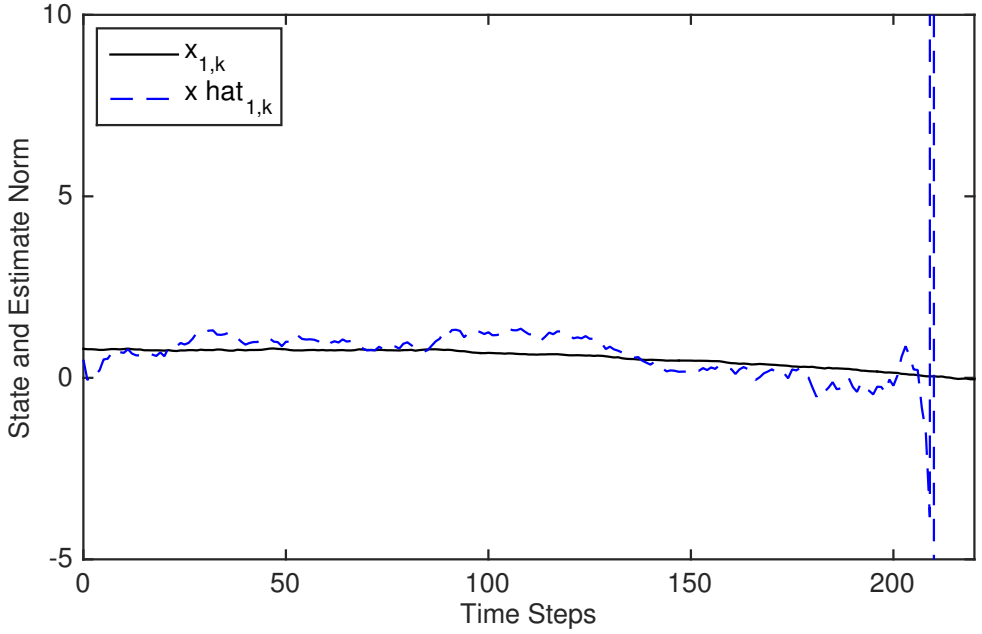

Figure 3.4: Second order system, Case 2 - State, $x_{1,k}$, and estimate, $\hat{x}_{1,k}$

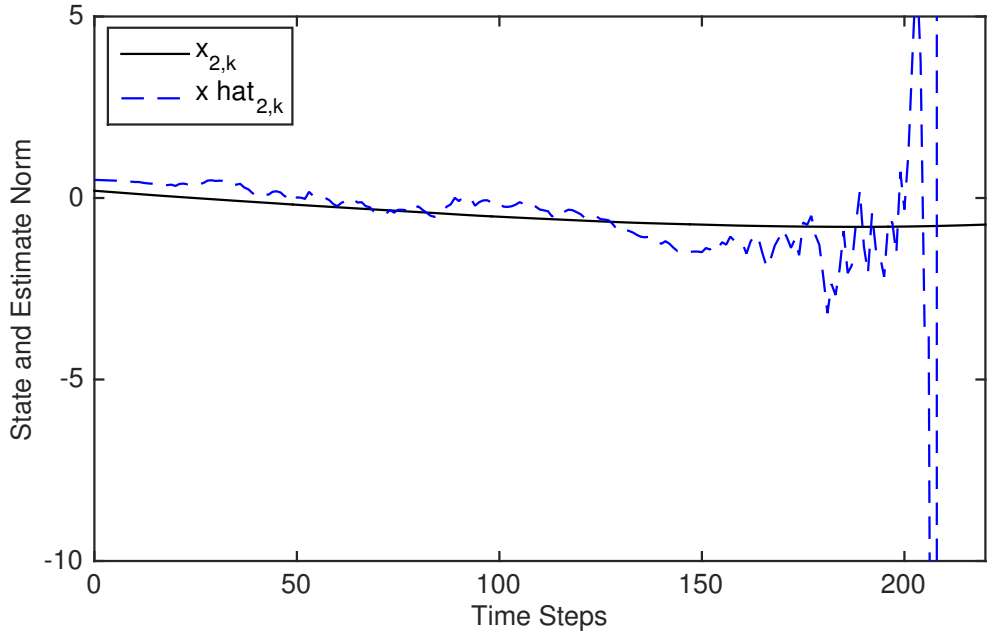

Figure 3.5: Second order system, Case 2 - State, $x_{2,k}$, and estimate, $\hat{x}_{2,k}$

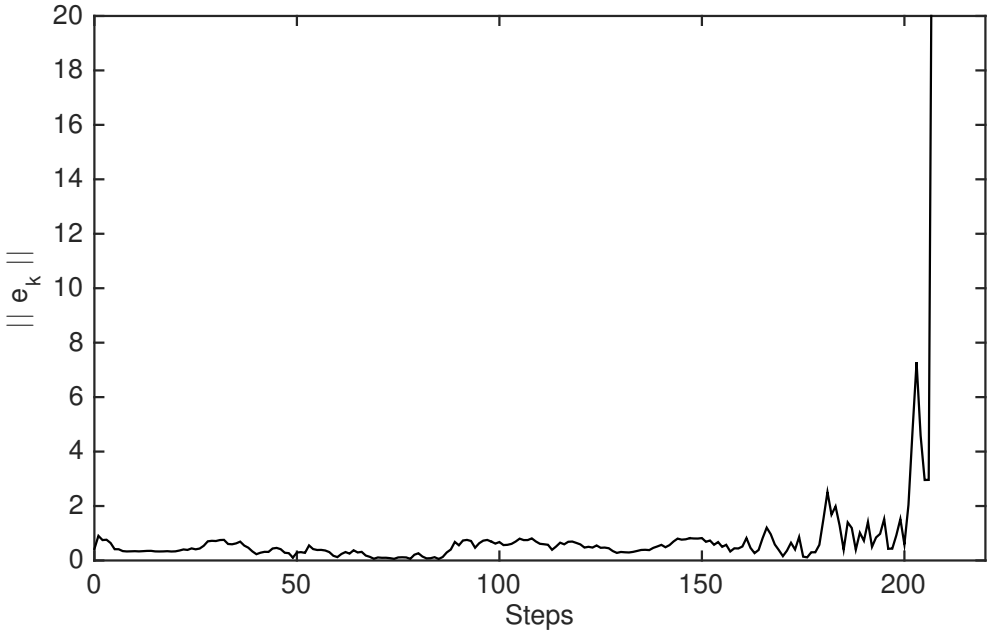

Figure 3.6: Second order system, Case 2 - Norm of the estimation error

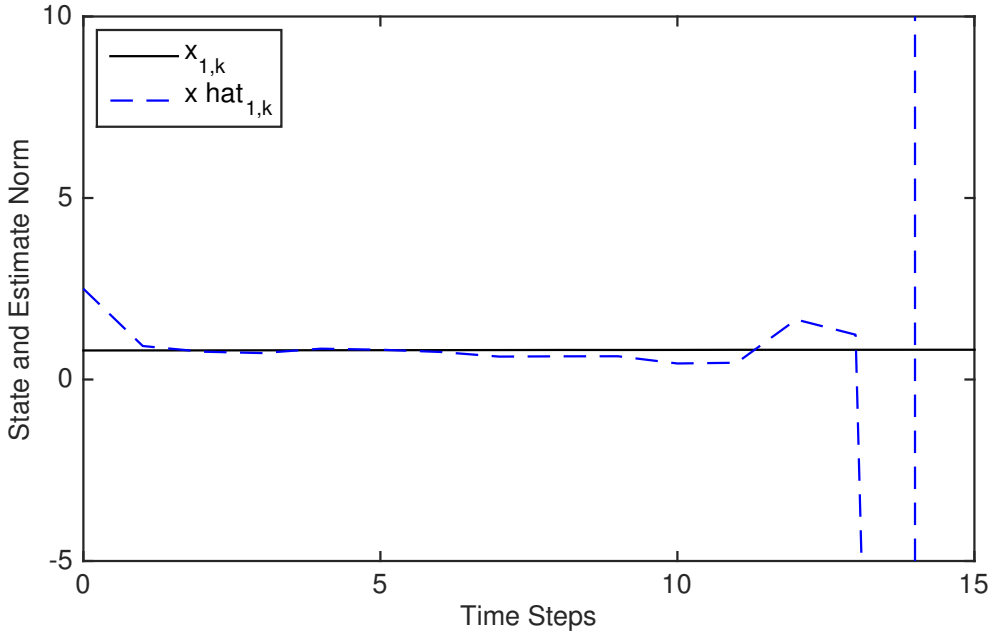

Figure 3.7: Second order system, Case 3 - State, $x_{1,k}$, and estimate, $\hat{x}_{1,k}$

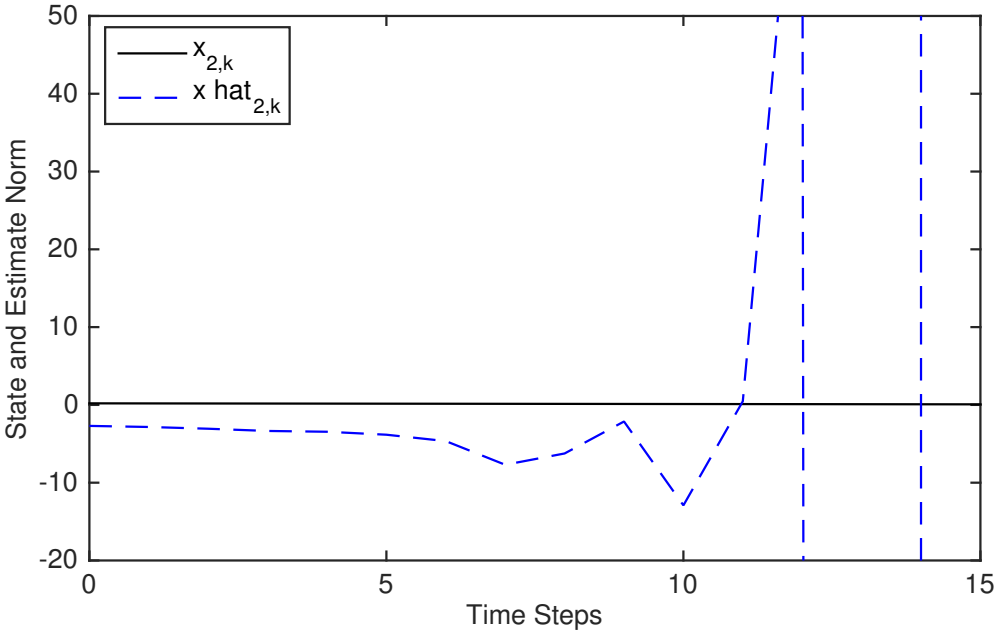

Figure 3.8: Second order system, Case 3 - State, $x_{2,k}$, and estimate, $\hat{x}_{2,k}$

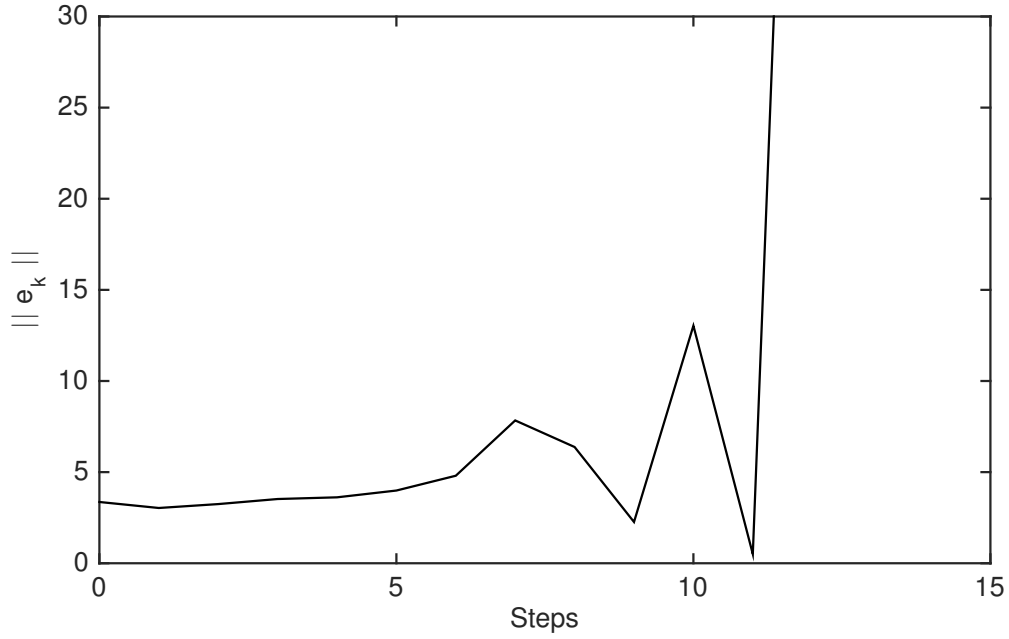

Figure 3.9: Second order system, Case 3 - Norm of the estimation error

3.4.2 Simulation H_∞-Gain to Theoretical H_∞-Bound Comparison

Scalar System

A scalar system shown below has also been analyzed to facilitate the comparison of the H_∞-gain from simulation to the theoretical bound to give insight into the validity and conservativeness of the result. The system is

$$x_{k+1} = x_k + 0.01 \sin x_k + 10\delta w_k \tag{3.45}$$

$$y_k = x_k + 0.1\delta w_k \tag{3.46}$$

with $w_k \in \ell_2$. The variable δ is swept from -50 to 50 in 0.2 increments to observe how the H_∞-gain from simulation and theoretical bound vary with disturbance magnitude. The H_∞-gain is calculated as the left hand side of (3.35) for each δ for a run time of $T = 1000$. Since this is a stochastic system, a 100 run Monte Carlo simulation is used for the analysis.

Figure 3.10 is a co-plot of the gain from simulation and the theoretical bound that shows for this system that the gain is close to the bound for all δ. For a better sense of the relationship between these values, the ratio of the calculated H_∞-gain to the theoretical bound is shown in Figure 3.11. This ratio is obtained using (3.35), where the error energy is found by calculating the 2-norm of the error at each instant in time, each 2-norm is then squared, the sample mean of the squared 2-norms is calculated, and then all of these are added together. The same process is performed for the disturbance energy. The right hand side of (3.35) is evaluated by finding $\lambda_{min}(P_k^{-1} - \mathcal{A}_k^T P_{k+1} \mathcal{A}_k)$ at each instant in time and then taking the minimum of these minimums to obtain φ_1. Similarly, φ_2 is found by calculating $\lambda_{max}(\mathcal{F}_k^T P_{k+1} \mathcal{F}_k)$ at each instant in time and then taking the maximum of these maximums.

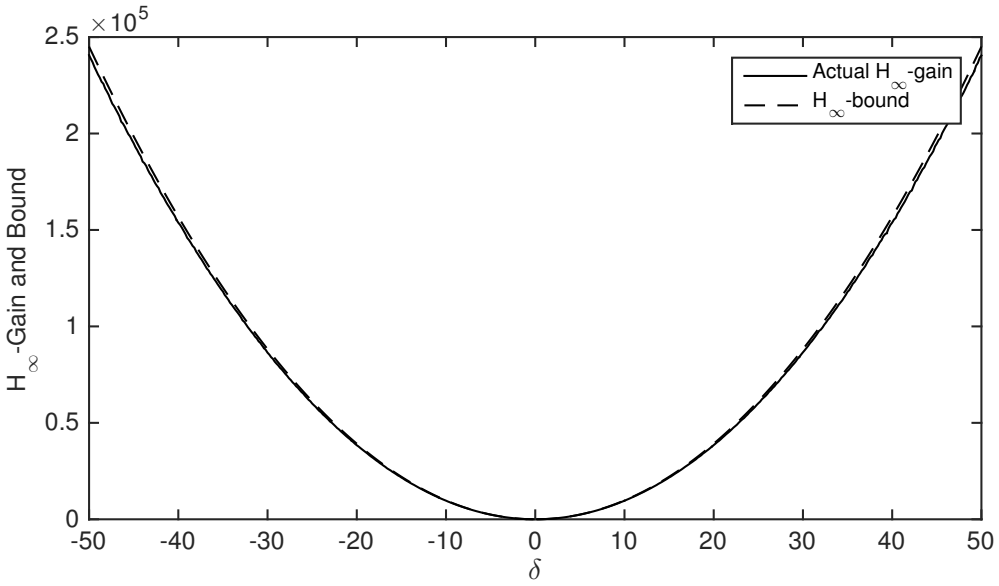

Figure 3.10: Co-plot of H_∞-gain and theoretical bound for a scalar system with a sinusoidal nonlinearity

Similar to the ratio analyzed in Chapter 2, the calculated H_∞-gain to the theoretical bound ratio has certain properties: 1) the ratio should be greater than zero and less than one and 2) the closer the ratio is to one, the less conservative the result. Figure 3.11 shows that the theoretical bound is very close to the H_∞-gain from simulation for all δ with the ratio remaining between 0.97 and 1.00 for this system. This ratio will be further analyzed to determine if this tightness in the bound is system dependent by studying second order systems.

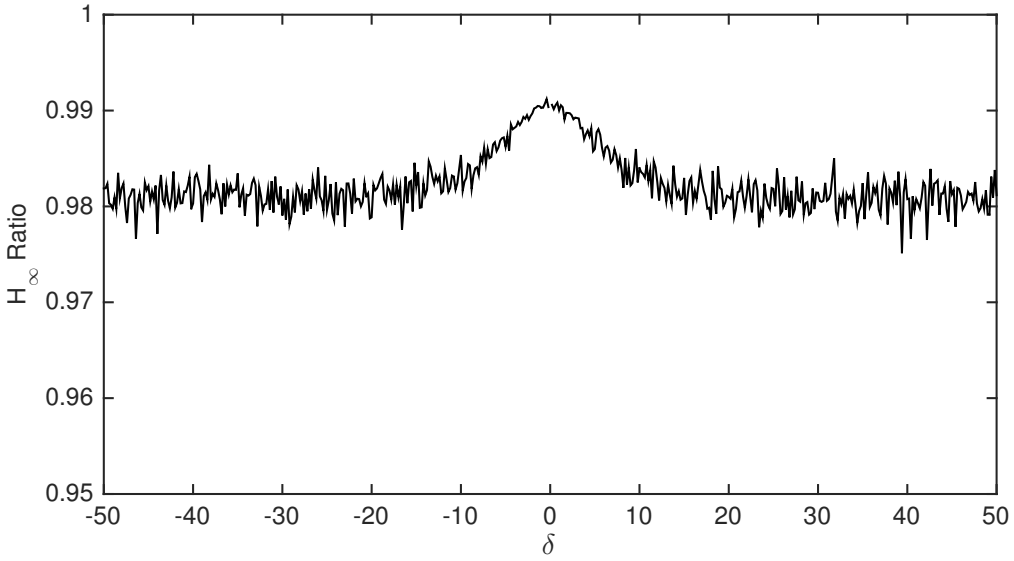

Figure 3.11: Ratio of H_∞-gain to theoretical bound for a scalar system with a sinusoidal nonlinearity

Second Order Systems with Various Nonlinearity Severities

As mentioned in the introduction to this section, various nonlinearity severities will now be analyzed. The nonlinearities from least severe to most severe are: sinusoidal, quadratic, and cubic. The severity of these nonlinearities is based on their first derivative. These systems are similar to the form given in Section 2.4, where the continuous-time system is defined as a

mass-spring-damper with a nonlinear spring

$$\ddot{y} = -b\dot{y} - f(y) \tag{3.47}$$

which is converted to state-space form, is discretized and has noise added to it as

$$x_{k+1} = \begin{bmatrix} 1 & \tau \\ 0 & (1-\tau b) \end{bmatrix} x_k + \begin{bmatrix} 0 \\ -\tau f(x_{1,k}) \end{bmatrix} + \delta \begin{bmatrix} 0.02 & 0.1 \\ 0 & 0.01 \end{bmatrix} w_k \tag{3.48}$$

$$y_k = \begin{bmatrix} 1 & 0 \end{bmatrix} x_k + \delta \begin{bmatrix} 0.1 & 0.1 \end{bmatrix} w_k \tag{3.49}$$

with $f(y) = \{sin(y), y^2, y^3\}$ used in the simulation, $b = 5$ is the damping coefficient, and $w_k \in \ell_2$. The disturbance multiplier, δ is swept from -1 to 1 in 0.01 increments and the ratio of the H_∞-gain from simulation to the theoretical bound is calculated using the method described earlier in this section.

Figure 3.12 shows that this ratio is smaller for these systems, implying that the bound is more conservative in these cases. Additionally, it is seen from Figure 3.12 that the least severe nonlinearity, the sinusoidal represented by the black line, has the most accurate bound out of the three nonlinearities studies.

3.5 Summary

The H_∞-property was shown for the discrete-time extended Kalman filter used as a nonlinear observer in the presence of random finite-energy disturbances. The H_2-property of the estimation error when the disturbance is absent follows as a special case of this result. Various simulation studies were performed to demonstrate convergence as well as H_∞. In the convergence simulations, it was seen that the estimation error would converge for relatively small initial error and disturbance magnitudes. A study on the validity and conservativeness of the H_∞-bound was performed on a scalar system and three second order systems with varying nonlinearity severities. The scalar system

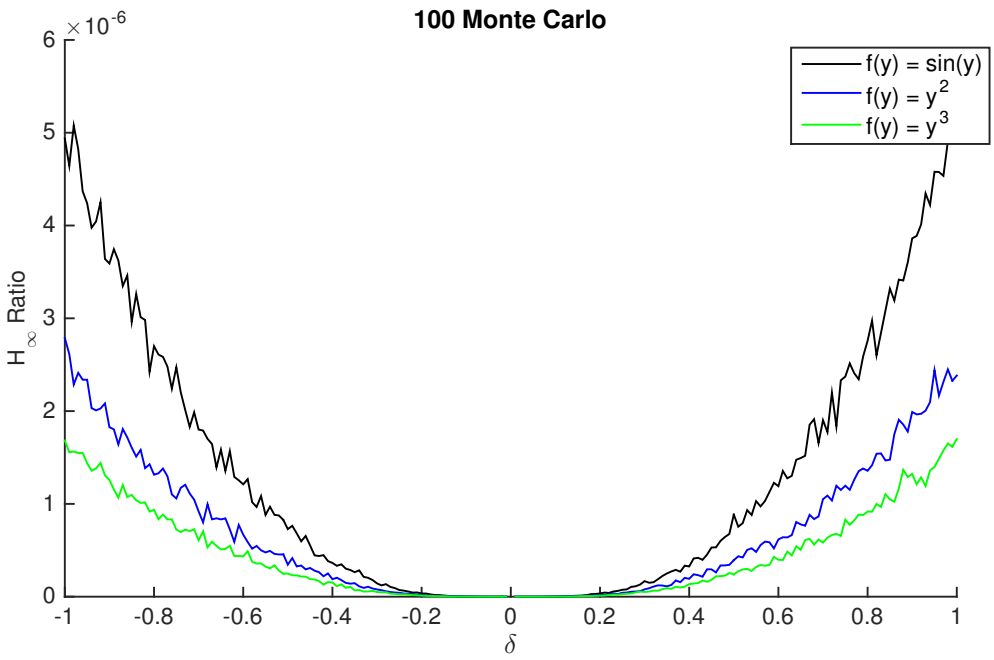

Figure 3.12: Three nonlinearities - Ratio of H_∞-gain to theoretical bound (100 run Monte Carlo)

simulation showed that the bound on the H_∞-gain is very tight. However, the additional simulations on second order systems show that the tightness of the bound is system dependent. The second order simulations also showed that for larger disturbance magnitudes, the least severe nonlinearity was the least conservative of the three studied. The following chapters will focus on the analysis of EKFs designed for the uncertain measurement model.

CHAPTER 4

H_∞-PROPERTY OF THE DISCRETE-TIME EXTENDED KALMAN FILTER FOR SYSTEMS WITH INDIVIDUALLY FAILING MEASUREMENTS

Recall the uncertain measurement model as described in Section 1.2.2 with an example shown in Figure 1.4, this is the model focused on in this chapter. A variation of the EKF that was designed for systems with zero mean, white noise and correlation between the process and measurement as well as uncertainty in the measurement has been analyzed for systems that have stochastic ℓ_2 type disturbances. It will be shown that this variation of the EKF has the finite-time H_∞-property. Simulations are provided that analyze the effect of the run time as well as various levels of nonlinearity severity.

4.1 System Description and the EKF as a Nonlinear Observer

Consider the nonlinear discrete-time system and measurement equations,

$$x_{k+1} = f(x_k) + F_k w_k \tag{4.1}$$

$$y_k = \Gamma_k h(x_k) + H_k w_k \tag{4.2}$$

where $x_k \in \Re^n$ is the state, $y_k \in \Re^p$ is the measurement, $f(x_k)$ and $h(x_k)$ are known analytic vector functions, the state and measurement disturbance coefficient matrices are $F_k \in \Re^{n\times l}$ and $H_k \in \Re^{p\times l}$, respectively, where the disturbance $w_k \in \Re^l$ is zero mean, white, and identity covariance resulting in $F_k F_k^T > 0$ as the process noise, $H_k H_k^T > 0$ as the measurement noise, and $F_k H_k^T$ as the correlation between the process and measurement noise. It is assumed that the measurement nonlinearity is uniformly bounded as $\|h(x)\| \leq \alpha_h$ for all $x \in \Re^n$. The coefficient matrix, Γ_k is of the form

$$\Gamma_k = diag(\gamma_k^1, \gamma_k^2, \ldots, \gamma_k^p) \tag{4.3}$$

where γ_k^i are Bernoulli random variables, taking values of 0 or 1, uncorrelated in time, representing whether sensor i contains data and noise or noise only. These Bernoulli random variables have known mean, $E\{\Gamma_k\} = \overline{\Gamma} = diag(\overline{\gamma}_i)$ for $i = 1, 2, \ldots, p$ and variance $E\{(\Gamma_k - \overline{\Gamma})(\Gamma_k - \overline{\Gamma})^T\} = diag(\overline{\gamma}_i(1 - \overline{\gamma}_i)) \triangleq \Upsilon$.

The EKF derived in this chapter is a modification of the resilient EKF developed in [23] for systems with correlation between the system state and measurement noise and without uncertainty in the gain. By the definition of the measurement model, when a measurement is received it is uncertain if each sensor is recording signal and noise or noise only. For this reason, the estimate uses only the statistical reliability information for the sensors or the mean of Γ_k and is computed as

$$\hat{x}_{k+1} = f(\hat{x}_k) + K_k(y_k - \overline{\Gamma}h(\hat{x}_k)) \tag{4.4}$$

where $K_k \in \Re^{n \times p}$ will be the minimum variance gain. Similarly, the nonlinearities are approximated using a Taylor Series expansion about the current estimate yielding

$$f(x_k) \cong f(\hat{x}_k) + A_k(x_k - \hat{x}_k) \tag{4.5}$$

$$h(x_k) \cong h(\hat{x}_k) + C_k(x_k - \hat{x}_k) \tag{4.6}$$

with the Jacobians defined as

$$A_k = \left.\frac{\partial f(x_k)}{\partial x}\right|_{x_k = \hat{x}_k} \tag{4.7}$$

$$C_k = \left.\frac{\partial h(x_k)}{\partial x}\right|_{x_k = \hat{x}_k} \tag{4.8}$$

The nonlinear observer error defined as the difference between the current state and the estimate,

$$e_k = x_k - \hat{x}_k \tag{4.9}$$

has the following dynamics

$$\begin{aligned} e_{k+1} &= x_{k+1} - \hat{x}_{k+1} \\ &= f(x_k) + F_k w_k - f(\hat{x}_k) - K_k(\Gamma_k h(x_k) + H_k w_k - \overline{\Gamma} h(\hat{x}_k)) \\ &= f(\hat{x}_k) + A_k e_k + F_k w_k - f(\hat{x}_k) - K_k(\Gamma_k h(\hat{x}_k) + \Gamma_k C_k e_k + H_k w_k - \overline{\Gamma} h(\hat{x}_k)) \end{aligned} \tag{4.10}$$

The difference between the actual Γ_k and the mean is defined as

$$\widetilde{\Gamma}_k \triangleq \Gamma_k - \overline{\Gamma} \tag{4.11}$$

which has zero mean and variance Υ. Using the definition in (4.11), cancelling terms, and collecting similar terms, (4.10) simplifies to

$$e_{k+1} \cong \mathcal{A}_k e_k + \mathcal{F}_k w_k - K_k \widetilde{\Gamma}_k h(\hat{x}_k) \tag{4.12}$$

with

$$\mathcal{A}_k = A_k - K_k \Gamma_k C_k \tag{4.13}$$

and

$$\mathcal{F}_k = F_k - K_k H_k \tag{4.14}$$

As a note, the initial estimate is generally chosen as the expected value of the state, $e_0 = x_0 - \overline{x}_0$; therefore, taking the expectation of the initial error results in $\overline{e}_0 = \overline{x}_0 - \overline{x}_0 = 0$. Since $E\{e_0\} = 0$, $E\{w_k\} = 0$, and $E\{\widetilde{\Gamma}_k\} = 0$, the expected value for the error is $E\{e_k\} = 0$, determined by taking the expectation of (4.12).

The goal of the EKF is to minimize the error covariance,

$$P_k = E\left\{e_k e_k^T\right\} \tag{4.15}$$

which is done through analysis of the error covariance dynamics

$$\begin{aligned} P_{k+1} &= E\left\{e_{k+1}e_{k+1}^T\right\} \\ &\cong E\left\{(\mathcal{A}_k e_k + \mathcal{F}_k w_k - K_k\widetilde{\Gamma}_k h(\hat{x}_k))(\mathcal{A}_k e_k + \mathcal{F}_k w_k - K_k\widetilde{\Gamma}_k h(\hat{x}_k))^T\right\} \\ &= E\left\{\begin{array}{c} \mathcal{A}_k e_k e_k^T\mathcal{A}_k^T + \mathcal{A}_k e_k w_k^T\mathcal{F}_k^T + \mathcal{A}_k e_k h^T(\hat{x}_k)\widetilde{\Gamma}_k^T K_k^T \\ +\mathcal{F}_k w_k e_k^T\mathcal{A}_k^T + \mathcal{F}_k w_k w_k^T\mathcal{F}_k^T + \mathcal{F}_k w_k h^T(\hat{x}_k)\widetilde{\Gamma}_k^T K_k^T \\ +K_k\widetilde{\Gamma}_k h(\hat{x}_k)e_k^T\mathcal{A}_k^T + K_k\widetilde{\Gamma}_k h(\hat{x}_k)w_k^T\mathcal{F}_k^T + K_k\widetilde{\Gamma}_k h(\hat{x}_k)h^T(\hat{x}_k)\widetilde{\Gamma}_k^T K_k^T \end{array}\right\} \end{aligned} \tag{4.16}$$

The expectation operator is linear, therefore it can be applied separately to each term while also removing known terms from the expectation operation

$$\begin{aligned} P_{k+1} \cong & E\left\{\mathcal{A}_k e_k e_k^T\mathcal{A}_k^T\right\} + E\left\{\mathcal{A}_k e_k w_k^T\right\}\mathcal{F}_k^T + E\left\{\mathcal{A}_k e_k h^T(\hat{x}_k)\widetilde{\Gamma}_k^T\right\}K_k^T \\ & + \mathcal{F}_k E\left\{w_k e_k^T\mathcal{A}_k^T\right\} + \mathcal{F}_k E\left\{w_k w_k^T\right\}\mathcal{F}_k^T + \mathcal{F}_k E\left\{w_k h^T(\hat{x}_k)\widetilde{\Gamma}_k^T\right\}K_k^T \\ & + K_k E\left\{\widetilde{\Gamma}_k h(\hat{x}_k)e_k^T\mathcal{A}_k^T\right\} + K_k E\left\{\widetilde{\Gamma}_k h(\hat{x}_k)w_k^T\right\}\mathcal{F}_k^T + K_k E\left\{\widetilde{\Gamma}_k h(\hat{x}_k)h^T(\hat{x}_k)\widetilde{\Gamma}_k^T\right\}K_k^T \end{aligned} \tag{4.17}$$

The first term is simplified by applying the definition of the error covariance,

$$E\left\{\mathcal{A}_k e_k e_k^T\mathcal{A}_k^T\right\} = E\left\{\mathcal{A}_k P_k\mathcal{A}_k^T\right\} \tag{4.18}$$

Terms two, three, four, six, seven, and eight in (4.17) are zero due to w_k, e_k, and $\widetilde{\Gamma}_k$ being uncorrelated and having zero mean. Term five is simplified by applying the definition of identity covariance for the noise,

$$\mathcal{F}_k\overline{w_k w_k^T}\mathcal{F}_k^T = \mathcal{F}_k\mathcal{F}_k^T \tag{4.19}$$

These simplifications result in

$$P_{k+1} \cong \overline{\mathcal{A}_k P_k\mathcal{A}_k} + \mathcal{F}_k\mathcal{F}_k^T + K_k\overline{\widetilde{\Gamma}_k h(\hat{x}_k)h^T(\hat{x}_k)\widetilde{\Gamma}_k^T}K_k^T \tag{4.20}$$

which will be the form used during analysis; however, the EKF should be designed in terms of known values, so further simplifications are necessary.

To further analyze the error covariance dynamics in terms of known variables such as $\overline{\Gamma}$, the remaining terms will be processed individually. The first term of (4.20) is expanded using (4.11) and (4.13) as

$$\begin{aligned}\overline{\mathcal{A}_k P_k \mathcal{A}_k^T} &= \overline{(A_k - K_k\overline{\Gamma}C_k - K_k\widetilde{\Gamma}_k C_k)P_k(A_k - K_k\overline{\Gamma}C_k - K_k\widetilde{\Gamma}_k C_k)^T} \\ &= (A_k - K_k\overline{\Gamma}C_k)P_k(A_k - K_k\overline{\Gamma}C_k)^T - (A_k - K_k\overline{\Gamma}C_k)\overline{P_k C_k^T\widetilde{\Gamma}_k^T}K_k^T \\ &- K_k\overline{\widetilde{\Gamma}_k C_k P_k}(A_k - K_k\overline{\Gamma}C_k)^T + K_k\overline{\widetilde{\Gamma}_k C_k P_k C_k^T\widetilde{\Gamma}_k^T}K_k^T\end{aligned} \tag{4.21}$$

Since the estimation error, e_k and $\widetilde{\Gamma}_k$ are uncorrelated, the expectation of their product is equal to the product of their expectations,

$$\overline{\mathcal{A}_k P_k \mathcal{A}_k^T} = \mathbb{A}_k P_k \mathbb{A}_k^T - \mathbb{A}_k P_k C_k^T\overline{\widetilde{\Gamma}_k}^T K_k^T - K_k\overline{\widetilde{\Gamma}_k}C_k P_k\mathbb{A}_k + K_k\overline{\widetilde{\Gamma}_k C_k P_k C_k^T\widetilde{\Gamma}_k^T}K_k^T \tag{4.22}$$

where

$$\mathbb{A}_k \triangleq A_k - K_k\overline{\Gamma}C_k \tag{4.23}$$

and, as mentioned previously, $\widetilde{\Gamma}_k$ is zero mean, resulting in

$$\overline{\mathcal{A}_k e_k e_k^T \mathcal{A}_k^T} = \mathbb{A}_k P_k \mathbb{A}_k^T + K_k\overline{\widetilde{\Gamma}_k C_k P_k C_k^T\widetilde{\Gamma}_k^T}K_k^T \tag{4.24}$$

Substituting (4.24) into (4.20) and grouping terms yields

$$P_{k+1} \cong \mathbb{A}_k P_k \mathbb{A}_k^T + \mathcal{F}_k\mathcal{F}_k^T + K_k\overline{\widetilde{\Gamma}_k(C_k P_k C_k^T + h(\hat{x}_k)h^T(\hat{x}_k))\widetilde{\Gamma}_k^T}K_k^T \tag{4.25}$$

Corollary 7.1 can be applied to the third term of (4.25) as

$$P_{k+1} \cong \mathbb{A}_k P_k \mathbb{A}_k^T + \mathcal{F}_k\mathcal{F}_k^T + K_k(\Upsilon \circ (C_k P_k C_k^T + h(\hat{x}_k)h^T(\hat{x}_k)))K_k^T \tag{4.26}$$

To minimize the error covariance over the gain, K_k, (4.26) is expanded to obtain the form for use with Lemma 1

$$\begin{aligned}P_{k+1} \cong & A_k P_k A_k^T - A_k P_k C_k^T\overline{\Gamma}^T K_k^T - K_k\overline{\Gamma}C_k P_k A_k^T + K_k\overline{\Gamma}C_k P_k C_k^T\overline{\Gamma}^T K_k^T + F_k F_k^T \\ & - F_k H_k^T K_k^T - K_k H_k F_k^T + K_k H_k H_k^T K_k^T + K_k(\Upsilon \circ (C_k P_k C_k^T + h(\hat{x}_k)h^T(\hat{x}_k)))K_k^T\end{aligned} \tag{4.27}$$

followed by grouping terms with respect to K_k which yields

$$P_{k+1} \cong A_k P_k A_k^T + F_k F_k^T - (A_k P_k C_k^T \overline{\Gamma}^T + F_k H_k^T) K_k^T - K_k (\overline{\Gamma} C_k P_k A_k^T + H_k F_k^T) \quad (4.28)$$
$$+ K_k \left(\Upsilon \circ (C_k P_k C_k^T + h(\hat{x}_k) h^T(\hat{x}_k)) + \overline{\Gamma} C_k P_k C_k^T \overline{\Gamma}^T + H_k H_k^T \right) K_k^T$$

Recognizing that (4.28) is now of the form in Lemma 1 where the corresponding terms are

$$A = \Upsilon \circ (C_k P_k C_k^T + h(\hat{x}_k) h^T(\hat{x}_k)) + \overline{\Gamma} C_k P_k C_k^T \overline{\Gamma}^T + H_k H_k^T \quad (4.29)$$

$$B = -(A_k P_k C_k^T \overline{\Gamma}^T + F_k H_k^T)^T \quad (4.30)$$

$$C = A_k P_k A_k^T + F_k F_k^T \quad (4.31)$$

$$D = P_{k+1} \quad (4.32)$$

$$X = K_k \quad (4.33)$$

so that applying Lemma 1 to (4.28) results in the locally optimal gain that minimizes (4.28),

$$K_k = (A_k P_k C_k^T \overline{\Gamma}^T + F_k H_k^T) \times \quad (4.34)$$
$$(\Upsilon \circ (C_k P_k C_k^T + h(\hat{x}_k) h^T(\hat{x}_k)) + \overline{\Gamma} C_k P_k C_k^T \overline{\Gamma}^T + H_k H_k^T)^{-1}$$

Therefore, the extended Kalman filter for the system in (4.1) and (4.2) is defined by the following

- State estimate

$$\hat{x}_{k+1} = f(\hat{x}_k) + K_k (y_k - \overline{\Gamma} h(\hat{x}_k)) \quad (4.35)$$

- Kalman Gain

$$K_k = (A_k P_k C_k^T \overline{\Gamma}^T + F_k H_k^T) \times \quad (4.36)$$
$$(\Upsilon \circ (C_k P_k C_k^T + h(\hat{x}_k) h^T(\hat{x}_k)) + \overline{\Gamma} C_k P_k C_k^T \overline{\Gamma}^T + H_k H_k^T)^{-1}$$

- Riccati Difference Equation

$$P_{k+1} = \mathbb{A}_k P_k \mathbb{A}_k^T + \mathcal{F}_k \mathcal{F}_k^T + K_k(\Upsilon \circ (C_k P_k C_k^T + h(\hat{x}_k)h^T(\hat{x}_k)))K_k^T \tag{4.37}$$

or equivalently

$$P_{k+1} = \overline{\mathcal{A}_k P_k \mathcal{A}_k} + \mathcal{F}_k \mathcal{F}_k^T + K_k \overline{\widetilde{\Gamma}_k h(\hat{x}_k) h^T(\hat{x}_k) \widetilde{\Gamma}_k^T} K_k^T \tag{4.38}$$

where

$$\mathbb{A}_k = A_k - K_k \overline{\Gamma}_k C_k \tag{4.39}$$

$$\mathcal{A}_k = A_k - K_k \Gamma_k C_k \tag{4.40}$$

$$\mathcal{F}_k = F_k - K_k H_k \tag{4.41}$$

with $\mathcal{F}_k \mathcal{F}_k^T > 0$ and A_k and C_k in (4.7) and (4.8), respectively.

4.2 Convergence Analysis of EKF Used on Systems with Uncertain Measurements and Finite Energy Noise

Consider the nonlinear discrete-time system and measurement equations,

$$x_{k+1} = f(x_k) + F_k w_k \tag{4.42}$$

$$y_k = \Gamma_k h(x_k) + H_k w_k \tag{4.43}$$

where $w_k \in \ell_2$ is now zero mean, identity covariance, uncorrelated in time, and finite-energy. The coefficient matrix, Γ_k is still of the form

$$\Gamma_k = diag(\gamma_k^1, \gamma_k^2, \ldots, \gamma_k^p) \tag{4.44}$$

where γ_k^i are Bernoulli random variables, taking values of 0 or 1, uncorrelated in time, representing whether sensor i contains data and noise or noise only. These Bernoulli random variables have known mean, $E\{\Gamma_k\} = \overline{\Gamma} = diag(\overline{\gamma}_i)$ for

$i = 1, 2, \ldots, p$ and variance $E\{(\Gamma_k - \overline{\Gamma})(\Gamma_k - \overline{\Gamma})^T\} = diag(\overline{\gamma}_i(1 - \overline{\gamma}_i)) \triangleq \Upsilon$. With the error defined in (4.9), the error dynamics are

$$e_{k+1} = \mathcal{A}_k e_k + \mathcal{F}_k w_k - K_k \widetilde{\Gamma}_k h(\hat{x}_k) \tag{4.45}$$

with $\mathcal{A}_k$ and $\mathcal{F}_k$ in (4.13) and (4.14).

Assumption 4.1. *The pair (A_k, C_k) is uniformly observable, with $\|A_k\|_i \leq \bar{a}$, $\|C_k\|_i \leq \bar{c}$, $\|F_k\|_i \leq \bar{f}$, $\|H_k\|_i \leq \bar{h}$, and $\|h(x_k)\| \leq \alpha_h$ uniformly bounded in time.*

Theorem 4.1. *Consider the nonlinear system* (4.42) *and measurement equation* (4.43)*, with uncertain measurements, the noise taken as an element of stochastic ℓ_2 and $\mathcal{F}_k \mathcal{F}_k^T > 0$ with $\mathcal{F}_k$ in* (4.14)*. Let the state be estimated using an extended Kalman filter based on this model, which was designed for white noise with zero mean and identity covariance, with gain K_k from* (4.36)*. With Assumption 4.1, Lemma 6 holds. With these conditions, the energy of the estimation error is finite-time bounded, for any integer $0 < T < \infty$, as follows*

$$\sum_{k=0}^{T} \overline{\|e_k\|^2} \leq \frac{1}{\varphi_1} \left(\overline{e_0^T P_0^{-1} e_0} + \varphi_2 \sum_{k=0}^{T} \overline{\|w_k\|^2} + \varphi_3 (T+1) \right) \tag{4.46}$$

where

$$\varphi_1 \triangleq \inf_k (\lambda_{min}(P_k^{-1} - \overline{\mathcal{A}_k^T P_{k+1}^{-1} \mathcal{A}_k})) \tag{4.47}$$

$$\varphi_2 \triangleq \sup_k (\lambda_{max}(\mathcal{F}_k^T P_{k+1}^{-1} \mathcal{F}_k)) \tag{4.48}$$

$$\varphi_3 \triangleq \sup_k (\lambda_{max}(h^T(\hat{x}_k) \overline{\widetilde{\Gamma}_k^T K_k^T P_{k+1}^{-1} K_k \widetilde{\Gamma}_k} h(\hat{x}_k))) \tag{4.49}$$

Proof. With Assumption 4.1, Lemma 6 states that the solution to the Riccati equation, P_k, and the Kalman gain, K_k, are uniformly upper and lower bounded, which is essential throughout the proof. Stochastic Lyapunov analysis is used to

determine the stability of the estimation error and obtain the finite-time H_∞-gain. The Lyapunov function candidate,

$$V_k = e_k^T P_k^{-1} e_k \tag{4.50}$$

is analyzed along the dynamics of the error (4.45) to verify that the average energy decreases over time. To this end, consider the following stochastic Lyapunov difference

$$\begin{aligned} &E\{V_{k+1}|e_k, e_{k-1}, \dots\} - V_k \\ &= E\{e_{k+1}^T P_{k+1}^{-1} e_{k+1}|e_k, e_{k-1}, \dots\} - e_k^T P_k^{-1} e_k < 0 \end{aligned} \tag{4.51}$$

With substitution from (4.45), the inequality in (4.51) when expanded is

$$\begin{aligned} &- e_k^T \left(P_k^{-1} - \overline{\mathcal{A}_k^T P_{k+1}^{-1} \mathcal{A}_k}\right) e_k + 2\overline{w_k^T \mathcal{F}_k^T P_{k+1}^{-1} \mathcal{A}_k} e_k \\ &- 2\overline{h^T(\hat{x}_k)\widetilde{\Gamma}_k^T K_k^T P_{k+1}^{-1} \mathcal{A}_k} e_k + \overline{w_k^T \mathcal{F}_k^T P_{k+1}^{-1} \mathcal{F}_k w_k} \\ &- 2\overline{\widetilde{\Gamma}_k h^T(\hat{x}_k) K_k^T P_{k+1}^{-1} \mathcal{F}_k w_k} \\ &+ \overline{h^T(\hat{x}_k)\widetilde{\Gamma}_k K_k^T P_{k+1}^{-1} K_k \widetilde{\Gamma}_k h(\hat{x}_k)} < 0 \end{aligned} \tag{4.52}$$

Because $\mathcal{F}_k$, $\mathcal{A}_k$, $\hat{x}_k$, and therefore e_k, P_k and K_k are functions of w_{k-1} and Γ_{k-1} and since w_k and Γ_k are uncorrelated in time and w_k is zero mean, the second and fifth terms can be rewritten so that (4.52) becomes

$$\begin{aligned} &- e_k^T \left(P_k^{-1} - \overline{\mathcal{A}_k^T P_{k+1}^{-1} \mathcal{A}_k}\right) e_k + 2\overline{w_k^T} \left(\overline{\mathcal{F}_k^T P_{k+1}^{-1} \mathcal{A}_k}\right) e_k \\ &- 2\overline{h^T(\hat{x}_k)\widetilde{\Gamma}_k^T K_k^T P_{k+1}^{-1} \mathcal{A}_k} e_k + \overline{w_k^T \mathcal{F}_k^T P_{k+1}^{-1} \mathcal{F}_k w_k} \\ &- 2\left(\overline{h^T(\hat{x}_k)\widetilde{\Gamma}_k^T K_k^T P_{k+1}^{-1} \mathcal{F}_k}\right) \overline{w_k} \\ &+ \overline{h^T(\hat{x}_k)\widetilde{\Gamma}_k^T K_k^T P_{k+1}^{-1} K_k \widetilde{\Gamma}_k h(\hat{x}_k)} < 0 \end{aligned} \tag{4.53}$$

leading to

$$\begin{aligned} &- e_k^T \left(P_k^{-1} - \overline{\mathcal{A}_k^T P_{k+1}^{-1} \mathcal{A}_k}\right) e_k - 2\overline{h^T(\hat{x}_k)\widetilde{\Gamma}_k^T K_k^T P_{k+1}^{-1} \mathcal{A}_k} e_k \\ &+ \overline{w_k^T \mathcal{F}_k^T P_{k+1}^{-1} \mathcal{F}_k w_k} + \overline{h^T(\hat{x}_k)\widetilde{\Gamma}_k^T K_k^T P_{k+1}^{-1} K_k \widetilde{\Gamma}_k h(\hat{x}_k)} < 0 \end{aligned} \tag{4.54}$$

To ensure (4.54) is negative, the development for an overall upper bound is provided next. The first term is lower bounded using Lemma 3

$$-\varphi_1 e_k^T e_k - 2\overline{h^T(\hat{x}_k)\widetilde{\Gamma}_k^T K_k^T P_{k+1}^{-1}\mathcal{A}_k e_k} + \overline{w_k^T \mathcal{F}_k^T P_{k+1}^{-1}\mathcal{F}_k w_k} + \overline{h^T(\hat{x}_k)\widetilde{\Gamma}_k^T K_k^T P_{k+1}^{-1} K_k \widetilde{\Gamma}_k h(\hat{x}_k)} < 0 \tag{4.55}$$

with φ_1 defined in (4.47). Such a φ_1 always exists, if for all $k = 0, 1, 2, \ldots$

$$P_k^{-1} - \mathcal{A}_k^T P_{k+1}^{-1}\mathcal{A}_k > 0 \tag{4.56}$$

The inequality in (4.56) is shown by using Lemma 4 resulting in the following conditions being equivalent

$$\begin{bmatrix} P_k^{-1} & \mathcal{A}_k^T \\ \mathcal{A}_k & P_{k+1} \end{bmatrix} > 0 \tag{4.57}$$

$$\mathcal{A}_k P_k \mathcal{A}_k^T + \mathcal{F}_k \mathcal{F}_k^T + K_k \widetilde{\Gamma}_k h(\hat{x}_k) h^T(\hat{x}_k) \widetilde{\Gamma}_k K_k^T - \mathcal{A}_k P_k \mathcal{A}_k^T > 0 \tag{4.58}$$

with $\mathcal{F}_k \mathcal{F}_k^T > 0$ and $K_k \widetilde{\Gamma}_k h(\hat{x}_k) h^T(\hat{x}_k) \widetilde{\Gamma}_k^T K_k^T \geq 0$, therefore, for all $k = 0, 1, 2, \ldots$

$$P_k^{-1} - \overline{\mathcal{A}_k^T P_{k+1}^{-1}\mathcal{A}_k} > 0 \tag{4.59}$$

To obtain an upper bound on the third term in (4.55), it is shown that for all $k = 0, 1, 2, \ldots$

$$\mathcal{F}_k^T P_{k+1}^{-1}\mathcal{F}_k \leq I_l \tag{4.60}$$

by using Lemma 4 and using (4.14), the following conditions are equivalent to (4.60)

$$\begin{bmatrix} I_l & \mathcal{F}_k^T \\ \mathcal{F}_k & P_{k+1} \end{bmatrix} \geq 0 \tag{4.61}$$

$$\mathcal{A}_k P_k \mathcal{A}_k^T + \mathcal{F}_k \mathcal{F}_k^T + K_k \widetilde{\Gamma}_k h(\hat{x}_k) h^T(\hat{x}_k) \widetilde{\Gamma}_k^T K_k^T - \mathcal{F}_k \mathcal{F}_k^T \geq 0 \tag{4.62}$$

which agrees with

$$\mathcal{A}_k P_k \mathcal{A}_k^T + K_k \widetilde{\Gamma}_k h(\hat{x}_k) h^T(\hat{x}_k) \widetilde{\Gamma}_k^T K_k^T \geq 0 \tag{4.63}$$

Therefore, it has been shown that I_l is a valid upper bound as shown in (4.60) and Lemma 3 can be applied, resulting in φ_2 in (4.48) which is guaranteed to be bounded.

Using this same technique, the fourth term is bounded by

$$h^T(\hat{x}_k) \widetilde{\Gamma}_k^T K_k^T P_{k+1}^{-1} K_k \widetilde{\Gamma}_k h(\hat{x}_k) \leq 1 \tag{4.64}$$

and Lemma 3 can be applied, resulting in φ_3 in (4.49) which is guaranteed to be bounded. These bounds result in

$$-\varphi_1 e_k^T e_k - 2\overline{h^T(\hat{x}_k) \widetilde{\Gamma}_k^T K_k^T P_{k+1}^{-1} \mathcal{A}_k e_k} + \varphi_2 \overline{w_k^T w_k} + \varphi_3 < 0 \tag{4.65}$$

Lastly, taking the expected value of (4.65) and using Lemma 5 results in

$$-\varphi_1 \overline{e_k^T e_k} - 2\overline{h^T(\hat{x}_k) \widetilde{\Gamma}_k^T K_k^T P_{k+1}^{-1} \mathcal{A}_k} \, (\overline{e_k}) + \varphi_2 \overline{w_k^T w_k} + \varphi_3 < 0 \tag{4.66}$$

Due to the unbiasedness, $E\{e_k\} = 0$, $k \geq 0$, of the estimator by design, (4.66) can be further reduced to

$$\overline{V_{k+1}} - \overline{V_k} < -\varphi_1 \overline{e_k^T e_k} + \varphi_2 \overline{w_k^T w_k} + \varphi_3 < 0 \tag{4.67}$$

To obtain the finite-time H_∞-property, the ratio of the estimation error energy to the disturbance energy is analyzed; the summation of (4.67) is taken from $k = 0$ to $k = T$ (for any integer $0 < T < \infty$) giving

$$\overline{V_T} - \overline{V_0} < -\varphi_1 \sum_{k=0}^{T} \overline{\|e_k\|^2} + \varphi_2 \sum_{k=0}^{T} \overline{\|w_k\|^2} + \varphi_3 (T+1) \tag{4.68}$$

and for $\overline{V_T} \geq 0$,

$$-\overline{V_0} < -\varphi_1 \sum_{k=0}^{T} \overline{\|e_k\|^2} + \varphi_2 \sum_{k=0}^{T} \overline{\|w_k\|^2} + \varphi_3 (T+1) \tag{4.69}$$

which is rearranged as

$$\sum_{k=0}^{T} \overline{\|e_k\|^2} < \frac{1}{\varphi_1} \left(\overline{V_0} + \varphi_2 \sum_{k=0}^{T} \overline{\|w_k\|^2} + \varphi_3 (T+1) \right) \tag{4.70}$$

This result indicates that the energy of the estimation error has an upper bound proportional to the initial estimation error, $\overline{V_0} = \overline{e_0^T P_0^{-1} e_0}$, the disturbance energy, $\sum_{k=0}^{T} \overline{\|w_k\|^2}$, and a linear function of time, where the proportionality constants φ_1, φ_2 and φ_3 are defined in (4.47), (4.48), and (4.49). ■

4.3 Significance

To consider the finite-time H_∞ property of the EKF in this chapter, the result (4.70) is taken as

$$\sum_{k=0}^{T} \overline{\|e_k\|^2} < \frac{\varphi_2}{\varphi_1} \sum_{k=0}^{T} \overline{\|w_k\|^2} \tag{4.71}$$

for any integer $0 < T < \infty$, where φ_1 and φ_2 are defined in (4.47) and (4.48).

On the other hand, if there is no noise in the system for $k = 0, 1, 2, \ldots$, then (4.70) is taken as a special case that presents a bound on the estimation error energy in terms of the initial conditions, $\overline{V_0} = \overline{e_0^T P_0^{-1} e_0}$, i.e. the finite-time H_2-property of the EKF

$$\sum_{k=0}^{T} \overline{\|e_k\|^2} < \frac{1}{\varphi_1} \overline{V_0} \tag{4.72}$$

4.4 Simulations

Two studies are performed similar to those in the previous chapter. First, the effect of initial conditions and disturbance magnitude on the convergence of the error is analyzed. It is shown that for small initial error and small disturbance magnitudes, the estimation error will converge. On the other hand, for large initial error or large disturbance magnitudes, the estimation error will diverge. In addition to these three cases, the initial error is held constant while the

disturbance magnitude is varied and the resulting H_∞-bound is calculated. The other study analyzes the H_∞-property of three second order nonlinear systems with varying levels of severity. These systems have a variable disturbance multiplier that is utilized to observe how different disturbance magnitudes affect the H_∞-gain and bound. Simulations are performed to analyze both the effects of the run time, T, as well as severity of the nonlinearity by plotting the ratio between the H_∞-gain from simulation to the theoretical bound. This ratio gives insight into both the validity and the degree of conservativeness of our result. To reduce the effect of outliers in the stochastic data, a 100 run Monte Carlo simulation is used for each case study.

The systems in this section are similar to those of the form given in Section 2.4, shown here for convenience, where the continuous-time system is defined as

$$\ddot{y} = -f(y) \tag{4.73}$$

which is converted to state-space form, is discretized and has noise added to it as

$$x_{k+1} = \begin{bmatrix} 1 & \tau \\ 0 & 1 \end{bmatrix} x_k + \begin{bmatrix} 0 \\ -\tau f(x_{1,k}) \end{bmatrix} + \delta \begin{bmatrix} 0.02 & 0.1 \\ 0 & 0.01 \end{bmatrix} w_k \tag{4.74}$$

$$y_k = \Gamma_k \begin{bmatrix} x_{1,k} \\ x_{2,k} \end{bmatrix} + \delta \begin{bmatrix} 0.1 & 0.1 \\ 0 & 0.001 \end{bmatrix} w_k \tag{4.75}$$

In the first simulation study, the system will have a quadratic nonlinearity, $f(y) = y^2$, which will be simulated with three combinations of initial error and disturbance magnitude. In the second study, the nonlinearity in the system will vary as $f(y) = \{sin(y), y^2, y^3\}$. Each of these three nonlinear systems will be simulated with the run time varying and then the run time will be held constant while the three nonlinear systems are compared.

4.4.1 Effect of Initial Conditions and Disturbance Magnitude

Consider the system given in the introduction of this section with

$$f(y) = y^2 \tag{4.76}$$

$$x_0 = \begin{bmatrix} 0.2 & 0.5 \end{bmatrix}^T \tag{4.77}$$

where $\tau = 0.01s$ is the sampling time, $T = 30$ is the run time, $\overline{\Gamma} = 0.9 * I_2$ is the Bernoulli random variable statistics, and $w_k \in \ell_2$ is the finite-energy disturbance. Three different cases are simulated as shown in Table 4.1 along with a qualitative finite-time convergence analysis and H_∞ calculations. Each case is discussed in further detail below. To determine if a time response is finite-time bounded, the error magnitude is considered bounded if $|e_{i,k}| < 15$ for all integer $k \geq 0$ and $i = 1, 2$.

Table 4.1: Effect of initial values and disturbance magnitude

	Case 1	**Case 2**	**Case 3**
$\hat{x}_0$	$[-1.8\ ,\ 2.5]^T$	$[-1.8\ ,\ 2.5]^T$	$[14.2\ ,\ -13.5]^T$
δ	5	100	5
Error Boundedness	Within bounded	Exceeds bound	Exceeds bound
H_∞-Gain	0.8307	—	—
Figures	4.1, 4.2, 4.3	4.4, 4.5, 4.6	4.7, 4.8, 4.9

Case 1 considers a system with small error in the initial estimate along with small disturbance magnitudes, which results in a finite-time bounded response of

the error. Figures 4.1 and 4.2 show that the estimate tracks the actual state well throughout the run time, which corresponds to the bounded error in Figure 4.3.

Case 2 consists of small error with large disturbance magnitude, where the state and estimate time responses are shown in Figures 4.4 and 4.5. Again, the estimate appears to be tracking the state relatively well; however, analyzing the estimation error in Figure 4.6 shows that it does not remain within the defined bound.

The last case considered has a large initial estimation error and a small disturbance magnitude. The time responses in Figures 4.7, 4.8, and 4.9 show that even though the system ends with a small estimation error, the error corresponding to $x_{1,k}$ increases up to and above the defined bound during the first four time steps. Through this study, it was observed that the initial estimation error and the disturbance magnitudes play a role in the finite-time bound on the estimation error as signified in the main result of this chapter.

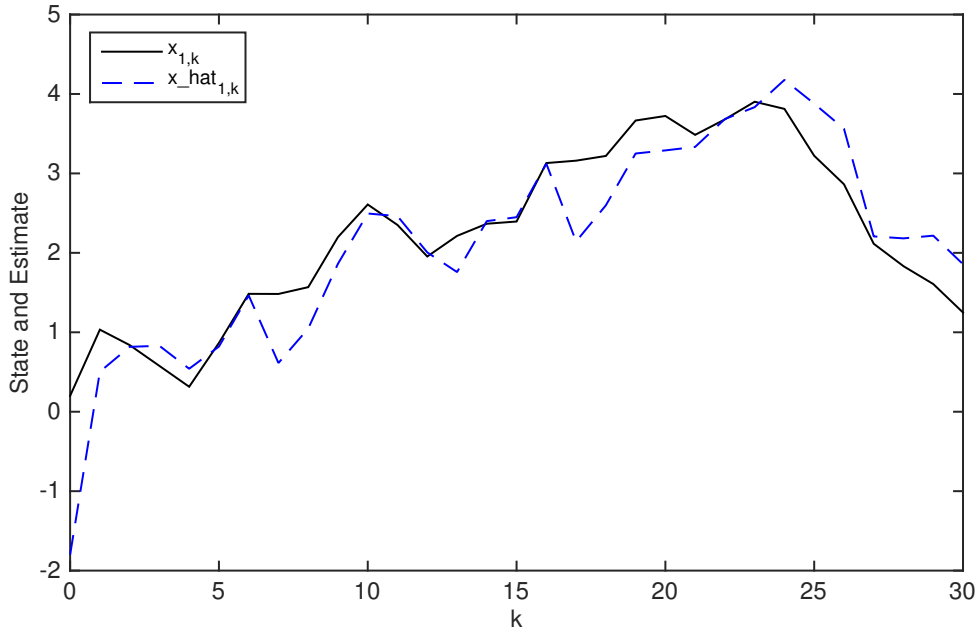

Figure 4.1: Quadratic nonlinearity, Case 1 - State, $x_{1,k}$, and estimate, $\hat{x}_{1,k}$

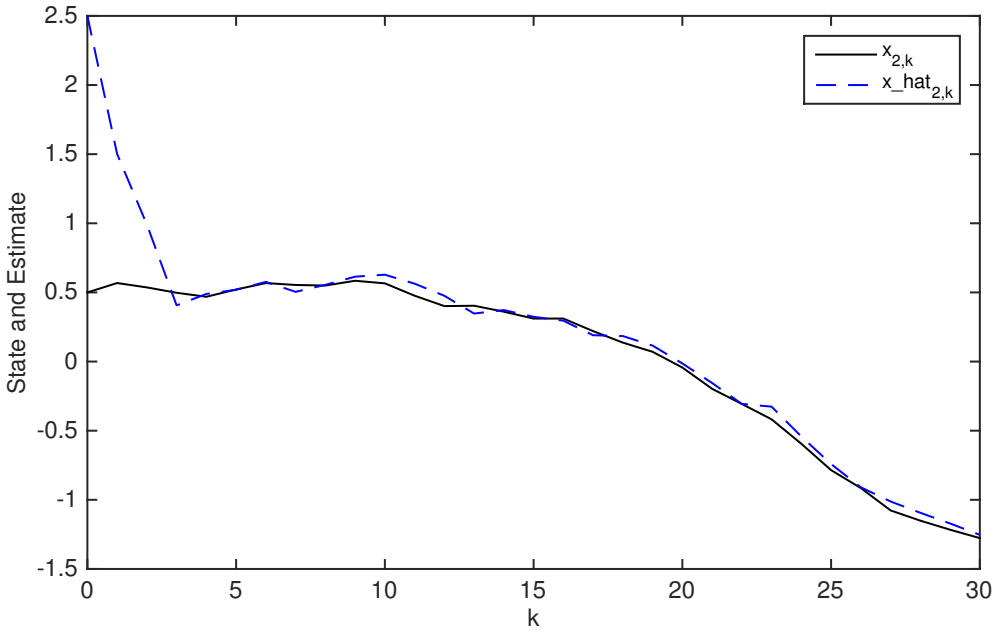

Figure 4.2: Quadratic nonlinearity, Case 1 - State, $x_{2,k}$, and estimate, $\hat{x}_{2,k}$

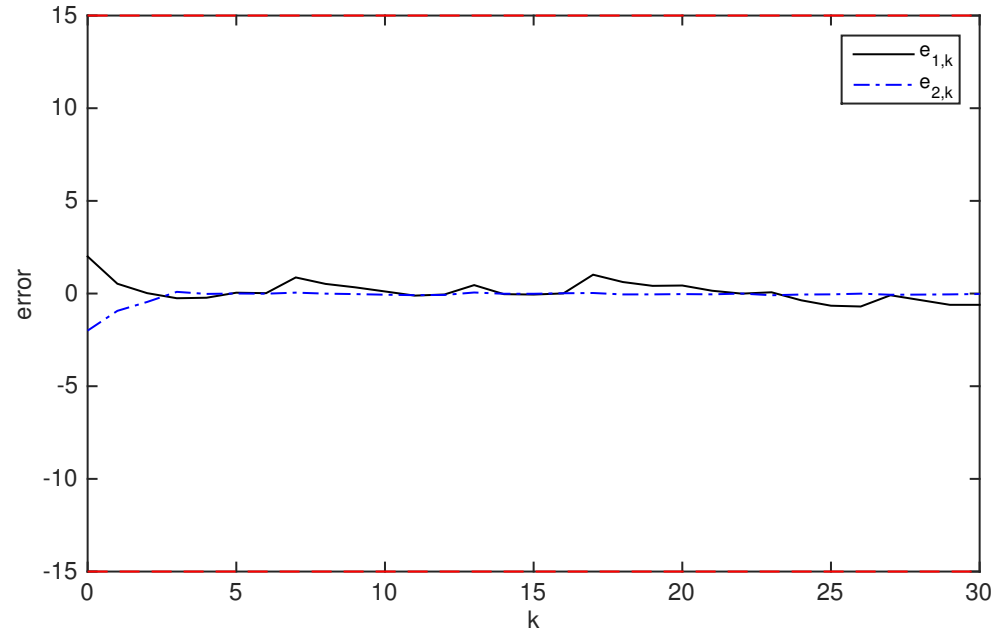

Figure 4.3: Quadratic nonlinearity, Case 1 - Estimation error, $e_{1,k}$ and $e_{2,k}$

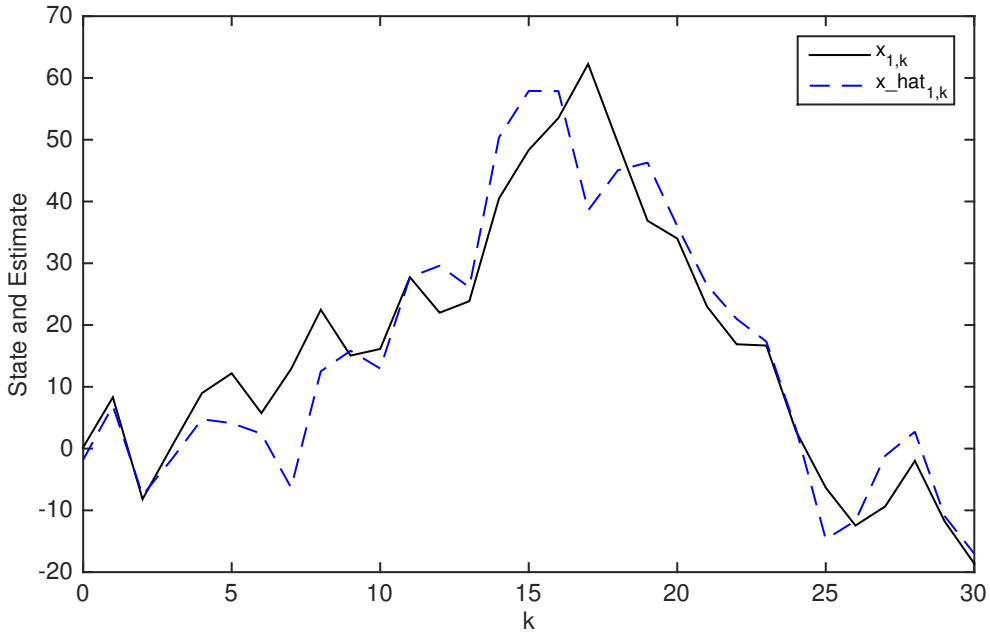

Figure 4.4: Quadratic nonlinearity, Case 2 - State, $x_{1,k}$, and estimate, $\hat{x}_{1,k}$

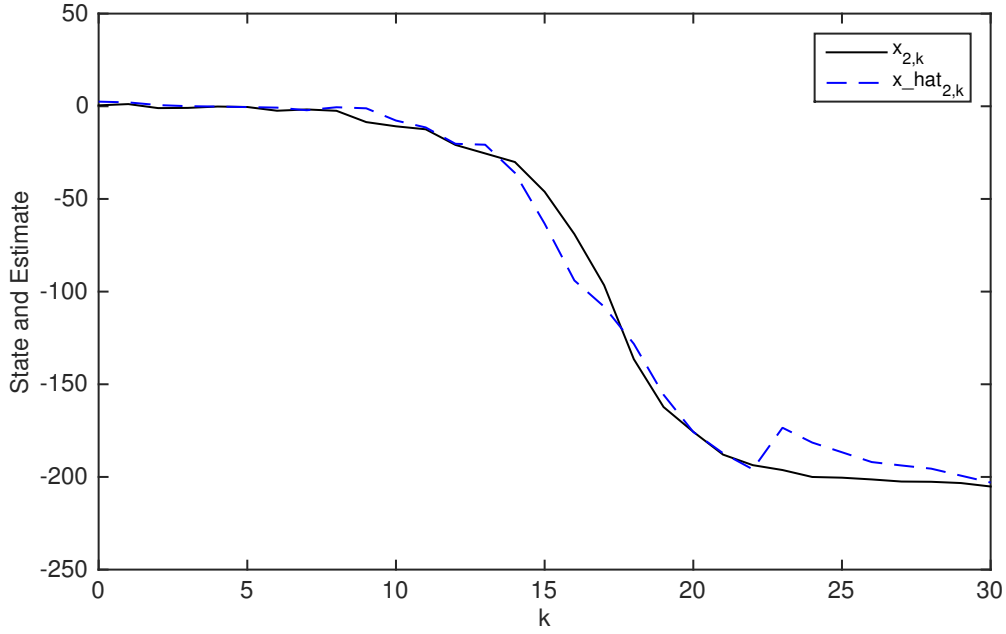

Figure 4.5: Quadratic nonlinearity, Case 2 - State, $x_{2,k}$, and estimate, $\hat{x}_{2,k}$

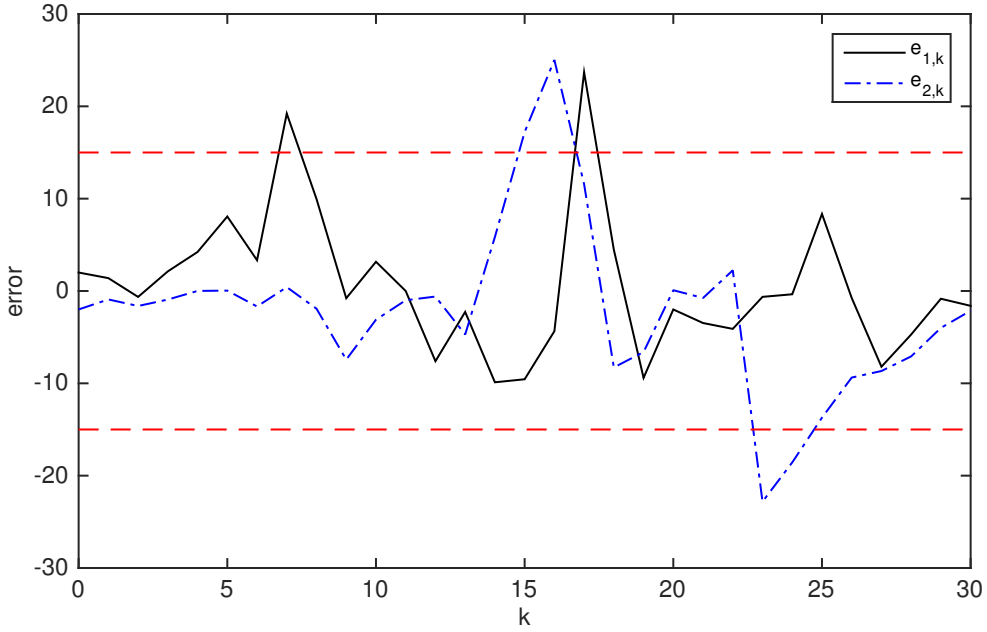

Figure 4.6: Quadratic nonlinearity, Case 2 - Estimation error, $e_{1,k}$ and $e_{2,k}$

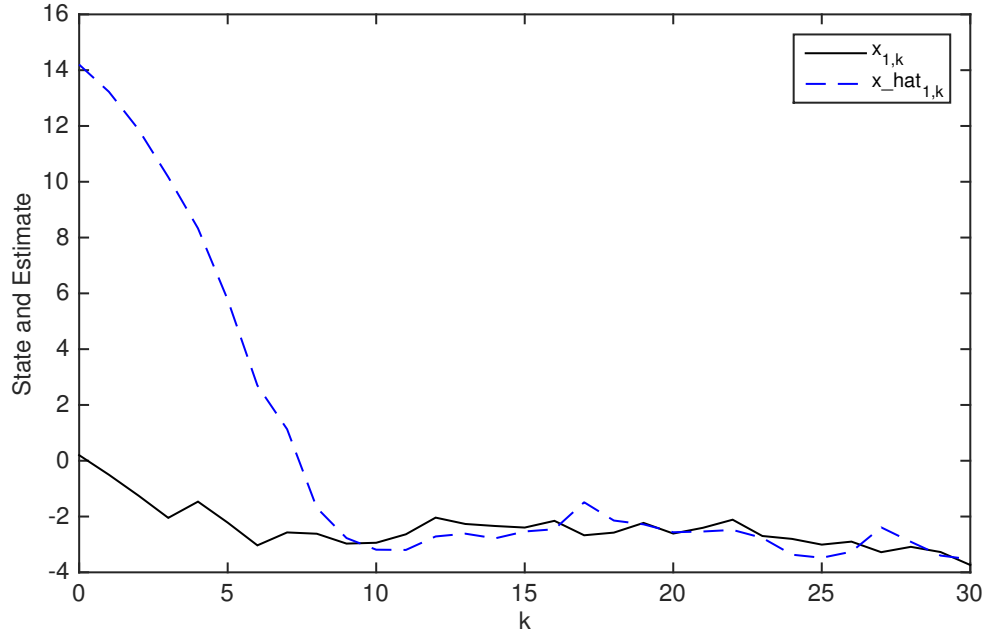

Figure 4.7: Quadratic nonlinearity, Case 3 - State, $x_{1,k}$, and estimate, $\hat{x}_{1,k}$

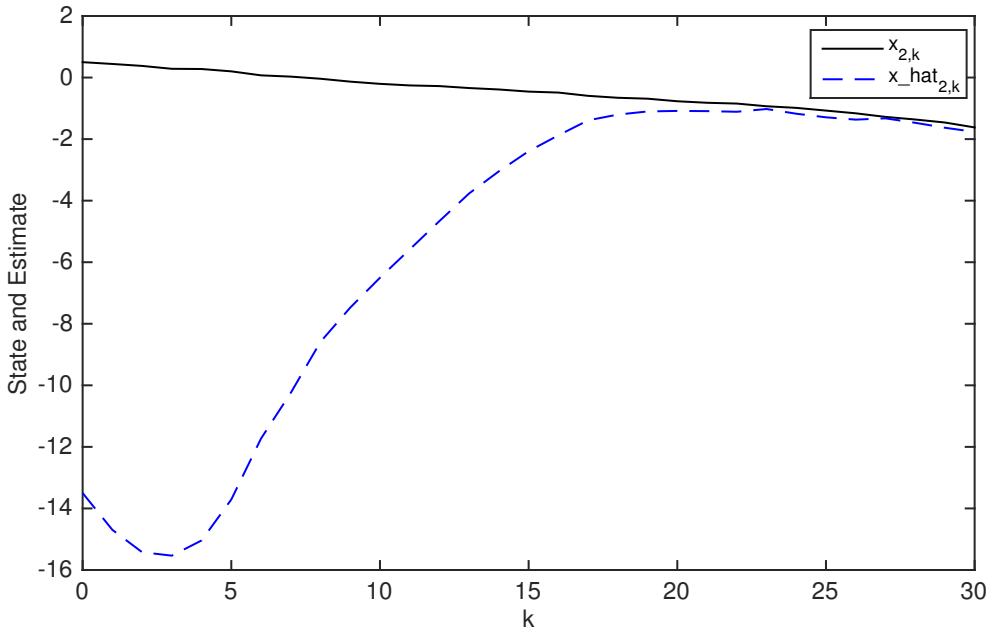

Figure 4.8: Quadratic nonlinearity, Case 3 - State, $x_{2,k}$, and estimate, $\hat{x}_{2,k}$

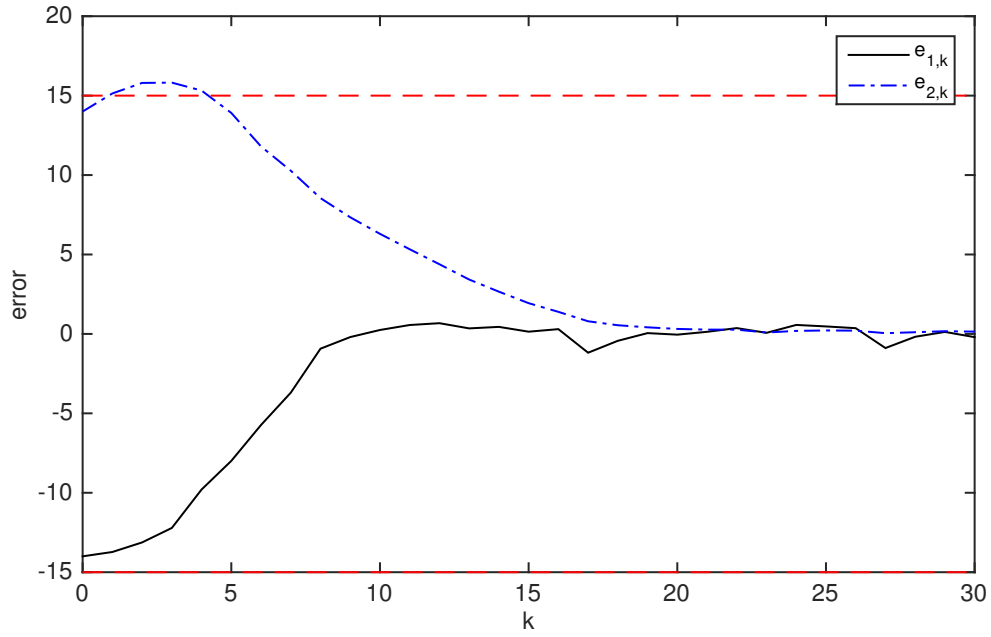

Figure 4.9: Quadratic nonlinearity, Case 3 - Estimation error, $e_{1,k}$ and $e_{2,k}$

With the initial error used in Case 1, the disturbance magnitude is varied from 1 to 10 and the H_∞ gain, bound, and ratio are calculated for each disturbance magnitude as shown in Table 4.2. The data in the table shows that both the H_∞-gain and bound are increasing with the disturbance magnitude. It is observed from the values of the ratio that the H_∞-gain is increasing at a faster rate than the H_∞-bound, which informs us that the theoretical bound is not as sensitive to the disturbance magnitude as the H_∞-gain. This table highlights one method a designer could use to take advantage of the results in this dissertation. Each of the H_∞-bound results in the various chapters is calculated using simulation, which can aid a designer in the choice of filter for their system.

Table 4.2: H_∞-gain and bound for a second order system with a quadratic nonlinearity

δ	**H_∞-gain**	**H_∞-bound**	**Ratio**
1	0.4740	1.6377	0.2894
2	0.4878	1.6561	0.2946
3	0.5079	1.6447	0.3088
4	0.5335	1.6135	0.3307
5	0.5643	1.6337	0.3454
6	0.5995	1.6493	0.3635
7	0.6385	1.6602	0.3846
8	0.6808	1.6685	0.4080
9	0.7257	1.6753	0.4332
10	0.7730	1.7705	0.4366

4.4.2 Sinusoidal Nonlinearity

The least severe nonlinearity is the sinusoidal, $f(y) = sin(y)$, with $w_k \in \ell_2$ and Γ_k generated such that the mean is $\overline{\Gamma} = 0.9I_2$. The variable δ is swept from -20 to 20 in 0.1 increments to observe how the finite-time H_∞-bound varies with the disturbance magnitude as well as with the run time, T. In the analysis provided in this section, (4.71) is rearranged as

$$\frac{\sum_{k=0}^{T} \overline{\|e_k\|^2}}{\sum_{k=0}^{T} \overline{\|w_k\|^2}} < \frac{\varphi_2}{\varphi_1} \tag{4.78}$$

and T takes the values $T = \{10, 30, 50\}$.

Figure 4.10 is a plot of the ratio in (4.78) for each run time, $T = \{10, 30, 50\}$. This figure shows that the bound is valid in the range of δ and T values being analyzed because the ratios remain between zero and one. Additionally the plot shows that there is an effect on the ratio due to the run time, T, where the smallest run time is the most conservative for small δ, but for $|\delta| > 17$, the smallest run time is the least conservative.

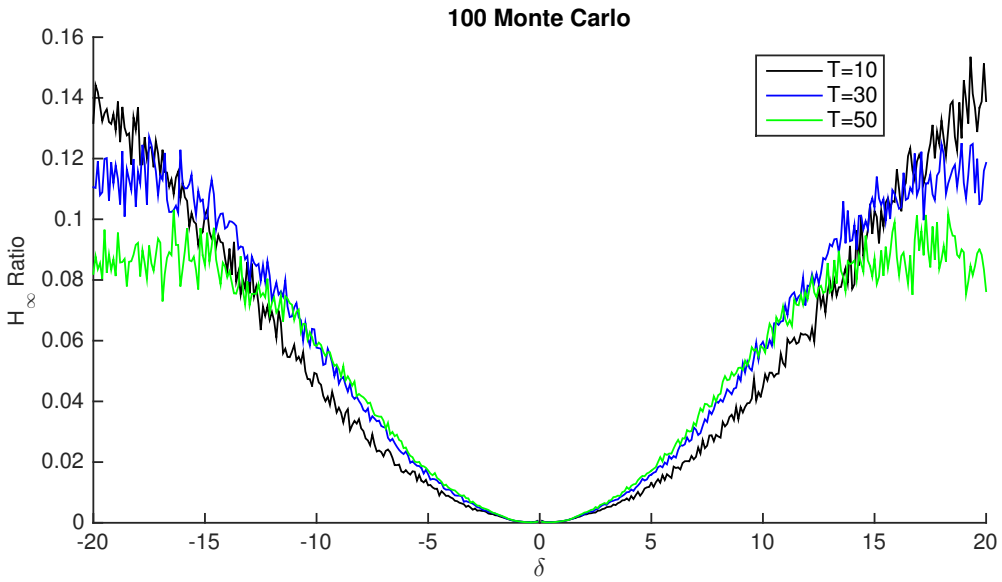

Figure 4.10: Sinusoidal nonlinearity - H_∞-gain to theoretical bound ratio

4.4.3 Quadratic Nonlinearity

The next nonlinearity considered is the quadratic, $f(y) = y^2$, with $w_k \in \ell_2$ and Γ_k generated such that the mean is $\overline{\Gamma} = 0.9I_2$. The variable δ is swept from -20 to 20 in 0.1 increments to observe how the finite-time H_∞-bound varies with the disturbance magnitude as well as with the runTime, T. Again, T takes the values $T = \{10, 30, 50\}$.

Figure 4.11 is a plot of the ratio in (4.78) for each run time, $T = \{10, 30, 50\}$. This figure shows similar results to those seen with the sinusoidal nonlinearity. The ratio is smaller overall, which would mean that this nonlinear system produces a more conservative H_∞-bound than that seen from the sinusoidal system. The bound is valid in the range of δ and T values being analyzed because the ratios remain between zero and one, and the plot shows that there is an effect on the ratio due to the run time, T, where the smallest run time is the most conservative for small δ, but for $|\delta| > 10$, the smallest run time is the least conservative.

4.4.4 Cubic Nonlinearity

The most severe nonlinearity is the cubic, $f(y) = y^3$, with $w_k \in \ell_2$ and Γ_k generated such that the mean is $\overline{\Gamma} = 0.9I_2$. The variable δ is swept from -20 to 20 in 0.1 increments to observe how the finite-time H_∞-bound varies with the disturbance magnitude as well as with the run time, T taking the values $T = \{10, 30, 50\}$.

Figure 4.12 is a plot of the ratio in (4.78) for each run time, $T = \{10, 30, 50\}$. As with the previous cases, this figure shows that the bound is valid in the range of δ and T values being analyzed because the ratios remain between zero and one. The ratio is smaller overall than both of the other nonlinearities, which would

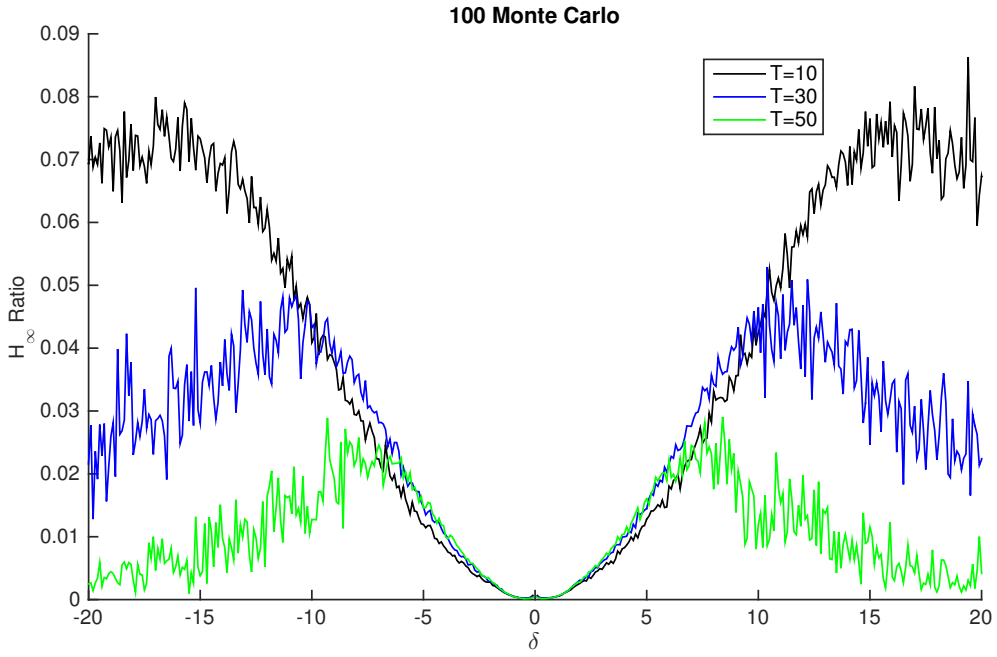

Figure 4.11: Quadratic nonlinearity - H_∞-gain to theoretical bound ratio

imply that systems with more severe nonlinearities might have more conservative bounds due to the Taylor series approximations. Figure 4.12 shows that there is an effect on the ratio due to the run time, T, where the smallest run time is the most conservative for small δ, but for $|\delta| > 6$, the smallest run time is the least conservative.

4.4.5 Side-by-Side Comparison of Results from Three Nonlinearities

Lastly, the run time will be held constant to $T = 30$ and now the three types of nonlinearities covered will be co-plotted. Figure 4.13 shows that while for $|\delta| > 9$, the initial assumption that the least severe nonlinearity is the least conservative, it also shows that for $|\delta| < 9$, the three types of nonlinearities considered have very similar results.

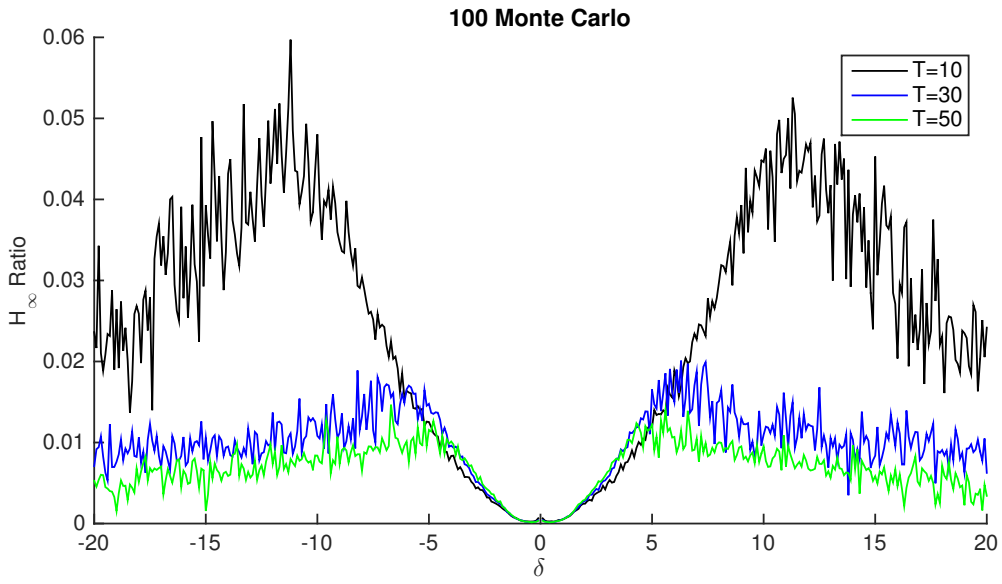

Figure 4.12: Cubic nonlinearity - H_∞-gain to theoretical bound ratio

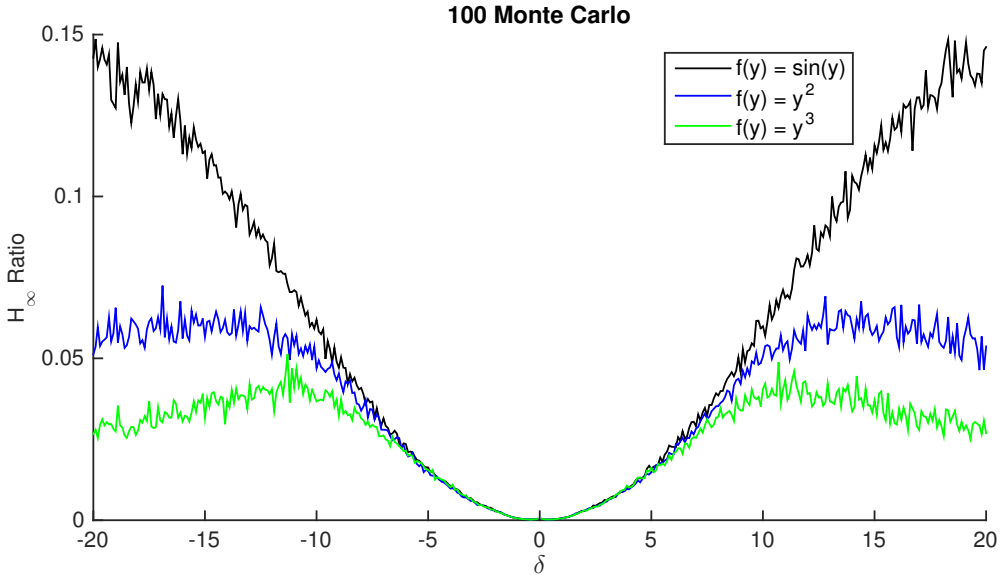

Figure 4.13: All three nonlinearities, T=30 - H_∞-gain to theoretical bound ratio

4.5 Summary

Convergence, H_2, and H_∞ analysis were performed on the discrete-time extended Kalman filter used as a nonlinear observer applied to systems with

finite-energy random disturbances and uncertain observations. Additional terms in the error that result from the uncertain measurements cause the energy analysis to be for finite-time only. Simulation studies were presented that demonstrated the effect of the run time as well as the effect of the severity of the nonlinearity on the conservativeness of the result. It was found that for larger disturbance magnitudes, short run times and less severe nonlinearities produced the least conservative results. A special case of this model is when the sensors no longer fail individually, they fail all at once. The EKF designed for this model will be analyzed in the next chapter.

CHAPTER 5

H_∞-PROPERTY OF THE DISCRETE-TIME EXTENDED KALMAN FILTER FOR SYSTEMS WITH SIMULTANEOUSLY FAILING MEASUREMENTS

A special case of the EKF designed in Chapter 4 is analyzed for convergence, H_2, and H_∞. The EKF is designed for systems with zero mean, white noise, and correlation between the process and measurement as well as grouped uncertainty in the measurement and is analyzed for systems that have stochastic ℓ_2 type disturbances. Simulations are provided to compare the effect of run time as well as the "severity" of the nonlinearity.

5.1 EKF Formulation

Consider the nonlinear discrete-time system and measurement equations,

$$x_{k+1} = f(x_k) + F_k w_k \tag{5.1}$$

$$y_k = \gamma_k h(x_k) + H_k w_k \tag{5.2}$$

where $x_k \in \Re^n$ is the state, $y_k \in \Re^p$ is the measurement, $f(x_k)$ and $h(x_k)$ are known analytic vector functions, the state and measurement disturbance coefficient matrices are $F_k \in \Re^{n\times l}$ and $H_k \in \Re^{p\times l}$, respectively, where the disturbance $w_k \in \Re^l$ is white, zero mean, and identity covariance. It is assumed that the measurement nonlinearity is uniformly bounded as $\|h(x)\| \leq \alpha_h$ for all $x \in \Re^n$. The coefficient $\gamma_k \in \Re$ is a Bernoulli random variable, taking values of 0 or 1, uncorrelated in time with known mean and variance, $E\{\gamma_k\} = \overline{\gamma}$ and $E\{(\gamma_k - \overline{\gamma})^2\} = \overline{\gamma}(1-\overline{\gamma}) \triangleq \Gamma$ respectively, and represents whether all of the measurements are present or not, therefore $\overline{\gamma}$ represents the probability of successfully receiving a multi-dimensional signal.

The details for the EKF for the general case were given in Chapter 4. The EKF for the special case, when the Bernoulli random variable is a scalar, follows

directly from the EKF equations for the general case. For this reason, the EKF in this chapter will not be derived; the EKF equations are given directly as the following

- State estimate

$$\hat{x}_{k+1} = f(\hat{x}_k) + K_k(y_k - \overline{\gamma}h(\hat{x}_k)) \tag{5.3}$$

- Kalman Gain

$$\begin{aligned} K_k = (\overline{\gamma}A_k P_k C_k^T + F_k H_k^T)\times \\ (\Gamma(C_k P_k C_k^T + h(\hat{x}_k)h^T(\hat{x}_k)) + \overline{\gamma}^2 C_k P_k C_k^T + H_k H_k^T)^{-1} \end{aligned} \tag{5.4}$$

- Riccati Difference Equation

$$P_{k+1} = \mathbb{A}_k P_k \mathbb{A}_k^T + \mathcal{F}_k \mathcal{F}_k^T + \Gamma K_k(C_k P_k C_k^T + h(\hat{x}_k)h^T(\hat{x}_k))K_k^T \tag{5.5}$$

or equivalently

$$P_{k+1} = \overline{\mathcal{A}_k P_k \mathcal{A}_k^T} + \mathcal{F}_k \mathcal{F}_k^T + \Gamma K_k h(\hat{x}_k)h^T(\hat{x}_k)K_k^T \tag{5.6}$$

where

$$\mathbb{A}_k = A_k - \overline{\gamma}K_k C_k \tag{5.7}$$

$$\mathcal{A}_k = A_k - \gamma_k K_k C_k \tag{5.8}$$

$$\mathcal{F}_k = F_k - K_k H_k \tag{5.9}$$

with $\mathcal{F}_k \mathcal{F}_k^T > 0$ and A_k and C_k in (4.7) and (4.8), respectively.

5.2 Convergence Analysis of EKF Used on Systems with Grouped Uncertain Measurements and Finite Energy Noise

Consider the nonlinear discrete-time system and measurement equations,

$$x_{k+1} = f(x_k) + F_k w_k \tag{5.10}$$

$$y_k = \gamma_k h(x_k) + H_k w_k \tag{5.11}$$

where $w_k \in \ell_2$ is now zero mean, identity covariance, uncorrelated in time, and finite-energy. The coefficient, γ_k is still a Bernoulli random variable uncorrelated

in time representing whether all sensors contain data and noise or noise only. This Bernoulli random variable has known mean, $E\{\gamma_k\} = \overline{\gamma}$ and variance $E\{(\gamma_k - \overline{\gamma})^2\} = \overline{\gamma}(1 - \overline{\gamma})) \triangleq \Gamma$. With the error defined in (4.9), the error dynamics are

$$e_{k+1} = \mathcal{A}_k e_k + \mathcal{F}_k w_k - \widetilde{\gamma}_k K_k h(\hat{x}_k) \tag{5.12}$$

with $\mathcal{A}_k$ and $\mathcal{F}_k$ in (4.13) and (4.14) and

$$\widetilde{\gamma}_k = \gamma_k - \overline{\gamma} \tag{5.13}$$

is zero mean with covariance Γ.

Theorem 5.1. *Consider the nonlinear system* (5.10) *and measurement equation* (5.11)*, with grouped uncertain measurements, the noise taken as an element of stochastic* ℓ_2 *and* $\mathcal{F}_k \mathcal{F}_k^T > 0$ *with* $\mathcal{F}_k$ *in* (5.9)*. Let the state be estimated using an extended Kalman filter based on this model, which was designed for white noise with zero mean and identity covariance, with gain* K_k *from* (5.4)*. With Assumption 4.1, Lemma 6 holds. With these conditions, the energy of the estimation error is finite-time bounded for any integer* $0 < T < \infty$ *as follows*

$$\sum_{k=0}^{T} \overline{\|e_k\|^2} \leq \frac{1}{\varphi_1} \left(\overline{e_0^T P_0^{-1} e_0} + \varphi_2 \sum_{k=0}^{T} \overline{\|w_k\|^2} + \varphi_3 (T+1) \right) \tag{5.14}$$

where

$$\varphi_1 \triangleq \inf_k (\lambda_{min} (P_k^{-1} - \overline{\mathcal{A}_k^T P_{k+1}^{-1} \mathcal{A}_k})) \tag{5.15}$$

$$\varphi_2 \triangleq \sup_k (\lambda_{max} (\mathcal{F}_k^T P_{k+1}^{-1} \mathcal{F}_k)) \tag{5.16}$$

$$\varphi_3 \triangleq \sup_k (\lambda_{max} (\Gamma h^T (\hat{x}_k) K_k^T P_{k+1}^{-1} K_k h(\hat{x}_k))) \tag{5.17}$$

Proof. With Assumption 4.1, Lemma 6 states that the solution to the Riccati equation, P_k, and the Kalman gain, K_k, are uniformly upper and lower bounded,

which is essential throughout the proof. Stochastic Lyapunov analysis is used to determine the stability of the estimation error and obtain the H_∞-gain. The Lyapunov function candidate,

$$V_k = e_k^T P_k^{-1} e_k \tag{5.18}$$

is analyzed along the dynamics of the error (5.12) to verify that the average energy decreases over time. To this end, consider the following stochastic Lyapunov difference

$$\begin{aligned} &E\{V_{k+1}|e_k, e_{k-1}, \dots\} - V_k \\ &= E\{e_{k+1}^T P_{k+1}^{-1} e_{k+1}|e_k, e_{k-1}, \dots\} - e_k^T P_k^{-1} e_k < 0 \end{aligned} \tag{5.19}$$

With substitution from (5.12), the inequality in (5.19) is expanded as,

$$\begin{aligned} &- e_k^T \left(P_k^{-1} - \overline{\mathcal{A}_k^T P_{k+1}^{-1} \mathcal{A}_k}\right) e_k + 2\overline{w_k^T \mathcal{F}_k^T P_{k+1}^{-1} \mathcal{A}_k} e_k \\ &- 2\overline{\tilde{\gamma}_k h^T(\hat{x}_k) K_k^T P_{k+1}^{-1} \mathcal{A}_k} e_k + \overline{w_k^T \mathcal{F}_k^T P_{k+1}^{-1} \mathcal{F}_k w_k} \\ &- 2\overline{\tilde{\gamma}_k h^T(\hat{x}_k) K_k^T P_{k+1}^{-1} \mathcal{F}_k w_k} \\ &+ \overline{\tilde{\gamma}_k^2 h^T(\hat{x}_k) K_k^T P_{k+1}^{-1} K_k h(\hat{x}_k)} < 0 \end{aligned} \tag{5.20}$$

Because $\mathcal{F}_k$, $\mathcal{A}_k$, $\hat{x}_k$, and therefore e_k, P_k and K_k are functions of w_{k-1} and γ_{k-1} and since w_k and γ_k are uncorrelated in time and w_k is zero mean, the second and fifth terms can be rewritten so that (5.20) becomes

$$\begin{aligned} &- e_k^T \left(P_k^{-1} - \overline{\mathcal{A}_k^T P_{k+1}^{-1} \mathcal{A}_k}\right) e_k + 2\overline{w_k^T} \left(\overline{\mathcal{F}_k^T P_{k+1}^{-1} \mathcal{A}_k}\right) e_k \\ &- 2\overline{\tilde{\gamma}_k h^T(\hat{x}_k) K_k^T P_{k+1}^{-1} \mathcal{A}_k} e_k + \overline{w_k^T \mathcal{F}_k^T P_{k+1}^{-1} \mathcal{F}_k w_k} \\ &- 2\overline{\tilde{\gamma}_k} \left(\overline{h^T(\hat{x}_k) K_k^T P_{k+1}^{-1} \mathcal{F}_k}\right) \overline{w_k} \\ &+ \overline{\tilde{\gamma}_k^2} h^T(\hat{x}_k) K_k^T P_{k+1}^{-1} K_k h(\hat{x}_k) < 0 \end{aligned} \tag{5.21}$$

leading to

$$\begin{aligned} &- e_k^T \left(P_k^{-1} - \overline{\mathcal{A}_k^T P_{k+1}^{-1} \mathcal{A}_k} \right) e_k \\ &- 2\overline{\tilde{\gamma}_k h^T(\hat{x}_k) K_k^T P_{k+1}^{-1} \mathcal{A}_k e_k} \\ &+ \overline{w_k^T \mathcal{F}_k^T P_{k+1}^{-1} \mathcal{F}_k w_k} \\ &+ \Gamma h^T(\hat{x}_k) K_k^T P_{k+1}^{-1} K_k h(\hat{x}_k) < 0 \end{aligned} \tag{5.22}$$

To ensure (5.22) is negative, the development for an upper bound is provided next. The first term is lower bounded using Lemma 3

$$\begin{aligned} &- \varphi_1 e_k^T e_k - 2\overline{\tilde{\gamma}_k h^T(\hat{x}_k) K_k^T P_{k+1}^{-1} \mathcal{A}_k e_k} + \overline{w_k^T \mathcal{F}_k^T P_{k+1}^{-1} \mathcal{F}_k w_k} \\ &+ \Gamma h^T(\hat{x}_k) K_k^T P_{k+1}^{-1} K_k h(\hat{x}_k) < 0 \end{aligned} \tag{5.23}$$

with φ_1 defined in (5.15). Such a φ_1 always exists, since for all $k = 0, 1, 2, \ldots$

$$P_k^{-1} - \mathcal{A}_k^T P_{k+1}^{-1} \mathcal{A}_k > 0 \tag{5.24}$$

This is shown by using Lemma 4 twice such that the following conditions are equivalent to (5.24)

$$\begin{bmatrix} P_k^{-1} & \mathcal{A}_k^T \\ \mathcal{A}_k & P_{k+1} \end{bmatrix} > 0 \tag{5.25}$$

$$\begin{aligned} &\mathcal{A}_k P_k \mathcal{A}_k^T + \mathcal{F}_k \mathcal{F}_k^T + \Gamma K_k h(\hat{x}_k) h^T(\hat{x}_k) K_k^T \\ &- \mathcal{A}_k P_k \mathcal{A}_k^T > 0 \end{aligned} \tag{5.26}$$

and $\mathcal{F}_k \mathcal{F}_k^T > 0$ and $\Gamma K_k h(\hat{x}_k) h^T(\hat{x}_k) K_k^T \geq 0$, therefore, for all $k = 0, 1, 2, \ldots$

$$P_k^{-1} - \overline{\mathcal{A}_k^T P_{k+1}^{-1} \mathcal{A}_k} > 0 \tag{5.27}$$

To obtain an upper bound on the third term in (5.23), it is shown that for all $k = 0, 1, 2, \ldots$

$$\mathcal{F}_k^T P_{k+1}^{-1} \mathcal{F}_k \leq I_l \tag{5.28}$$

by substituting $\mathcal{F}_k$ from (5.9) and using Lemma 4 twice the following conditions are equivalent

$$\begin{bmatrix} I_l & \mathcal{F}_k^T \\ \mathcal{F}_k & P_{k+1} \end{bmatrix} \geq 0 \tag{5.29}$$

$$\begin{aligned} &\mathcal{A}_k P_k \mathcal{A}_k^T + \mathcal{F}_k \mathcal{F}_k^T + \Gamma K_k h(\hat{x}_k) h^T(\hat{x}_k) K_k^T \\ &- \mathcal{F}_k \mathcal{F}_k^T \geq 0 \end{aligned} \tag{5.30}$$

which agrees with

$$\mathcal{A}_k P_k \mathcal{A}_k^T + \Gamma K_k h(\hat{x}_k) h^T(\hat{x}_k) K_k^T \geq 0 \tag{5.31}$$

Therefore, it has been shown that I_l is a valid upper bound as shown in (5.28) and Lemma 3 can be applied, resulting in φ_2 in (5.16) which is guaranteed to be bounded.

Using this same technique, the third term is bounded by

$$\Gamma h^T(\hat{x}_k) K_k^T P_{k+1}^{-1} K_k h(\hat{x}_k) \leq 1 \tag{5.32}$$

and Lemma 3 can be applied, resulting in φ_3 in (5.17) which is guaranteed to be bounded. These bounds result in

$$\begin{aligned} &- \varphi_1 e_k^T e_k - 2\overline{\tilde{\gamma}_k h^T(\hat{x}_k) K_k^T P_{k+1}^{-1} \mathcal{A}_k} e_k \\ &+ \varphi_2 \overline{w_k^T w_k} + \varphi_3 < 0 \end{aligned} \tag{5.33}$$

Lastly, taking the expected value of (5.33) and using Lemma 5 results in

$$\begin{aligned} &- \varphi_1 \overline{e_k^T e_k} - 2\overline{\tilde{\gamma}_k h^T(\hat{x}_k) K_k^T P_{k+1}^{-1} \mathcal{A}_k} \, (\overline{e_k}) \\ &+ \varphi_2 \overline{w_k^T w_k} + \varphi_3 < 0 \end{aligned} \tag{5.34}$$

Due to the unbiasedness, $E\{e_k\} = 0$, $k \geq 0$, of the estimator by design, (5.34) can be further reduced to

$$\overline{V_{k+1}} - \overline{V_k} < -\varphi_1 \overline{e_k^T e_k} + \varphi_2 \overline{w_k^T w_k} + \varphi_3 < 0 \tag{5.35}$$

To obtain the finite-time H_∞-property, the ratio of the estimation error energy to the disturbance energy is analyzed; the summation of (5.35) is taken from $k = 0$ to $k = T$ (for any integer $T > 0$) giving

$$\overline{V_T} - \overline{V_0} < -\varphi_1 \sum_{k=0}^{T} \overline{\|e_k\|^2} + \varphi_2 \sum_{k=0}^{T} \overline{\|w_k\|^2} + \varphi_3(T+1) \tag{5.36}$$

and for $\overline{V_T} \geq 0$,

$$-\overline{V_0} < -\varphi_1 \sum_{k=0}^{T} \overline{\|e_k\|^2} + \varphi_2 \sum_{k=0}^{T} \overline{\|w_k\|^2} + \varphi_3(T+1) \tag{5.37}$$

which is rearranged as

$$\sum_{k=0}^{T} \overline{\|e_k\|^2} < \frac{1}{\varphi_1} \left(\overline{V_0} + \varphi_2 \sum_{k=0}^{T} \overline{\|w_k\|^2} + \varphi_3(T+1) \right) \tag{5.38}$$

This result indicates that the energy of the estimation error has an upper bound proportional to the summation of a function of the initial estimation error, $\overline{V_0} = \overline{e_0^T P_0^{-1} e_0}$, the disturbance energy, $\sum_{k=0}^{T} \overline{\|w_k\|^2}$, and a linear function of time where the proportionality constants φ_1, φ_2 and φ_3 are defined in (5.15), (5.16), and (5.17). ■

When the result of this chapter is compared to that in Chapter 4, it is seen that this chapter's result is a special case. Consider φ_3 from (4.49) and φ_3 from (5.17) provided in (5.39) and (5.40) for side-by-side comparison. What can be seen from this comparison is that if $\widetilde{\Gamma}_k$ is taken as a scalar, as is the case in this chapter, the two equations are equivalent. Therefore the result in Chapter 4 can be directly applied to this special case.

$$\text{Ch4: } \varphi_3 \triangleq \sup_k (\lambda_{max}(h^T(\hat{x}_k) \overline{\widetilde{\Gamma}_k^T K_k^T P_{k+1}^{-1} K_k \widetilde{\Gamma}_k} h(\hat{x}_k))) \tag{5.39}$$

$$\text{Ch5: } \varphi_3 \triangleq \sup_k (\lambda_{max}(\Gamma h^T(\hat{x}_k) K_k^T P_{k+1}^{-1} K_k h(\hat{x}_k))) \tag{5.40}$$

5.3 Significance

To consider the finite-time H_∞-property of the EKF in this chapter, the result (5.38) is taken as

$$\sum_{k=0}^{T} \overline{\|e_k\|^2} < \frac{\varphi_2}{\varphi_1} \sum_{k=0}^{T} \overline{\|w_k\|^2} \tag{5.41}$$

for any integer $0 < T < \infty$, where φ_1, φ_2, and φ_3 are defined in (5.15), (5.16), and (5.17).

On the other hand, if there is no noise in the system for $k = 0, 1, 2, \ldots$, then (5.38) is taken as a special case that presents a bound on the estimation error energy in terms of the initial conditions, $\overline{V_0} = \overline{e_0^T P_0^{-1} e_0}$, i.e. the finite-time H_2-property of the EKF

$$\sum_{k=0}^{T} \overline{\|e_k\|^2} < \frac{1}{\varphi_1} \overline{V_0} \tag{5.42}$$

5.4 Simulations

A scalar nonlinear system is considered with a variable disturbance magnitude. Simulations are performed to demonstrate the effect of the disturbance magnitude on the the finite-time H_∞-gain. The ratio of the left hand side and right hand side of (5.41) is analyzed to give insight to both the validity and the degree of conservativeness of our result. This ratio should remain between zero and one. Additionally, a study to observe the effects of the initial estimation error and disturbance magnitude is performed. Lastly, since the run time variable, T, appears in the result, the same simulation set up will be run for different values of T. From these simulations, it will be apparent that the run time has an effect on the validity and conservativeness of the result. To reduce the effect of outliers in the stochastic data, a 100 run Monte Carlo simulation is used for each case.

5.4.1 Scalar System

Consider the scalar nonlinear system

$$x_{k+1} = x_k + 0.01 \sin x_k + 10\delta w_k \tag{5.43}$$

$$y_k = \gamma_k x_k + 0.1\delta w_k \tag{5.44}$$

with $w_k \in \ell_2$ and γ_k such that the mean is $\overline{\gamma} = 0.9$. The variable δ is swept from -50 to 50 in 0.2 increments to observe how the result in (5.41) varies with the disturbance magnitude. The ratio of the left hand side of (5.41) over the right hand side is analyzed to show the validity of the result for each δ where $T = \{10, 30, 50\}$ for this study. The bound on the energy of the error is less conservative when the ratio in (5.41) is closer to one.

Figure 5.1 is a co-plot of the ratios in (5.41) for $T = \{10, 30, 50\}$. This figure shows that the bound is valid in all cases because the ratios remain between zero and one. Additionally this plot shows that the disturbance magnitude has a slight effect on the ratio for this system with the ratio being larger, i.e. the bound is less conservative, for smaller disturbance magnitudes. Additionally, the run time has a noticeable effect on the conservativeness of the result with a short run time providing a less conservative result. This implies that the bound on the energy of the observer error is more accurate for shorter run times; therefore this result would be best aimed towards H_∞ analysis of the transient response of a system.

5.4.2 Effect of Initial Conditions and Disturbance Magnitude

Consider a mass-spring-damper with a nonlinear spring where the continuous-time system is defined as

$$\ddot{y} = -b\dot{y} - f(y) \tag{5.45}$$

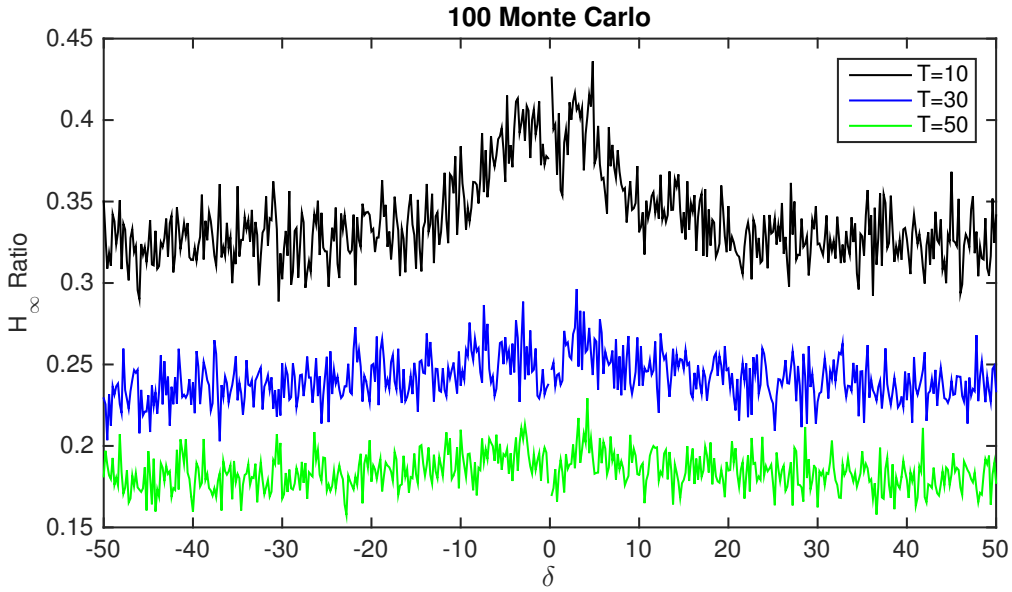

Figure 5.1: Calculate H_∞-gain to theoretical bound ratio

which is converted to state-space form, is discretized and has noise added to it as

$$x_{k+1} = \begin{bmatrix} 1 & \tau \\ 0 & (1-\tau b) \end{bmatrix} x_k + \begin{bmatrix} 0 \\ -\tau f(x_{1,k}) \end{bmatrix} + \delta \begin{bmatrix} 0.02 & 0.1 \\ 0 & 0.01 \end{bmatrix} w_k \tag{5.46}$$

$$y_k = \gamma_k \begin{bmatrix} x_{1,k} \\ x_{2,k} \end{bmatrix} x_k + \delta \begin{bmatrix} 0.1 & 0.1 \\ 0 & 0.001 \end{bmatrix} w_k \tag{5.47}$$

with

$$f(y) = y^2 \tag{5.48}$$

$$x_0 = \begin{bmatrix} 0.2 & 0.5 \end{bmatrix}^T \tag{5.49}$$

and $\tau = 0.01s$ is the sampling time, $T = 30$ is the run time, $b = 5$ is the damping coefficient, $\overline{\gamma} = 0.9$ is the Bernoulli random variable statistics, and $w_k \in \ell_2$ is the finite-energy disturbance. As in the previous chapter, three different cases are simulated with different values for the initial conditions and the disturbance magnitude. Table 5.1 consists of the initial estimate value and the disturbance magnitude used for each case along with a qualitative finite-time bounded

analysis and H_∞ calculations. Each case is discussed in further detail below. To determine if a time response is finite-time bounded, the error magnitude is considered bounded if $|e_{i,k}| < 15$ for all integer $k \geq 0$ and $i = 1, 2$.

Table 5.1: Effect of initial values and disturbance magnitude

	Case 1	Case 2	Case 3
$\hat{x}_0$	$[-1.8\ ,\ 1.5]^T$	$[-1.8\ ,\ 1.5]^T$	$[14.2\ ,\ -13.5]^T$
δ	5	60	5
Error Boundedness	Within bounded	Exceeds bound	Exceeds bound
H_∞-Gain	0.5185	—	—
Figures	5.2, 5.3, 5.4	5.5, 5.6, 5.7	5.8, 5.9, 5.10

Case 1 considers a system with small error in the initial estimate along with small disturbance magnitudes, which results in a finite-time bounded response of the error. Figures 5.2 and 5.3 show that the estimate tracks the actual state well throughout the run time, which corresponds to the bounded error in Figure 5.4.

Case 2 consists of small error with large disturbance magnitude, where the state and estimate time responses are shown in Figures 5.5 and 5.6. Again, the estimate appears to be tracking the state relatively well; however, analyzing the estimation error in Figure 5.7, it is observed that the estimation error does not remain within the defined bound.

The last case in this simulation study has a large initial estimation error and a small disturbance magnitude. The time responses in Figures 5.8 and 5.9, show the time responses of the state variables and their estimates. By analyzing

the response of the estimation error in Figure 5.10, it is seen that even though the initial error begins within the bounded region, it is unable to remain bounded for the entire run time. These three cases emphasize the effect disturbance magnitude and initial estimate have on the time response of the estimation error. The estimation error of the EKF designed for systems with uncertain measurements that have group failure rates will remain within a desired bound for sufficiently small initial error and sufficiently small disturbance magnitude.

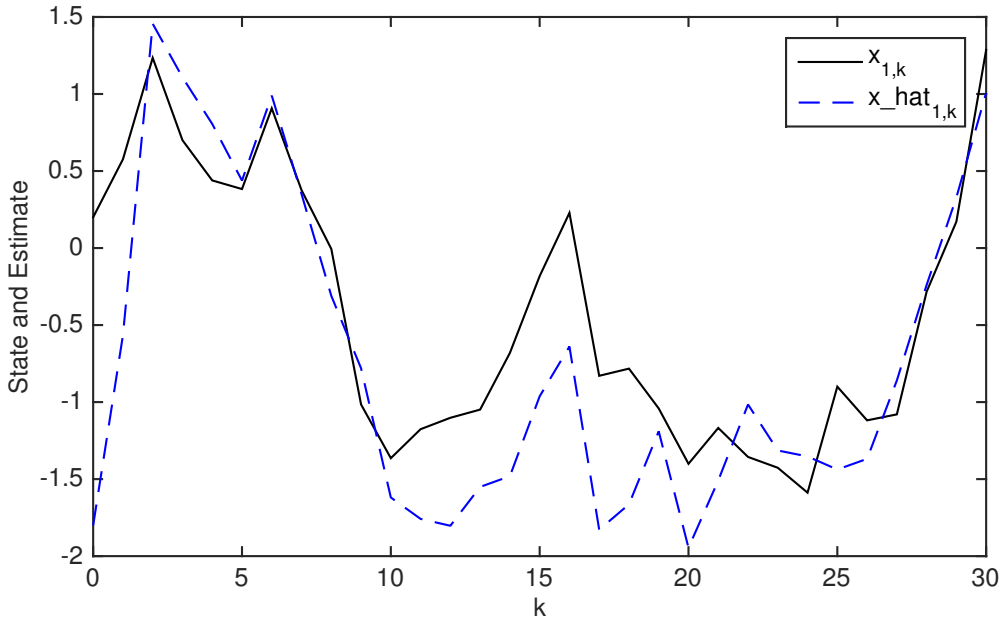

Figure 5.2: Quadratic Nonlinearity, Case 1 - State, $x_{1,k}$, and estimate, $\hat{x}_{1,k}$

5.4.3 Sinusoidal Nonlinearity

The system in state-space form in Section 5.4.2, with zero damping, $b = 0$, is used in this study for three different system nonlinearities, $f(y) = \{sin(y), y^2, y^3\}$. First, each of these nonlinear systems will be simulated with the run time varying and then the run time will be held constant while the

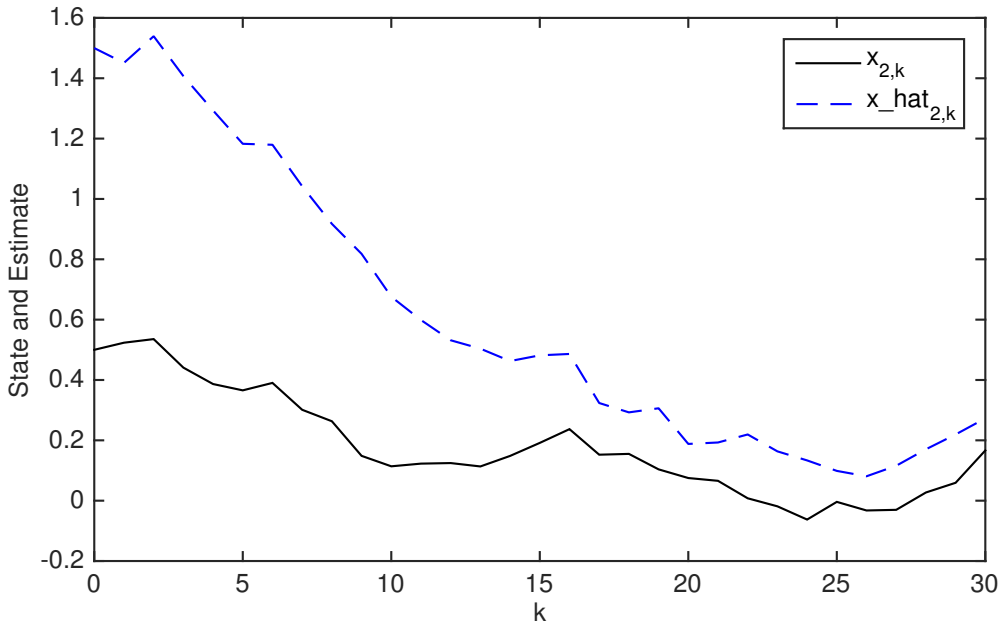

Figure 5.3: Quadratic Nonlinearity, Case 1 - State, $x_{2,k}$, and estimate, $\hat{x}_{2,k}$

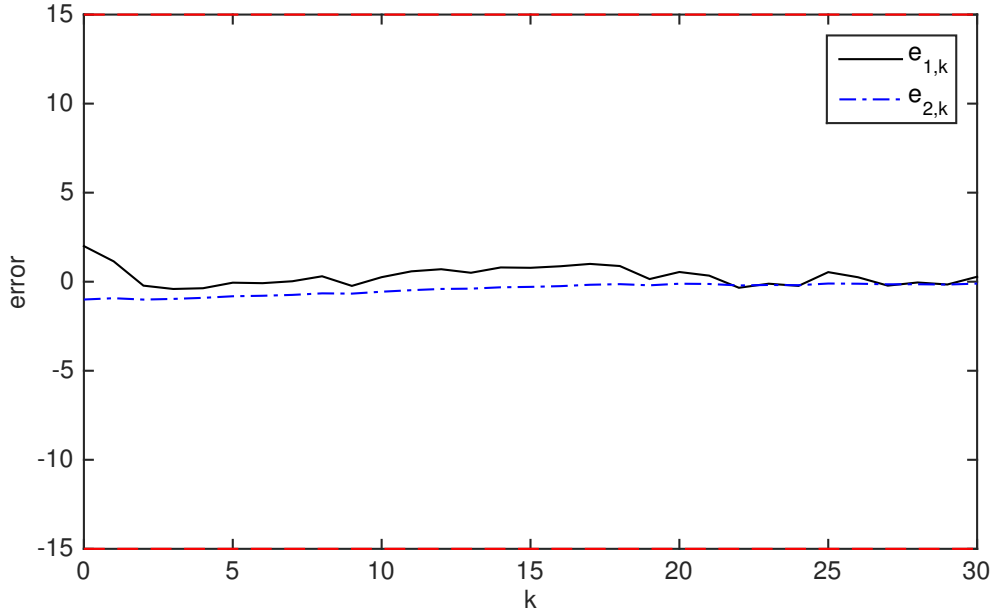

Figure 5.4: Quadratic Nonlinearity, Case 1 - Estimation error, $e_{1,k}$ and $e_{2,k}$

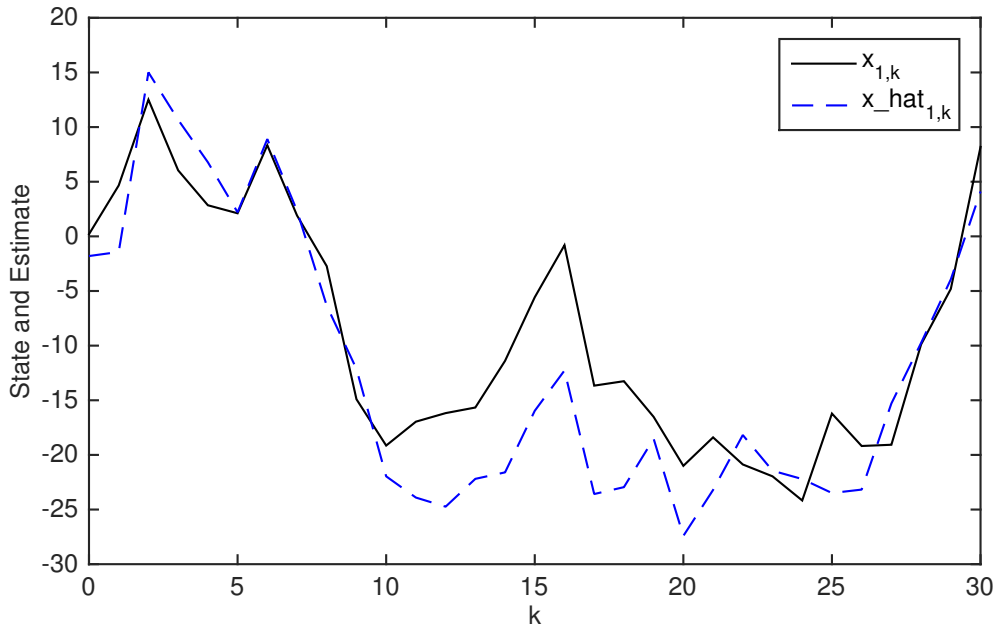

Figure 5.5: Quadratic Nonlinearity, Case 2 - State, $x_{1,k}$, and estimate, $\hat{x}_{1,k}$

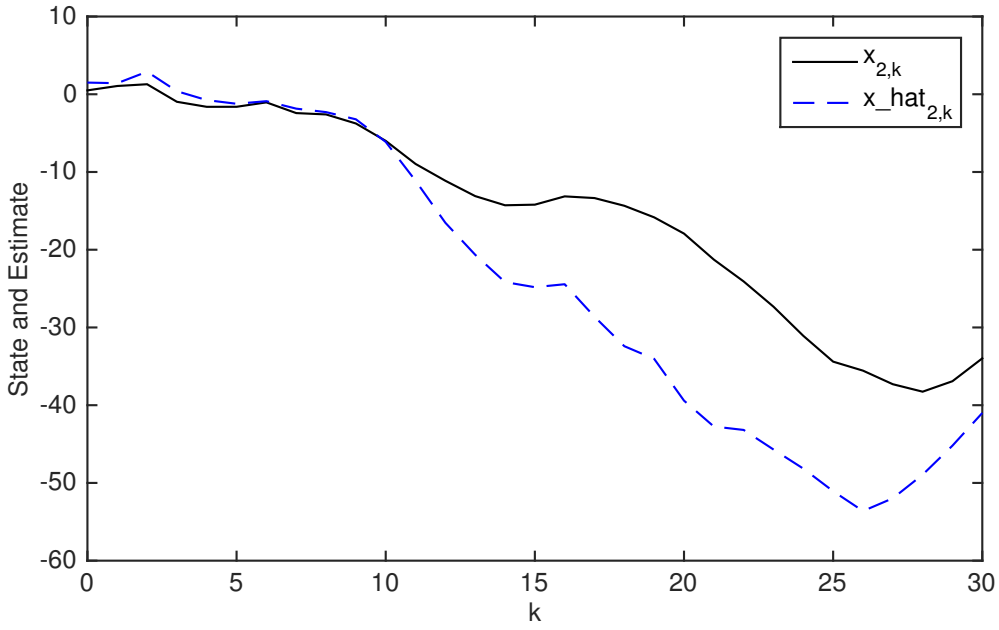

Figure 5.6: Quadratic Nonlinearity, Case 2 - State, $x_{2,k}$, and estimate, $\hat{x}_{2,k}$

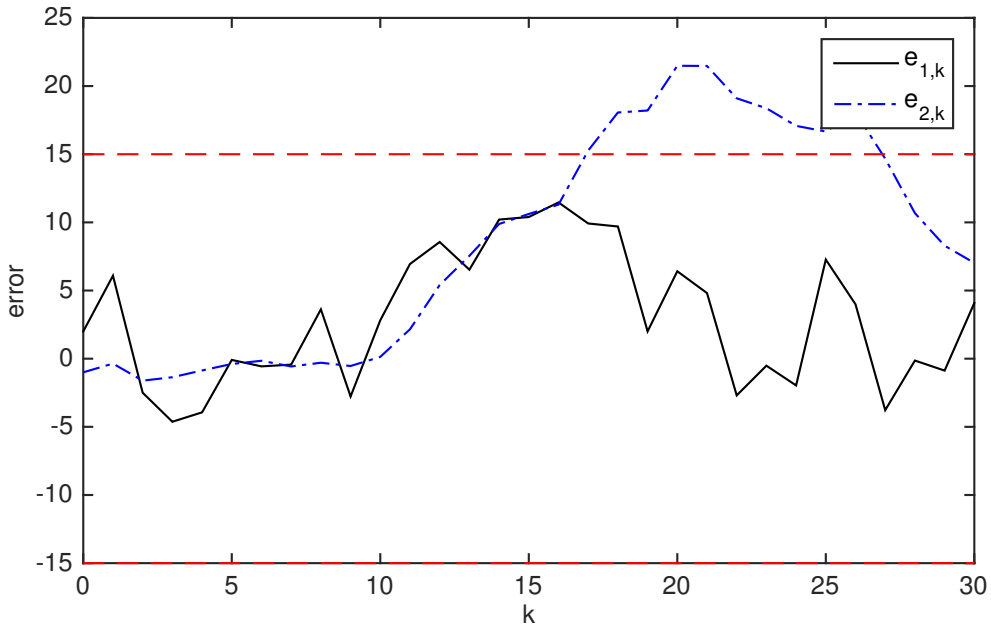

Figure 5.7: Quadratic Nonlinearity, Case 2 - Estimation error, $e_{1,k}$ and $e_{2,k}$

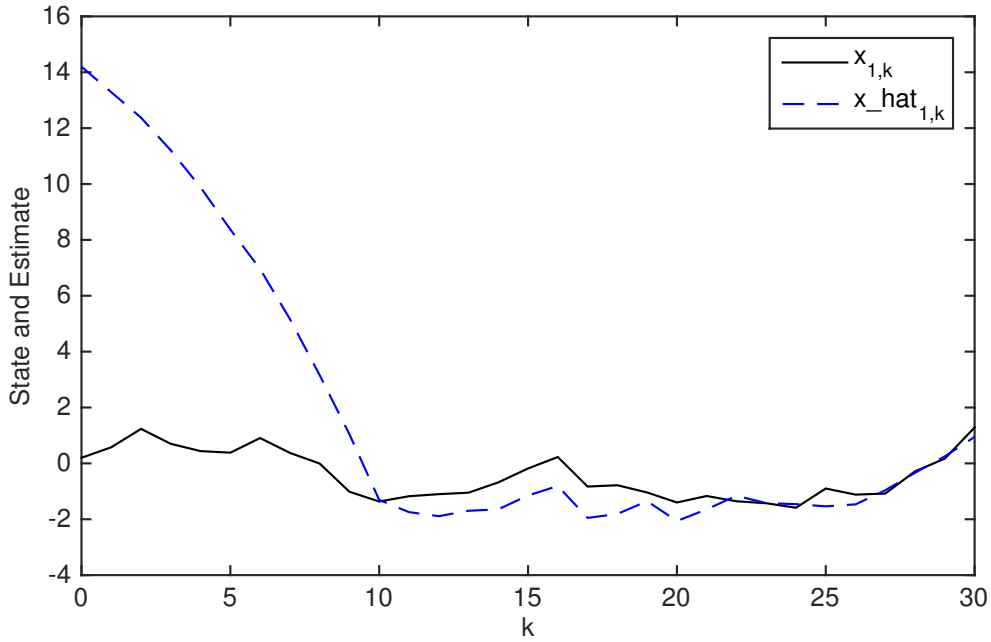

Figure 5.8: Quadratic Nonlinearity, Case 3 - State, $x_{1,k}$, and estimate, $\hat{x}_{1,k}$

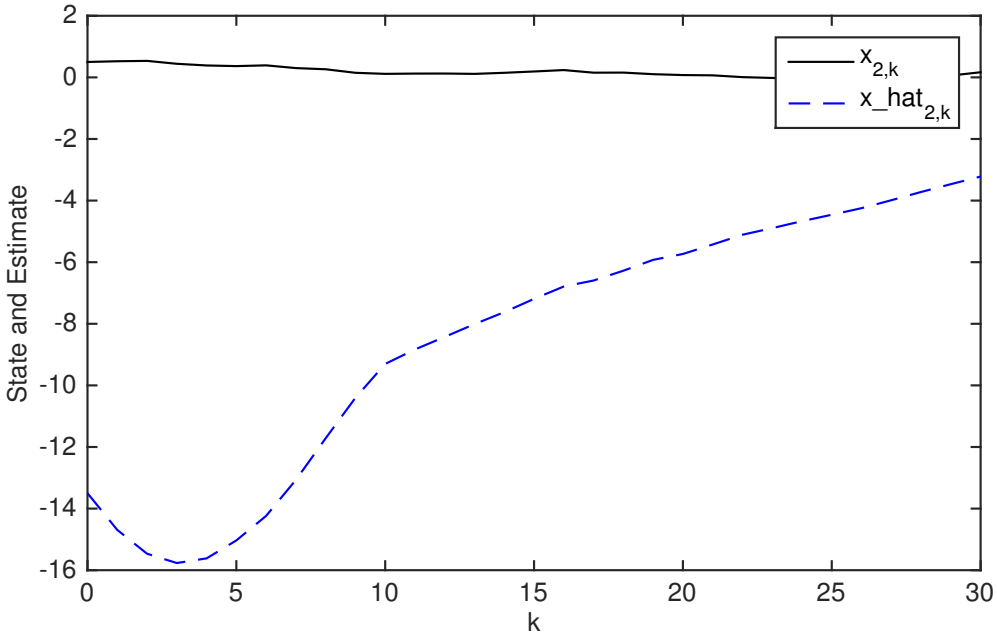

Figure 5.9: Quadratic Nonlinearity, Case 3 - State, $x_{2,k}$, and estimate, $\hat{x}_{2,k}$

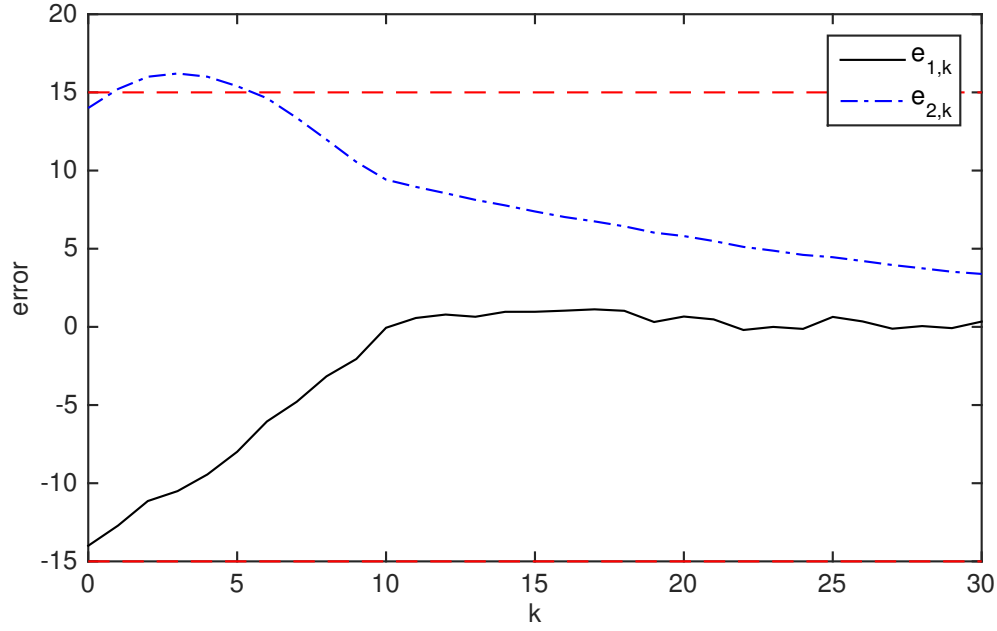

Figure 5.10: Quadratic Nonlinearity, Case 3 - Estimation error, $e_{1,k}$ and $e_{2,k}$

three nonlinear systems will be compared. The least "severe" nonlinearity is the sinusoidal, $f(y) = sin(y)$, with $w_k \in \ell_2$ and γ_k generated such that the mean is $\overline{\gamma} = 0.9$. The variable δ is swept from -15 to 15 in 0.1 increments to observe how the finite-time H_∞-bound varies with the disturbance magnitude as well as with the run time, T, which takes the values $\{10, 30, 50\}$.

Figure 5.11 is a plot of the ratio in (5.41) for each run time, $T = \{10, 30, 50\}$. This figure shows that the bound is valid in the range of δ and values of T being analyzed because the ratios remain between zero and one. Additionally the plot shows that there is an effect on the ratio due to the run time, T, though it is different than seen in the previous chapter. In Figure 5.11, the ratio resulting from $T = 10$ is consistently the most conservative result within this range of δ values.

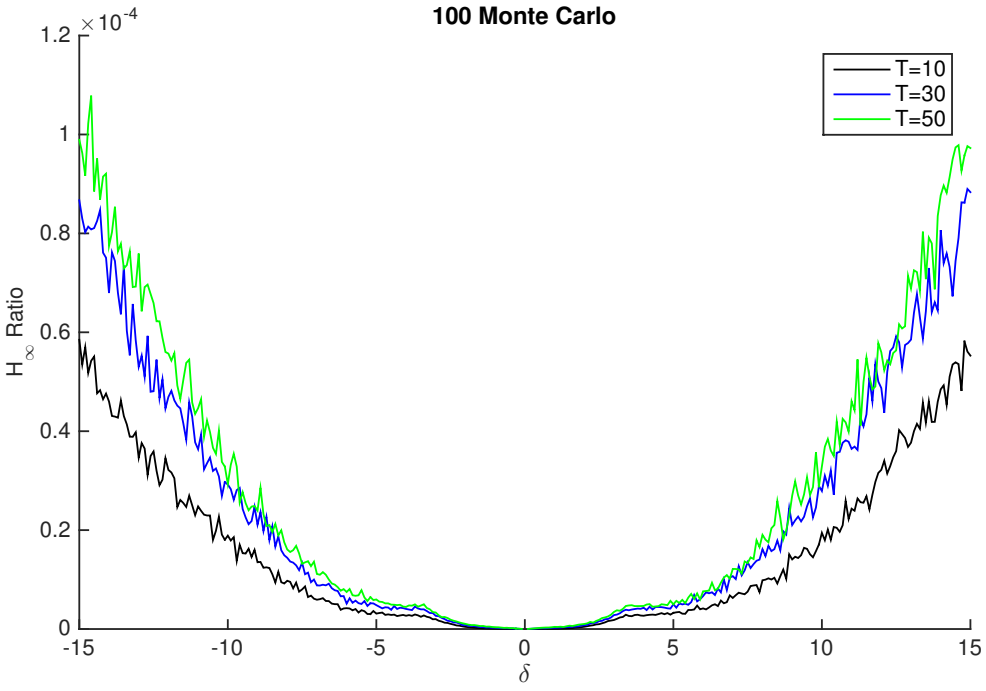

Figure 5.11: Sinusoidal nonlinearity - H_∞-gain to theoretical bound ratio

5.4.4 Quadratic Nonlinearity

The next nonlinearity considered is the quadratic, $f(y) = y^2$, with $w_k \in \ell_2$ and γ_k generated such that the mean is $\overline{\gamma} = 0.9$. The variable δ is swept from -20 to 20 in 0.1 increments to observe how the finite-time H_∞-bound varies with the disturbance magnitude as well as with the run time, T. Again, T takes the values $T = \{10, 30, 50\}$.

Figure 5.12 is a plot of the ratio in (5.41) for each run time, $T = \{10, 30, 50\}$. This figure shows similar results to those seen with the sinusoidal nonlinearity,

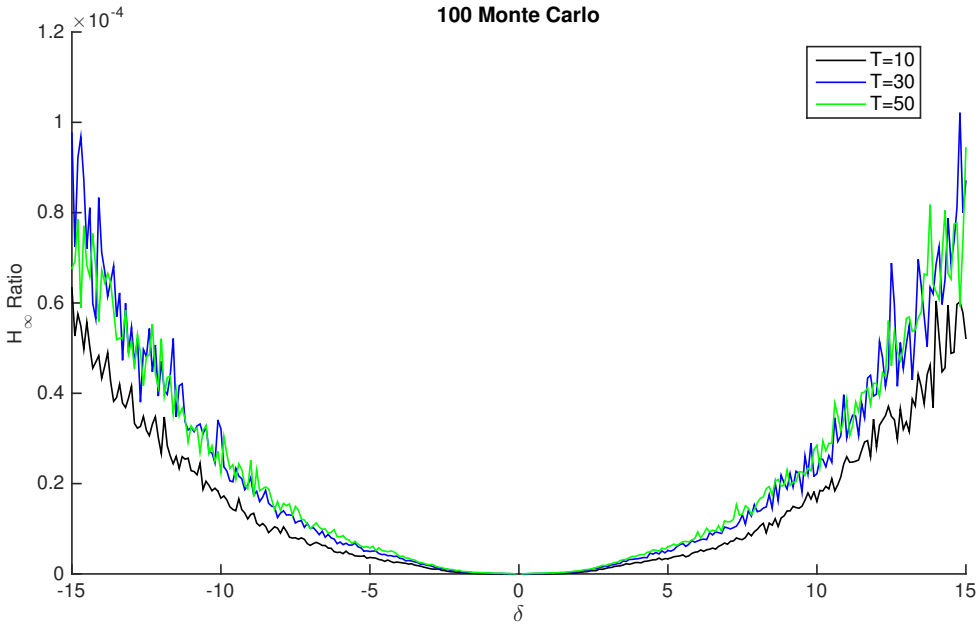

Figure 5.12: Quadratic nonlinearity - H_∞-gain to theoretical bound ratio

where the least/most conservative is rather indifferent for small δ but as δ increase, the result from $T = 10$ is the most conservative.

5.4.5 Cubic Nonlinearity

The most "severe" nonlinearity is the cubic, $f(y) = y^3$, with $w_k \in \ell_2$ and γ_k generated such that the mean is $\overline{\gamma} = 0.9$. The variable δ is swept from -20 to 20 in 0.1 increments to observe how the finite-time H_∞-bound varies with the disturbance magnitude as well as with the run time, T, which takes the values $T = \{10, 30, 50\}$.

Figure 5.13 is a plot of the ratio in (5.41) for each run time, $T = \{10, 30, 50\}$. As with the sinusoidal case in this chapter, this figure shows that the bound is valid in the range of δ and values of T being analyzed because the ratios remain between zero and one but the result for $T = 10$ is consistently the least conservative result for this range of disturbance magnitudes.

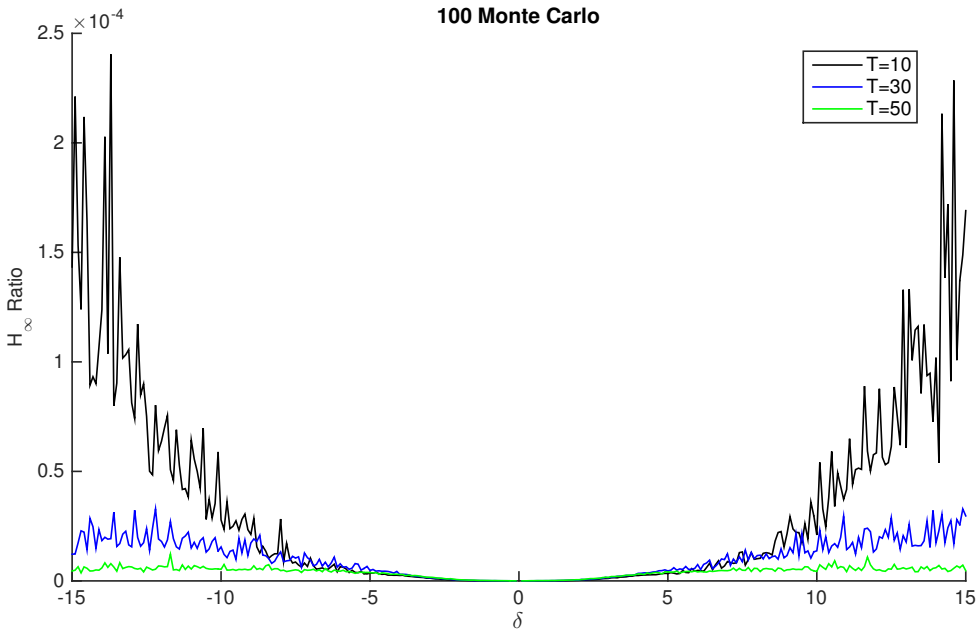

Figure 5.13: Cubic nonlinearity - H_∞-gain to theoretical bound ratio

5.4.6 Side-by-Side Comparison of Results from Three Nonlinearities

Lastly, the run time will be held constant to $T = 30$ and now the three types of nonlinearities covered will be co-plotted. Figure 5.14 shows that while for $|\delta| > 8$, the assumption that the least "severe" nonlinearity is the least conservative is true. It also shows that throughout the range of δ, the result for the sinusoidal and quadratic nonlinearities are very close.

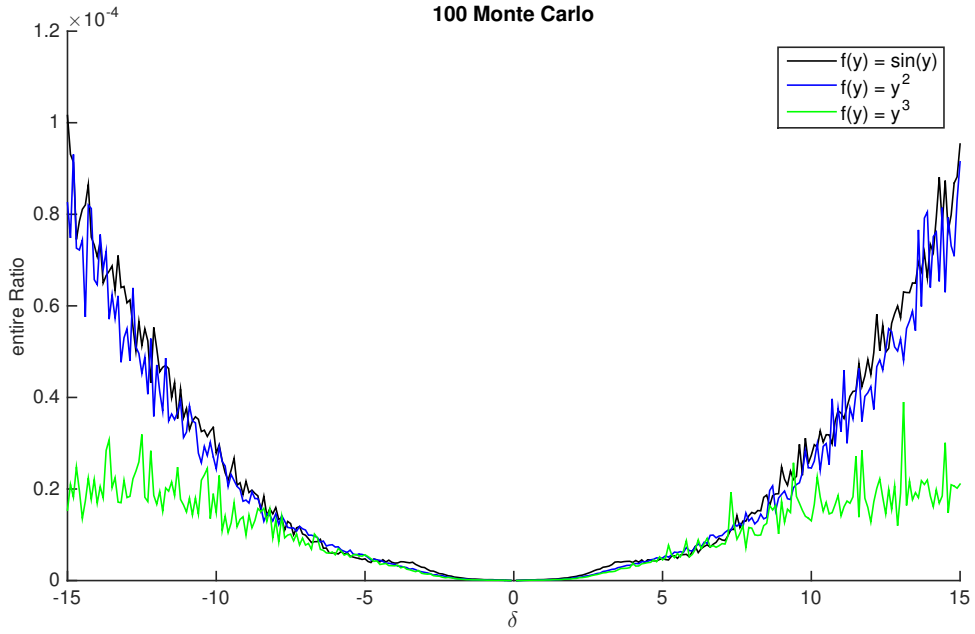

Figure 5.14: All three nonlinearities, T=30 - H_∞-gain to theoretical bound ratio

5.5 Summary

The discrete-time extended Kalman filter used as a nonlinear observer was analyzed for the finite-time H_∞-property in the presence of random disturbances and uncertain observations. The H_2-property of the estimation error when the disturbance is absent followed as a special case of this result. Simulation studies

were provided to demonstrate the effect of the run time on the validity and conservativeness of the finite-time H_∞-bound developed in this chapter. The results seen in this chapter were not as clear cut as those in Chapter 4, though when comparing the three levels of nonlinearity "severity" side-by-side, it was apparent that the most "severe" nonlinearity resulted in the most conservative result.

CHAPTER 6

EXTENSION: H_∞-PROPERTY OF THE CONTINUOUS-TIME EXTENDED KALMAN FILTER FOR SYSTEMS WITH $\mathcal{L}_2$ TYPE DISTURBANCES

Moving from the discrete-time domain to the continuous-time domain, the continuous-time EKF is analyzed. This EKF is designed for systems with zero mean white noise and correlation between the process and measurement and has been analyzed for systems that have $\mathcal{L}_2$ type disturbances. In previous work [9], Reif et al. consider the stochastic stability for this EKF; this work continues to move forward on the topic by analyzing the H_∞-property of this EKF.

6.1 System Description and the EKF as a Nonlinear Observer

Consider the nonlinear continuous-time system and measurement equations,

$$\dot{x} = f(x) + F_t w \tag{6.1}$$

$$y = h(x) + H_t w \tag{6.2}$$

where $x \in \Re^n$ is the state, $y \in \Re^p$ is the measurement, $f(x)$ and $h(x)$ are known analytic vector functions, the state and measurement disturbance coefficient matrices are $F_t \in \Re^{n\times l}$ and $H_t \in \Re^{p\times l}$, respectively, where the disturbance $w \in \Re^l$ is white with zero mean and identity covariance.

When the EKF [28] is used to estimate the state, the estimate is computed as

$$\dot{\hat{x}} = f(\hat{x}) + K_t(y - h(\hat{x})) \tag{6.3}$$

where $K_t \in \Re^{n\times p}$ is the Kalman gain

$$K_t = (P_t C_t^T + F_t H_t^T) R_t^{-1} \tag{6.4}$$

which is dependent on the solution of the associated matrix Riccati differential equation

$$\begin{aligned}\dot{P} =&(A_t - F_t H_t^T R_t^{-1} C_t)P_t + P_t(A_t - F_t H_t^T R_t^{-1} C_t)^T \\ &- P_t C_t^T R_t^{-1} C_t P_t + Q_t - F_t H_t^T R_t^{-1} H_t F_t^T\end{aligned} \tag{6.5}$$

where $Q \geq 0$ is an $n \times n$ matrix, $R > 0$ is a $p \times p$ matrix, and A_t and C_t are defined below. The matrices, Q and R, are chosen positive definite and chosen as $Q \triangleq F_t F_t^T + \epsilon I_n$ and $R \triangleq H_t H_t^T$ where $\epsilon > 0$ is arbitrary in the following development. Also, the Riccati equation for the inverse of $P_t > 0$ is used:

$$\begin{aligned}\frac{d(P_t^{-1})}{dt} =& - P_t^{-1}\mathcal{A}_t - \mathcal{A}_t^T P_t^{-1} \\ &+ C_t^T R_t^{-1} C_t - P_t^{-1} Q_t P_t^{-1} + P_t^{-1} F_t H_t^T R_t^{-1} H_t F_t^T P_t^{-1}\end{aligned} \tag{6.6}$$

with

$$\mathcal{A}_t = A_t - F_t H_t^T R_t^{-1} C_t \tag{6.7}$$

which is obtained from (6.5) using Lemma 8.

The EKF is set up by using first order approximations of the nonlinearities in the state and measurement using Taylor Series approximation evaluated at the state estimate such that

$$f(x) \cong f(\hat{x}) + A_t(x - \hat{x}) \tag{6.8}$$

$$h(x) \cong h(\hat{x}) + C_t(x - \hat{x}) \tag{6.9}$$

where

$$A_t = \left.\frac{\partial f(x)}{\partial x}\right|_{x=\hat{x}} \text{ and } C_t = \left.\frac{\partial h(x)}{\partial x}\right|_{x=\hat{x}} \tag{6.10}$$

Assumption 6.1. *The pair (A_t, C_t) is uniformly observable, with $\|A_t\|_i \leq \bar{a}$, $\|C_t\|_i \leq \bar{c}$ uniformly bounded in time.*

6.2 Error Analysis

The H_∞-property of the EKF for continuous-time systems is investigated for finite-energy disturbance, $w_k \in \mathcal{L}_2$. The estimation error is defined as

$$e = x - \hat{x} \tag{6.11}$$

The dynamics of the estimation error are obtained by using (6.1) and (6.3) in the time derivative of (6.11) to give

$$\dot{e} = f(x) + F_t w - f(\hat{x}) - K_t(y - h(\hat{x})) \tag{6.12}$$

By using (6.2) and regrouping terms, (6.12) becomes

$$\dot{e} = f(x) - f(\hat{x}) - K_t(h(x) - h(\hat{x})) + (F_t - K_t H_t)w \tag{6.13}$$

Applying the approximations in (6.8) and (6.9) to the error dynamics in (6.13) leads to

$$\dot{e} \cong (A_t - K_t C_t)e + (F_t - K_t H_t)w \tag{6.14}$$

which can also be written in matrix vector form as

$$\dot{e} \cong \begin{bmatrix} I_n & -K_t \end{bmatrix} \begin{bmatrix} A_t e + F_t w \\ C_t e + H_t w \end{bmatrix} \tag{6.15}$$

Theorem 6.1. *Consider the nonlinear system* (6.1) *and measurement equation* (6.2)*, with the disturbance taken as an element in* $\mathcal{L}_2$*. Let the state be estimated using an extended Kalman filter, which was designed for white noise with zero mean and unit covariance, with gain* K_t *from* (6.4)*. With the conditions in Assumption 6.1, Lemma 9 holds. With these conditions, the energy of the estimation error is bounded as follows*

$$\int_0^T \|e\|^2 dt \leq \frac{1}{\varphi_1}\left(e(0)^T P(0)^{-1} e(0) + \varphi_2 \int_0^T \|w\|^2 dt\right) \tag{6.16}$$

where

$$\varphi_1 \triangleq \inf_t(\lambda_{min}(\tilde{Q}_t)) - \beta \tag{6.17}$$

$$\varphi_2 \triangleq \beta^{-1} \sup_t(\lambda_{max}(\Phi_t)) \tag{6.18}$$

$$\Phi_t \triangleq \begin{bmatrix} F_t^T & H_t^T \end{bmatrix} \begin{bmatrix} P_t^{-1} \\ -K_t^T P_t^{-1} \end{bmatrix} \begin{bmatrix} P_t^{-1} & -P_t^{-1}K_t \end{bmatrix} \begin{bmatrix} F_t \\ H_t \end{bmatrix} \tag{6.19}$$

and

$$\widetilde{Q}_t \triangleq P_t^{-1}(Q_t - F_t H_t^T R_t^{-1} H_t F_t^T)P_t^{-1} + C_t^T R_t^{-1} C_t > 0 \tag{6.20}$$

when $\beta > 0$ is an arbitrary constant.

Proof. Lyapunov analysis is used to determine the convergence of the estimation error in the presence of finite energy disturbances and obtain the H_∞-gain. The Lyapunov energy function candidate,

$$V(t) = e^T P_t^{-1} e \tag{6.21}$$

is analyzed along the dynamics of the error (6.14) to verify that the energy decreases over time. To this end, consider the following Lyapunov differential equation

$$\dot{V}(t) = e^T \frac{d(P_t^{-1})}{dt} e + 2e^T P_t^{-1} \dot{e} \tag{6.22}$$

Applying the Kalman gain (6.4), and substituting (6.6) and (6.15) into (6.22) yields

$$\begin{aligned} \dot{V} \cong\ & e^T(-P_t^{-1}\mathcal{A}_t - \mathcal{A}_t^T P_t^{-1} + C_t^T R_t^{-1} C_t - P_t^{-1} Q_t P_t^{-1} + P_t^{-1} F_t H_t^T R_t^{-1} H_t F_t^T P_t^{-1})e \\ & + 2e^T P_t^{-1} \begin{bmatrix} I_n & -(P_t C_t^T + F_t H_t^T)R^{-1} \end{bmatrix} \begin{bmatrix} A_t e + F_t w \\ C_t e + H_t w \end{bmatrix} \end{aligned} \tag{6.23}$$

By collecting terms, (6.23) can be written as

$$\dot{V} = -e^T \widetilde{Q}_t e + 2e^T \begin{bmatrix} P_t^{-1} & -(C_t^T + P_t^{-1} F_t H_t^T)R^{-1} \end{bmatrix} \begin{bmatrix} F_t \\ H_t \end{bmatrix} w \tag{6.24}$$

where $\widetilde{Q}_t$ is given by (6.20).

To guarantee $\dot{V} < 0$, an overall upper bound for (6.24) is established by finding appropriate bounds for each term. The second term in (6.24) is bounded using Lemma 10, which yields

$$\begin{aligned} & e^T \begin{bmatrix} P_t^{-1} & -(C_t^T + P_t^{-1} F_t H_t^T) R^{-1} \end{bmatrix} \begin{bmatrix} F_t \\ H_t \end{bmatrix} w \\ & + w^T \begin{bmatrix} F_t^T & H_t^T \end{bmatrix} \begin{bmatrix} P_t^{-1} \\ -R^{-1}(C_t^T + P_t^{-1} F_t H_t^T)^T \end{bmatrix} e \\ & \leq \beta e^T e + \beta^{-1} w^T \Phi_t w \end{aligned} \tag{6.25}$$

with Φ_t in (6.19) and $\beta > 0$. Therefore, a sufficient condition for (6.22) to hold is

$$\dot{V} \leq -e^T (\widetilde{Q}_t - \beta I_n) e + \beta^{-1} w^T \Phi_t w \tag{6.26}$$

To obtain an overall upper bound, the negative term is lower bounded and the positive term is upper bounded using Lemma 3,

$$\widetilde{Q}_t - \beta I_n \geq \inf_t (\lambda_{min}(\widetilde{Q}_t)) - \beta \triangleq \varphi_1 \tag{6.27}$$

$$\beta^{-1} \left\| \Phi_t \right\|_i \leq \beta^{-1} \sup_t (\lambda_{max}(\Phi_t)) \triangleq \varphi_2 \tag{6.28}$$

yielding the inequality

$$\dot{V} \leq -\varphi_1 \|e\|^2 + \varphi_2 \|w\|^2 < 0 \tag{6.29}$$

Considering Lemma 9 in (6.27) and (6.28), φ_1 and φ_2 are both positive finite constants under Assumption 6.1 for sufficiently small values of β.

To obtain the H_∞-property, the ratio of the estimation error energy to the disturbance energy is analyzed; (6.29) is integrated from $t = 0$ to $t = T$ (for all $T \geq 0$) giving

$$V(T) - V(0) \leq -\varphi_1 \int_0^T \|e\|^2 dt + \varphi_2 \int_0^T \|w\|^2 dt \tag{6.30}$$

and for $V(T) \geq 0$,

$$-V(0) \leq -\varphi_1 \int_0^T \|e\|^2 dt + \varphi_2 \int_0^T \|w\|^2 dt \tag{6.31}$$

which can be rearranged as

$$\int_0^T \|e\|^2 dt \leq \frac{1}{\varphi_1} \left(V(0) + \varphi_2 \int_0^T \|w\|^2 dt \right) \tag{6.32}$$

This result shows the relationship of the energy of the error to the initial estimation error, $V(0) = e(0)P(0)^{-1}e(0)$, and the disturbance energy, $\int_0^T \|w\|^2 dt$, with φ_1 and φ_2 defined in (6.17) and (6.18). ■

6.3 Significance

If the initial estimate has zero error, the result (6.32) is the H_∞-property resulting in the H_∞-gain below,

$$\frac{\int_0^T \|e\|^2}{\int_0^T \|w\|^2} \leq \frac{\varphi_2}{\varphi_1} \tag{6.33}$$

where φ_1 and φ_2 are defined in (6.17) and (6.18), respectively.

On the other hand, if there is no disturbance in the system for $t \geq 0$, then (6.32) results in a special case that presents a bound on the estimation error energy in terms of the initial conditions, $V(0) = e(0)^T P(0)^{-1} e(0)$, i.e. the H_2-property of the EKF

$$\int_0^T \|e\|^2 \leq \frac{1}{\varphi_1} V(0) \tag{6.34}$$

6.4 Simulations

Simulations are presented that demonstrate the H_∞-property of the continuous-time EKF. First, three cases are analyzed to show the necessity for sufficiently small initial error and disturbance energy. These simulations show

that for sufficiently small error in the initial estimate and disturbances with sufficiently small energy, the estimation error is asymptotically stable, accommodating the effect of the disturbances with a finite bound on the energy gain. Then using the same initial estimate, simulations show that, even for a stable system, sufficiently large disturbances render the estimation error unstable. When the magnitude of the disturbance is reduced and the error in the initial estimate is increased, the simulations show that there is a limit to the amount of error allowed in the initial estimate. An additional study demonstrates how the H_∞-gain changes due to different disturbance magnitudes.

6.4.1 Effect of Initial Conditions and Disturbance Magnitude

The nonlinear system from [9] is used with modifications for a finite-energy disturbance given by

$$\dot{x} = \begin{bmatrix} x_2 \\ -x_1 + (x_1^2 + x_2^2 - 1)x_2 \end{bmatrix} + \begin{bmatrix} 0.2 & 1 \\ 0 & 0.1 \end{bmatrix} w \tag{6.35}$$

$$y = x_1 + \begin{bmatrix} 0.1 & 0.1 \end{bmatrix} w \tag{6.36}$$

$$w = \delta \begin{bmatrix} e^{-0.5t} \\ e^{-t} \end{bmatrix} \tag{6.37}$$

where δ is the disturbance magnitude that is varied in the simulation cases below and $x(0) = \begin{bmatrix} 0.8 & 0.2 \end{bmatrix}^T$.

Following the procedure for the EKF, the nonlinearities are linearized via a Taylor Series approximation around the state estimate

$$\left.\frac{\partial f}{\partial x}\right|_{x=\hat{x}} = \begin{bmatrix} 0 & 1 \\ -1 + 2\hat{x}_1\hat{x}_2 & \hat{x}_1^2 + 3\hat{x}_2^2 - 1 \end{bmatrix} = A_t \tag{6.38}$$

$$\left.\frac{\partial h}{\partial x}\right|_{x=\hat{x}} = \begin{bmatrix} 1 & 0 \end{bmatrix} = C_t \tag{6.39}$$

These time varying matrices are used to calculate the solution to the Riccati equation and the Kalman gain at each instance in time, with $Q = FF^T + I_2$, $R = HH^T$, and $P(0) = I_2$. The first three cases analyzed via MATLAB simulation are given in Table 6.1 along with the qualitative stability analysis.

Table 6.1: Initial values and disturbance magnitude effect on error

	Case 1	Case 2	Case 3
$\hat{x}(0)$	$\begin{bmatrix}0.9 & 0.3\end{bmatrix}^T$	$\begin{bmatrix}0.9 & 0.3\end{bmatrix}^T$	$\begin{bmatrix}2.8 & 2.2\end{bmatrix}^T$
Disturbance, δ	0.1	5	0.1
Error Stability	Stable	Unstable	Unstable
Figures	6.1, 6.2, 6.3	6.4, 6.5, 6.6	6.7, 6.8, 6.9

Case 1 consists of a small error in the initial state estimate as well as a small disturbance magnitude. Figures 6.1 and 6.2 show that for this asymptotically stable system, the estimate is also asymptotically stable resulting in the same performance for the estimation error, Figure 6.3. Using the same initial value for the estimate, case 2 has a large magnitude for the finite energy disturbance. Figures 6.4 and 6.5 show that with this larger disturbance, the estimate does not track both state variables with Figure 6.6 showing the estimation error as unstable. Case 3 has large error in the initial estimate of the state with a small magnitude of the disturbance. Figures 6.7 and 6.8 show that even though the state itself is stable, the estimate is unable to track it, causing the unstable error response in Figure 6.9.

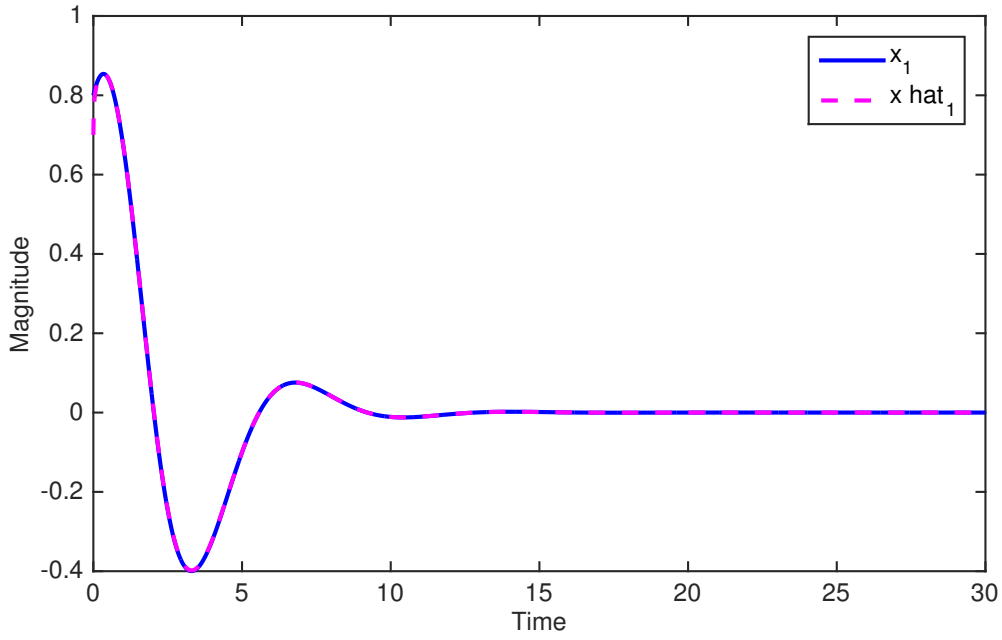

Figure 6.1: Case 1 - x_1 and the estimate of x_1

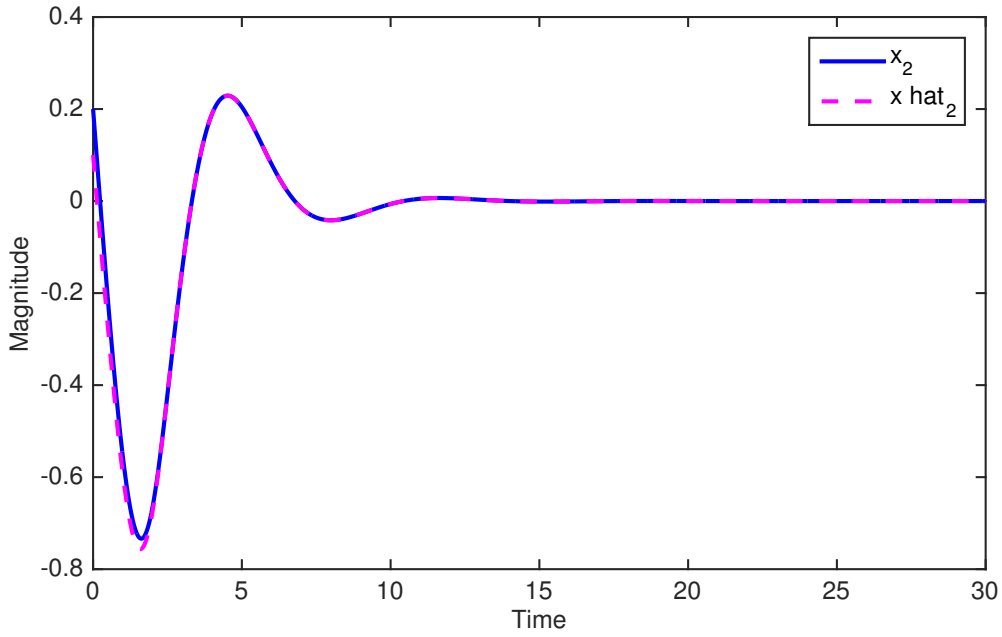

Figure 6.2: Case 1 - x_2 and the estimate of x_2

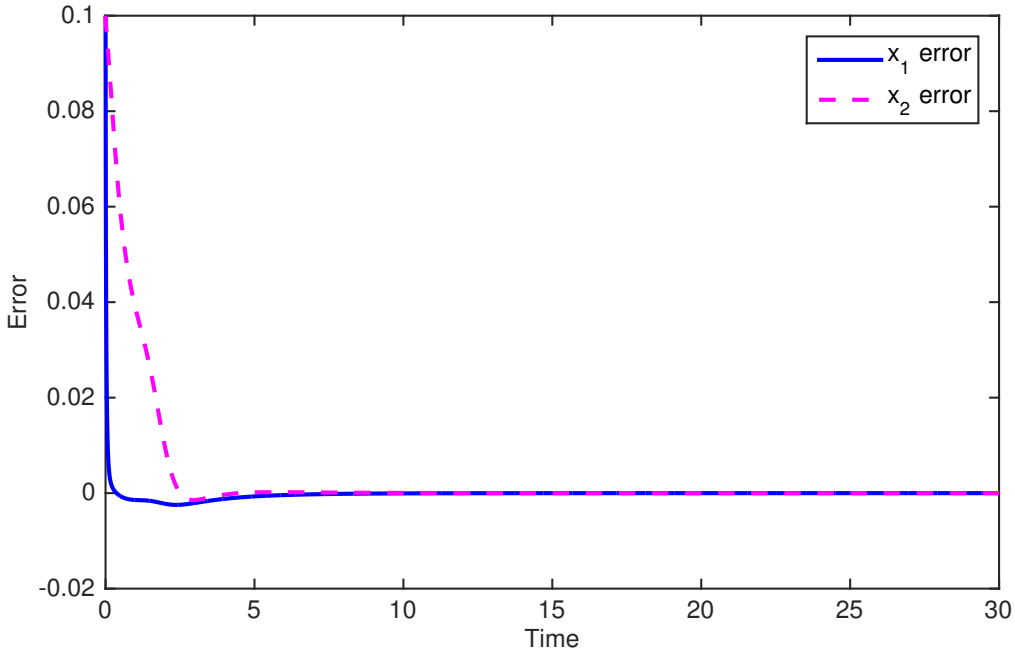

Figure 6.3: Case 1 - Error between the state and the estimate

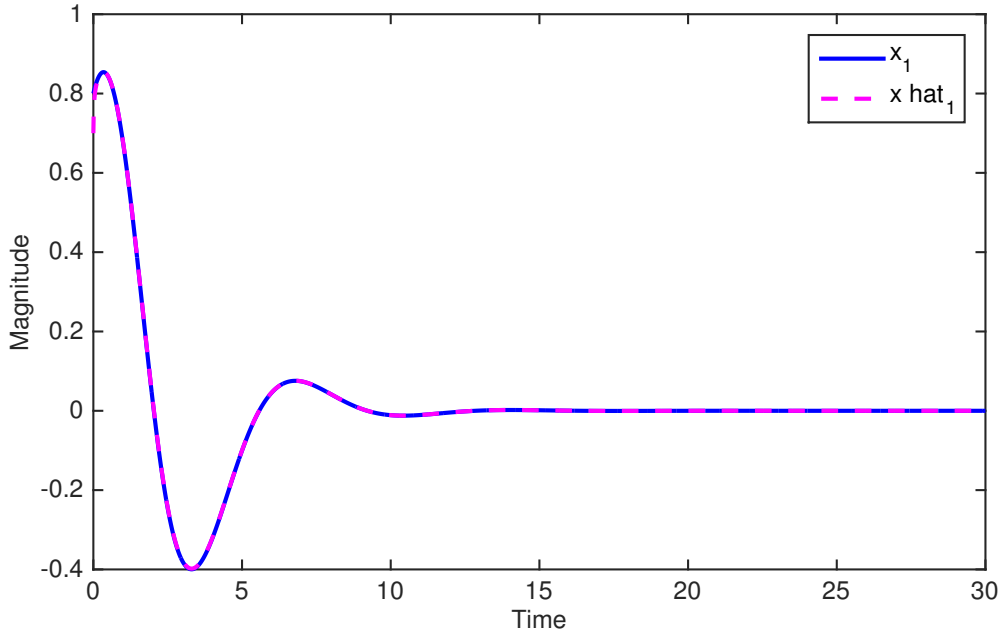

Figure 6.4: Case 2 - x_1 and the estimate of x_1

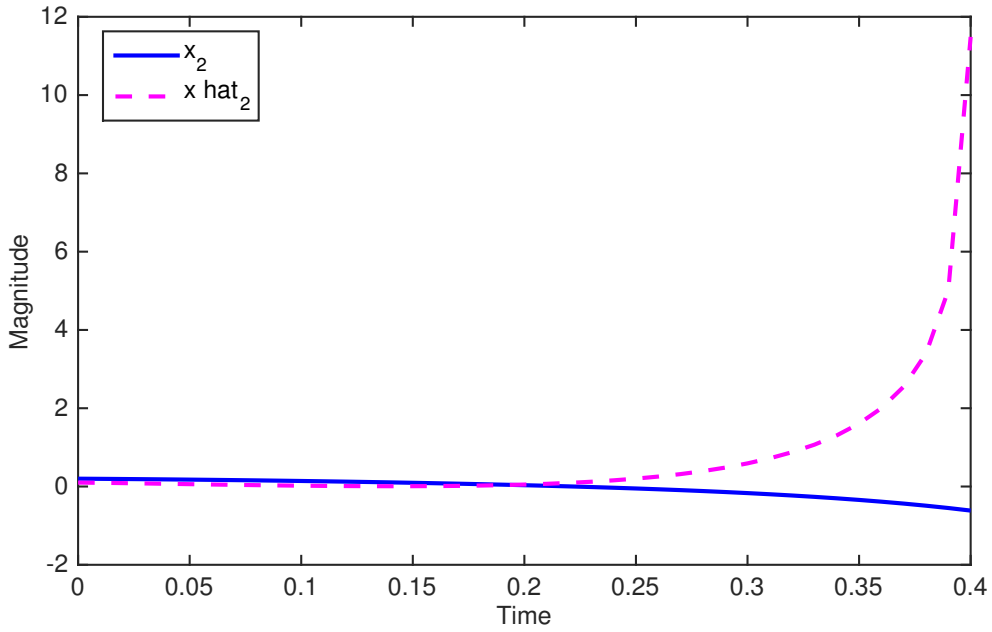

Figure 6.5: Case 2 - x_2 and the estimate of x_2

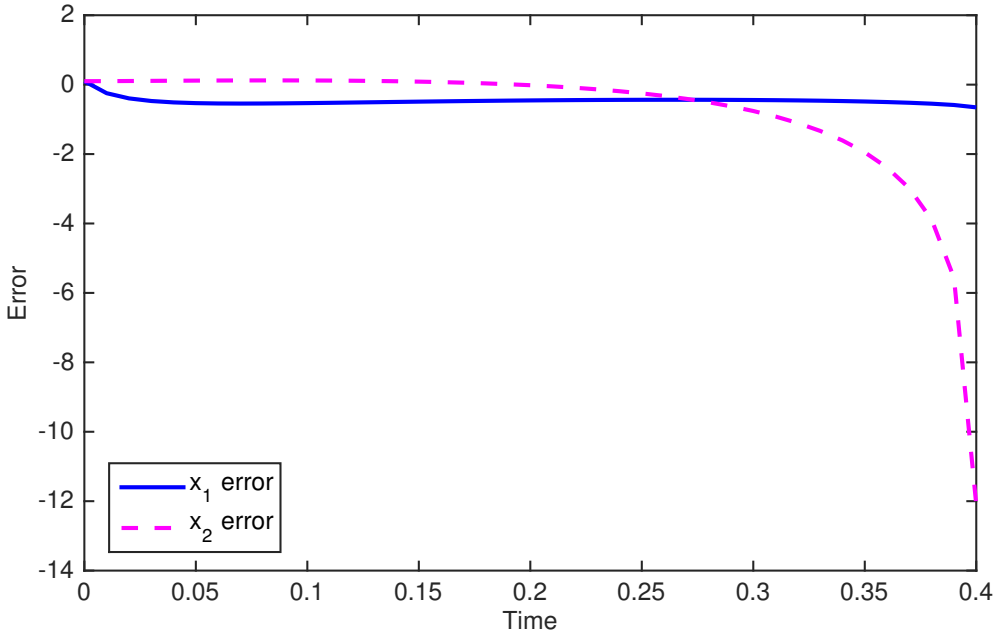

Figure 6.6: Case 2 - Error between the state and the estimate

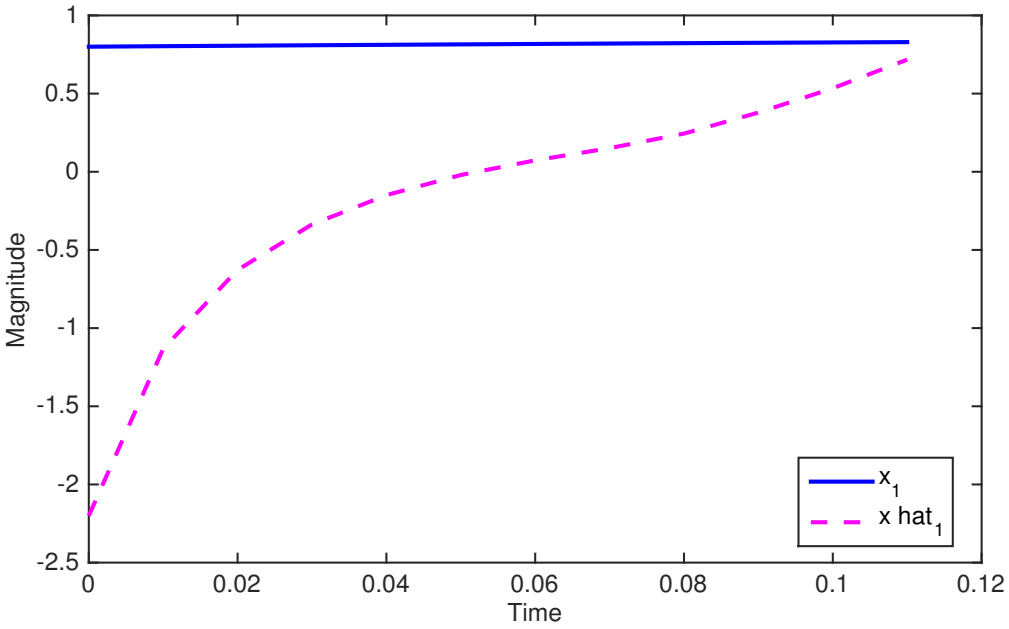

Figure 6.7: Case 3 - x_1 and the estimate of x_1

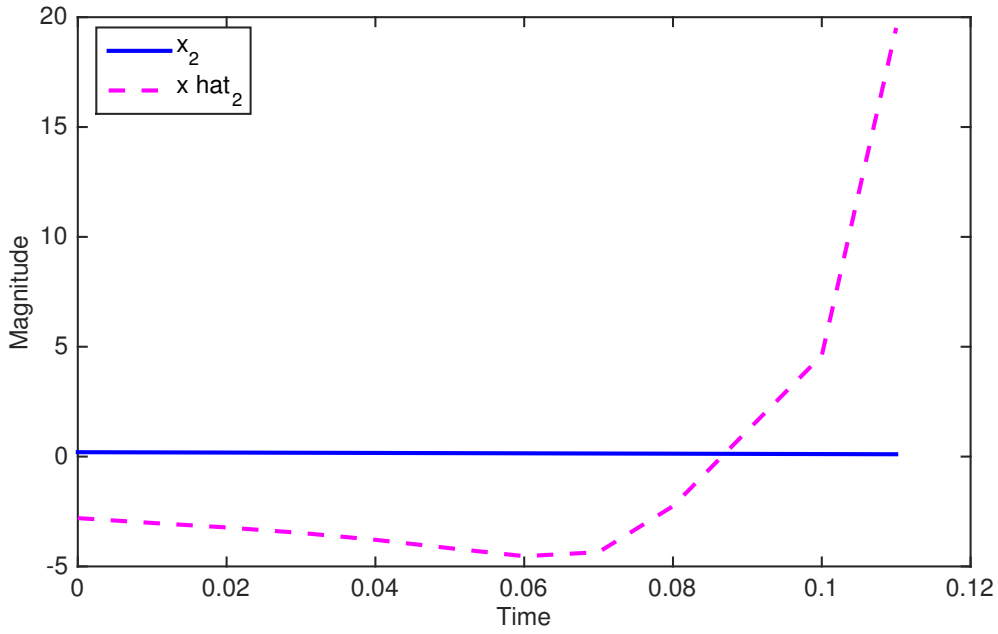

Figure 6.8: Case 3 - x_2 and the estimate of x_2

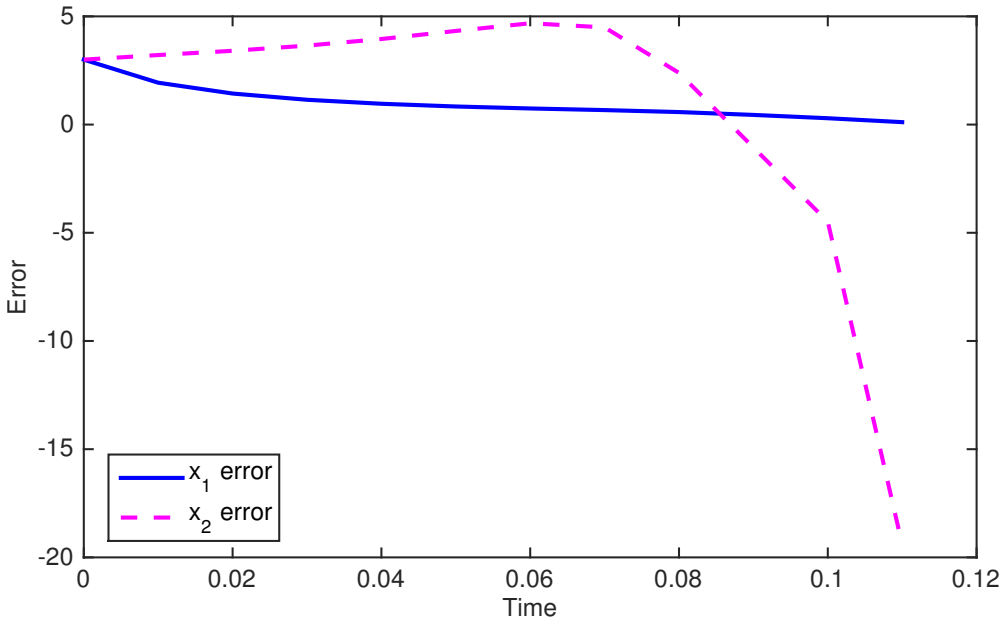

Figure 6.9: Case 3 - Error between the state and the estimate

In addition to these three cases, the H_∞-gain is studied for the same system by setting the initial estimation error equal to zero and changing the amplitude of the disturbance by varying δ from -0.2 to $+0.2$ in 0.004 increments. The left hand side of (6.33) is approximated as the ratio of the Riemann sums of the numerator and denominator. The results from this analysis are given in Figure 6.10, which shows that the relationship between the disturbance magnitude and the H_∞-gain is nonlinear. Note that when there is no disturbance, $\delta = 0$, one cannot obtain an H_∞-gain and is the reason for the gap at $\delta = 0$.

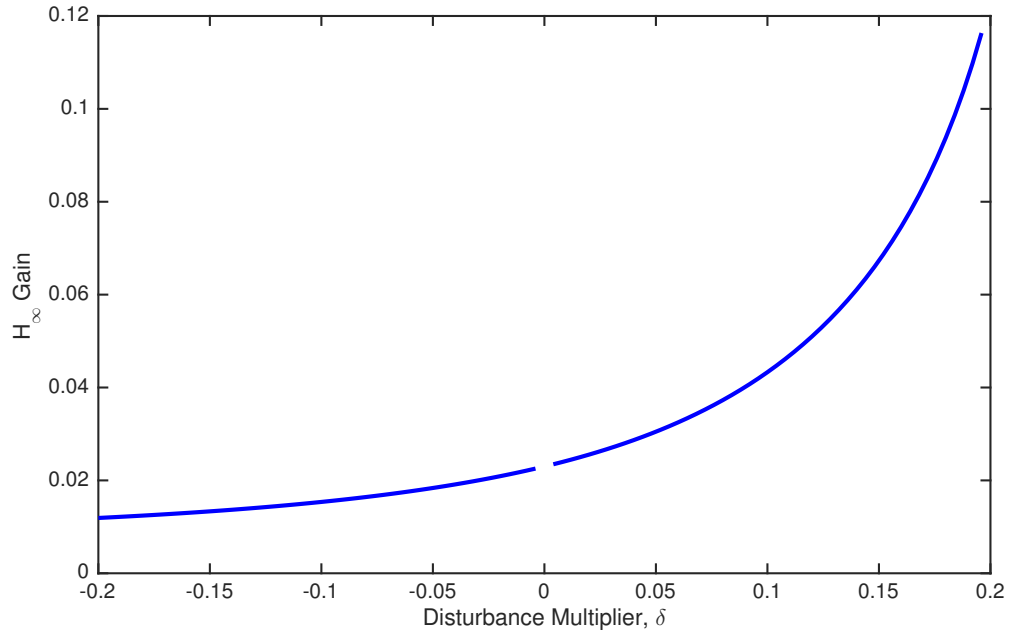

Figure 6.10: Second order system - H_∞ analysis

6.4.2 H_∞-Gain to Theoretical Bound Comparison - Sinusoidal Nonlinearity

Both the H_∞-gain and the H_∞-bound are analyzed for the following mass-spring-damper system with a spring that has a sinusoidal nonlinearity

$$\dot{x} = \begin{bmatrix} x_2 \\ -\sin(x_1) - bx_2 \end{bmatrix} + \begin{bmatrix} 0.2 & 1 \\ 0 & 0.1 \end{bmatrix} w \tag{6.40}$$

$$y = \begin{bmatrix} 1 & 0 \end{bmatrix} x + \begin{bmatrix} 0.1 & 0.1 \end{bmatrix} w \tag{6.41}$$

$$w = \delta \begin{bmatrix} e^{-1.5t} \\ e^{-3.5t} \end{bmatrix} \tag{6.42}$$

The initial conditions are

$$x(0) = \hat{x}(0) = \begin{bmatrix} 0.1 & 0.1 \end{bmatrix}^T \tag{6.43}$$

$$P(0) = \begin{bmatrix} 1 & 0 \\ 0 & 1 \end{bmatrix} \tag{6.44}$$

The disturbance magnitude, δ, is varied from -1 to $+1$ in 0.02 increments. The Riemann sum method is used to approximate the left hand side of (6.33), the H_∞-gain. In addition, the simulation data is used to determine the right hand side of (6.33), the H_∞-bound, with $\beta = 0.1$ and $\epsilon = 1$. These two values are compared via a ratio of the H_∞-gain from simulation to the theoretical H_∞-bound. Since the ratio in Figure 6.11 has values that are always positive and less than one, this shows the H_∞-bound is consistently greater than the H_∞-gain and therefore validates that, for this range of δ values, there is an H_∞-property.

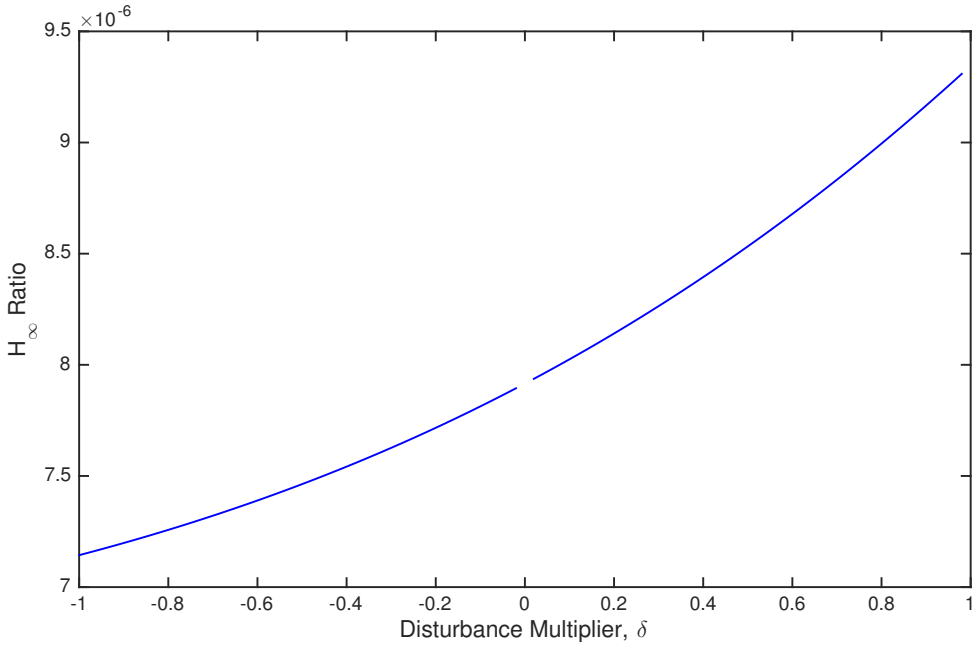

Figure 6.11: Sinusoidal nonlinear system: H_∞-gain and H_∞-bound ratio

Since the response of the ratio in Figure 6.11 verifies that this system has an H_∞ property, it is of interest to observe how the H_∞-gain itself varies with differing disturbance magnitudes. Figure 6.12 shows a nonlinear relationship between the H_∞-gain and the disturbance magnitudes, with a smaller gain for negative disturbance magnitudes and a larger response for disturbance

magnitudes greater than zero.

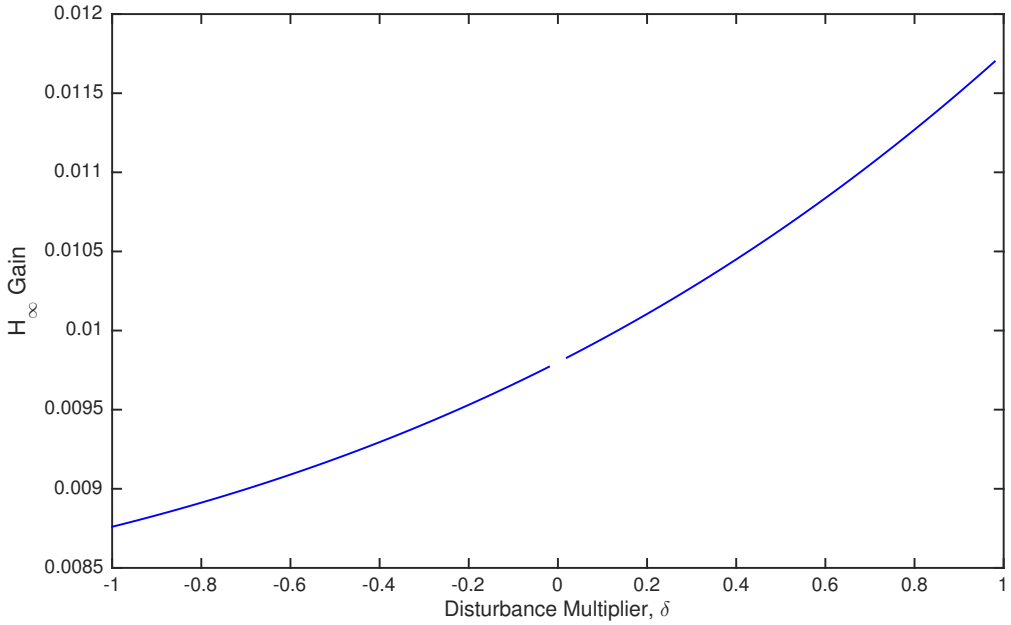

Figure 6.12: Sinusoidal nonlinear system: H_∞-gain

6.4.3 H_∞-Gain to Theoretical Bound Comparison - Cubic Nonlinearity

Again, the H_∞-gain and the H_∞-bound are analyzed, this time for the following mass-spring-damper system with a spring that has a cubic nonlinearity

$$\dot{x} = \begin{bmatrix} x_2 \\ -x_1^3 - bx_2 \end{bmatrix} + \begin{bmatrix} 0.2 & 1 \\ 0 & 0.1 \end{bmatrix} w \tag{6.45}$$

$$y = \begin{bmatrix} 1 & 0 \end{bmatrix} x + \begin{bmatrix} 0.1 & 0.1 \end{bmatrix} w \tag{6.46}$$

$$w = \delta \begin{bmatrix} e^{-1.5t} \\ e^{-3.5t} \end{bmatrix} \tag{6.47}$$

The initial conditions are

$$x(0) = \hat{x}(0) = \begin{bmatrix} 0.1 & 0.1 \end{bmatrix}^T \tag{6.48}$$

$$P(0) = \begin{bmatrix} 1 & 0 \\ 0 & 1 \end{bmatrix} \tag{6.49}$$

The disturbance magnitude, δ, is varied from -1 to $+1$ in 0.02 increments. The Riemann sum method is used to approximate the left hand side of (6.33), the H_∞-gain. In addition, the simulation data is used to determine the right hand side of (6.33), the H_∞-bound, with $\beta = 0.1$ and $\epsilon = 1$. These two values are compared via a ratio of the H_∞-gain from simulation to the theoretical H_∞-bound. Since the ratio in Figure 6.13 has values that are always positive and less than one, this shows the H_∞-bound is consistently greater than the H_∞-gain and therefore validates that, for this range of δ values, there is an H_∞-property.

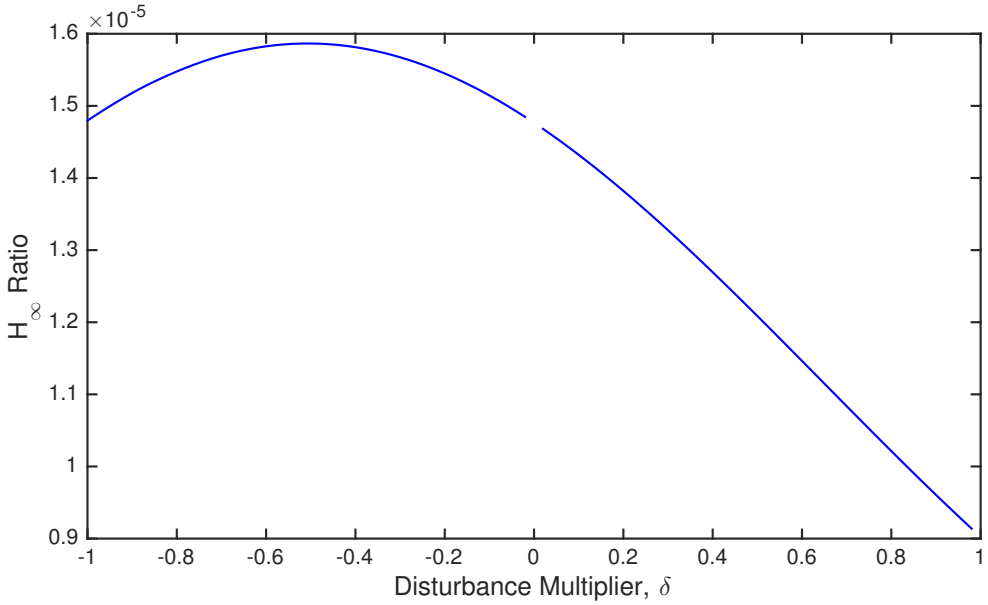

Figure 6.13: Cubic nonlinear system: H_∞-gain and H_∞-bound ratio

When observing how the H_∞-gain varies with differing disturbance magnitudes, Figure 6.14 shows a nonlinear relationship between the H_∞-gain and the disturbance magnitudes. This system has a different relationship to that seen for the system with the sinusoidal nonlinearity.

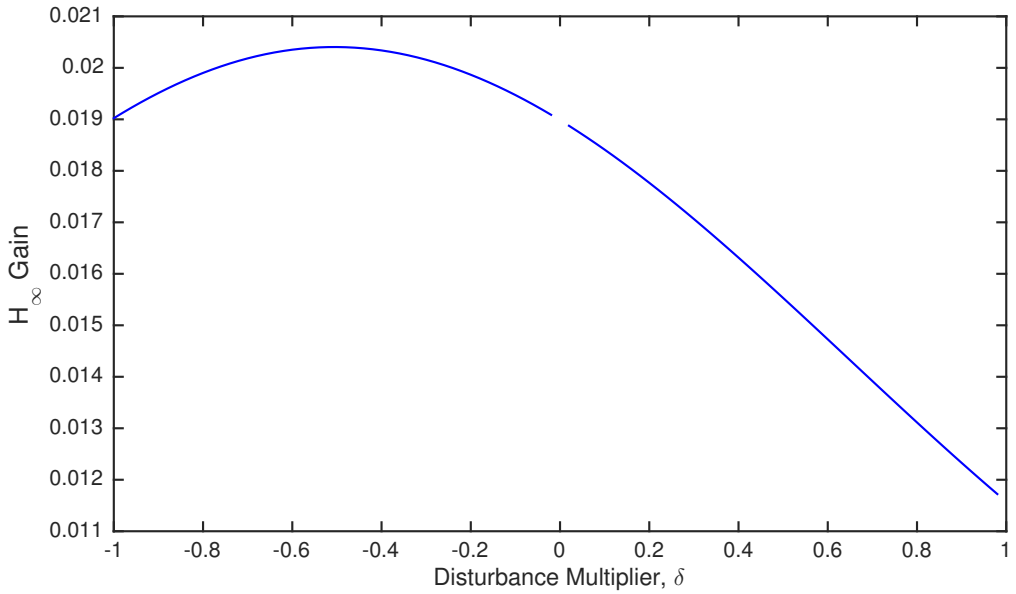

Figure 6.14: Cubic nonlinear system: H_∞-gain

These examples have highlighted various aspects regarding the H_∞-propety of the continuous-time EKF. The first case studies show that there is a limit to both the initial error as well as the amount of disturbance energy regarding the convergence of the estimation error. The second and third examples show that while both exhibit the H_∞-property in the respective disturbance magnitude ranges, the actual H_∞-gain is quite different for the two systems.

6.5 Summary

The continuous-time extended Kalman filter used as a nonlinear observer is analyzed for the H_∞-property. The H_2-property of the estimation error when

the disturbance is absent follows as a special case of this result. Simulation studies are presented to validate the results. It is proven mathematically and verified by simulations that, in addition to the noise filtering, the EKF has the H_∞-property, where the estimation error energy to disturbance energy ratio is finite if the initial estimation error and the disturbance magnitude are sufficiently small.

CHAPTER 7

CONCLUSION AND FUTURE WORK

The ubiquitous discrete-time extended Kalman filter is analyzed for its ability to attenuate finite-energy disturbances. The property of specific interest is the H_∞-property. Knowledge of this property gives a designer insight into the effectiveness of their extended Kalman filter in the face of finite-energy disturbances and it is shown that a bound can be calculated based on system parameters. Variations of the discrete-time extended Kalman filter are analyzed for both general convergence and the H_∞-property. Lastly, this work is extended to continuous-time, where the continuous-time extended Kalman filter is shown to also inherently possess the H_∞-property.

7.1 Summary

This dissertation began by introducing finite-energy disturbances, which are essential to consider H_∞. The definition of H_∞ is such that for a disturbance with bounded or finite-energy, the energy of the estimation error is also bounded. This works reveals the H_∞-property in EKFs designed for various models through the use of Lyapunov convergence techniques.

The first EKF that is analyzed is the basic EKF designed for systems with white noise. In Chapter 2, the development for this EKF in the direct form is provided rather than the more commonly used form of the EKF algorithm, the predict-update form. By using the EKF in the direct form, fewer assumptions are required on the system compared to previous works that analyze the EKF in the predict-update form. Once the EKF is defined, it is applied to a noise-free system and Lyapunov analysis is performed. In the Lyapunov analysis, there are steps in

the derivation where, by taking advantage of the direct form of the EKF, the inequalities are of a form to apply the Schur complement when proving positive definiteness making the derivations easier and with less restrictive results. At the end of the Lyapunov analysis, it is shown that the EKF used for a noise-free system would converge under Assumption 2.1, the pair (A_k, C_k) is uniformly observable, with $\|A_k\|_i \leq \bar{a}$, $\|C_k\|_i \leq \bar{c}$, $\|F_k\|_i \leq \bar{f}$, and $\|H_k\|_i \leq \bar{h}$ uniformly bounded in time, without having to make assumptions on the invertibility of the system Jacobian as in previous work. To analyze if the EKF also inherently has the H_2-property, the summation of both sides of the inequality is taken from 0 to any integer $T > 0$. Simulations are provided that compare the H_2-gain from simulation to the theoretical bound which validate the result by showing that the bound is never exceeded.

Similarly, the same EKF used in Chapter 2 is used in Chapter 3 for systems with finite-energy disturbances. Using the direct form of the EKF in the Lyapunov analysis, it is possible to show convergence of this EKF. Additionally, taking the summation of the resulting inequality from the Lyapunov analysis, bounds on the H_∞- and H_2-properties are developed. Simulations are provided to demonstrate that initial conditions and disturbance magnitude both affect the convergence of the estimation error. For sufficiently small disturbance magnitude and initial error, the estimation error of the EKF will converge. Additionally, the ratio between the H_∞-gain from simulation to the theoretical bound is analyzed and shows the bound is never exceeded.

In Chapter 4, the system used in the EKF design is a system model with uncertain measurements. Unlike the previous system model, this model has a measurement that always contains noise and randomly may or may not also include the measured signal. The development of this modified EKF is provided in the direct form. In the Lyapunov analysis, there are extra terms due to the

uncertainty in the measurements, which leads to finite-time H_∞- and H_2-properties. Simulations are performed that show the effect of the disturbance magnitude and initial conditions on the boundedness of the estimation error. Additionally the ratio of the H_∞-gain to theoretical bound is analyzed for varying disturbances magnitudes as well as different run time values. The simulations show that the bound is never exceeded for systems that met the conditions in Assumption 4.1, the pair (A_k, C_k) is uniformly observable, with $\|A_k\|_i \leq \bar{a}$, $\|C_k\|_i \leq \bar{c}$, $\|F_k\|_i \leq \bar{f}$, $\|H_k\|_i \leq \bar{h}$, and $\|h(x_k)\| \leq \alpha_h$ uniformly bounded in time. A special case of this result is shown in Chapter 5 for uncertain measurement models that have a simultaneously failing sensors. Simulations, similar to those in Chapter 4, are performed to observe the effect of initial conditions and disturbance magnitude on the H_∞-gain and bound.

Chapter 6 moved into the continuous-time domain, in which the continuous-time EKF was analyzed using Lyapunov analysis. It was shown that, similar to what was seen with the discrete-time EKF, this EKF inherently has the H_∞- and H_2-properties. Simulations show that these properties, along with general convergence, rely heavily on the initial conditions, disturbance magnitude, and the severity of the nonlinearities.

Additionally, the discrete-time EKFs applied to the various models in Chapters 2 through 5 are simulated using similar nonlinear systems with varying severity: sinusoidal, quadratic, and cubic. It is consistently seen in each chapter, that for large enough disturbance magnitudes, the least severe nonlinearity, sinusoidal, is the least conservative result while the most severe nonlinearity, cubic, is the most conservative result. Therefore, it is inferred through simulation that systems with more severe nonlinearities are more likely to fail system assumptions when there is a large initial error or large disturbance magnitude.

7.2 Conclusions

In conducting this research, it is discovered that the inherent relationship between the Riccati difference equation and the Lyapunov difference inequality could be exploited in the convergence analysis of the EKF. This relationship is used in combination with the Schur Complement, Lemma 4, to show positive definiteness in the Lyapunov convergence analysis. By applying the Schur complement in the Lyapunov inequality, an equivalent condition for positive definiteness is given. This new condition has many terms that cancel due to the similarities between the Riccati difference equation and the Lyapunov difference inequality. The benefit of this relationship to the convergence analysis is discovered due to the discrete-time EKF being analyzed in the direct form. The ability to exploit this relationship in the convergence proof can continue to be investigated with other variations of the discrete-time and continuous-time EKFs.

7.3 Future Work

This work is just the beginning of error convergence and energy analysis on extended Kalman filters represented in the direct form. Deeper analysis into simulation results presented in this dissertation can be performed. In Chapter 2, it can be investigated as to why Figure 2.3 has the minimum of the H_2 ratio of the gain from simulation to the theoretical bound approximately along the 30° line and the maximum approximately along the 120° line.

The sampling period used in many of the simulations was $T = 0.01s$. This caused the nonlinearity in some of the cases to appear negligible compared to the noise in the system. The investigation of the sample period's affect on the accuracy of the bound can be performed. Key points to consider are: 1) if the shape of the ratio between the gain from simulation to the theoretical bound

changes with different sampling periods and 2) how the sampling period affects the accuracy, based on whether the resulting ratio is larger or smaller than that presented in this dissertation.

The choice of the Lyapunov function candidate used throughout this dissertation enables the exploitation of the relationship between the Lyapunov difference inequality and the Riccati difference equations allowing for the proof of positive definiteness and upper boundedness at critical points in the derivations. However, the choice of the Lyapunov function candidate can be changed in an attempt to achieve a tighter bound.

This work could be extended to the most general EKF in [23] which would add uncertainty on the estimation gain. The techniques herein could also be applied to various EKFs for systems with stochastic nonlinearities [29], [30] or for systems with the nonlinearity as a function of both the state variables and the disturbances. Additionally, the linear unbiased state estimator for systems with random sensor delays [31] could be extended for nonlinear systems followed by convergence, H_2, and H_∞ analysis.

BIBLIOGRAPHY

[1] R. Kalman, "A new approach to linear filtering and prediction problems," *J. Basic Eng.*, vol. 82, no. 1, pp. 35–45, 1960.

[2] F. L. Lewis, *Optimal Estimation*. New York: Wiley, 1986.

[3] D. Simon, *Optimal State Estimation*. New Jersey: Wiley, 2006.

[4] H. Guo, H. Chen, F. Xu, F. Wang, and G. Lu, "Implementation of EKF for vehicle velocities estimation on FPGA," *IEEE Trans. Autom. Control*, vol. 60, no. 9, pp. 3823–3835, 2013.

[5] J. K. Rice and M. Verhaegen, "Efficient system identification of heterogeneous distributed systems via a structure exploiting extended Kalman filter," *IEEE Trans. Autom. Control*, vol. 56, no. 7, pp. 1713–1718, 2011.

[6] L. Ljung, "Asymptotic behavior of the extended Kalman filter as a parameter estimator for linear systems," *IEEE Trans. Autom. Control*, vol. AC-24, pp. 36–50, 1979.

[7] B. Ursin, "Asymptotic convergence properties of the extended Kalman filter using filtered state estimates," *IEEE Trans. Autom. Control*, vol. AC-25, pp. 1207–1211, 1980.

[8] L. A. Campbell and D. M. Wiberg, "Searching for convergence points of the continuous time extended Kalman filter used as a parameter estimator," in *Proc. of Signals, Syst. and Comput.*, 1991, pp. 252–256.

[9] K. Reif, S. Günther, E. Yaz, and R. Unbehauen, "Stochastic stability of the continuous-time extended Kalman filter," in *IEEE Proc. of Control Theory and Applicat.*, vol. 147, 2000, pp. 45–52.

[10] S. Bonnabel and J. Slotine, "A contraction theory based analysis of the stability of the deterministic extended Kalman filter," *IEEE Trans. Autom. Control*, vol. 60, no. 2, pp. 565–569, 2015.

[11] K. Reif, S. Günther, E. Yaz, and R. Unbehauen, "Stochastic stability of the discrete-time extended Kalman filter," *IEEE Trans. Autom. Control*, vol. 44, no. 4, pp. 714–728, 1999.

[12] M. Boutayeb, H. Rafaralahy, and M. Darouach, "Convergence analysis of the extended Kalman filter used as an observer for nonlinear deterministic

discrete-time systems," *IEEE Trans. Autom. Control*, vol. 42, no. 4, pp. 581–586, 1997.

[13] K. Reif and R. Unbehauen, "The extended Kalman filter as an exponential observer for nonlinear systems," *IEEE Trans. Signal Process.*, vol. 47, no. 8, pp. 2324–2328, 1999.

[14] Y. Song and J. W. Grizzle, "The extended Kalman filter as a local asymptotic observer for discrete-time nonlinear systems," *J. Math., Syst., Estimation, and Control*, vol. 5, no. 1, pp. 59–78, 1995.

[15] J. V. Candy, *Bayesian Signal Processing*. New Jersey: Wiley, 2009.

[16] B. Sinopoli, L. Schenato, M. Franceschetti, K. Poolla, M. Jordan, and S. Sastry, "Kalman filtering with intermittent observations," *IEEE Trans. Autom. Control*, vol. 49, no. 9, pp. 1453–1464, 2004.

[17] A.Vakili and B. Hassibi, "On the steady-state performance of Kalman filtering with intermittent observations for stable systems," in *IEEE Conf. Decision and Control*, 2009, pp. 6847–6852.

[18] S. Kluge, K. Reif, and M. Brokate, "Stochastic stability of the extended Kalman filter with intermittent observations," *IEEE Trans. Autom. Control*, vol. 55, no. 2, pp. 514–518, 2010.

[19] E. Rohr, D. Marelli, and M. Fu, "A unified framework for mean square stability of Kalman filters with intermittent observations," in *IEEE Int. Conf. on Control and Automat.*, 2011, pp. 177–182.

[20] ——, "Kalman filtering with intermittent observations: Bounds on the error covariance distribution," in *IEEE Conf. on Decision and Control and European Control Conf.*, 2011, pp. 2416–2421.

[21] K. A. E. M. H. Elamin and M. F. E. Taha, "On the steady-state error covariance matrix of Kalman filtering with intermittent observations in the presence of correlated noises at the same time," in *Int. Conf. on Computing, Elect. and Electron. Eng.*, 2013, pp. 15–22.

[22] E. Rohr, D. Marelli, and M. Fu, "Stability of Kalman filters subject to intermittent observations," in *IEEE Conf. Decision and Control*, 2013, pp. 7809–7814.

[23] X. Wang and E. E. Yaz, "Stochastically resilient extended Kalman filtering for discrete-time nonlinear systems with sensor failures," *Int. J. Syst. Sci.*, vol. 45,

no. 7, pp. 1393– 1401, 2014.

[24] E. E. Yaz, "EECE229 stochastic systems, estimation, and control," Spring 2009, class notes.

[25] R. A. Horn and C. R. Johnson, *Matrix Analysis*. New York: Cambridge University Press, 1986.

[26] A. Papoulis and S. U. Pillai, *Probability, Random Variables and Stochastic Processes*. New York: McGraw Hill, 2002.

[27] A. R. Amir-Moéz, "Extreme properties of eigenvalues of a hermitian transformation and singular values of the sum and product of linear transformations," *Duke Math. J.*, vol. 23, no. 3, pp. 463–476, 1956.

[28] R. G. Brown, *Introduction to Random Signal Analysis and Kalman Fitlering*. New York: Wiley, 1983.

[29] E. Yaz, "Linear state estimators for nonlinear stochastic systems with noisy nonlinear observers," *Int. J. Control*, vol. 48, pp. 2465–2475, 1988.

[30] E. E. Yaz and Y. I. Yaz, "State estimation of uncertain nonlinear stochastic systems with general criteria," *Applied Math. Letters*, vol. 14, no. 5, pp. 605–610, 2001.

[31] E. Yaz and A. Ray, "Linear unbiased state estimation under randomly varying bounded sensor delay," *Applied Math. Letters*, vol. 11, no. 4, pp. 27–32, 1998.

[32] B. Shen, Z. Wang, and H. Shu, *Nonlinear Stochastic Systems with Incomplete Information - Filtering and Control*. London: Springer, 2013.

[33] S. Sugathadasa, C. Martin, and W. P. Dayawansa, "Convergence of extended Kalman filter to locate a moving target in wild life telemetry," in *Proc. of IEEE Conf. Decision and Control*, 2000, pp. 2096–2099.

[34] B. D. de Senneville, S. Roujol, S. Hey, C. Moonen, and M. Ries, "Extended Kalman filtering for continuous volumetric MR-temperature imaging," in *IEEE Trans. on Med. Imag.*, vol. 32, 2013, pp. 711–718.

[35] K. Reif, F. F. Sonnenmann, E. Yaz, and R. Unbehauen, "An observer for nonlinear systems based on H_∞-filtering techniques," in *Proc. IEEE American Control Conf.*, 1997, pp. 2379– 2380.

[36] J. L. Bonniwell, S. C. Schneider, and E. E. Yaz, "H_∞-property of the discrete-time extended Kalman filter with stochastic ℓ_2 disturbances," in *IEEE Conf. Decision and Control*, 2015, pp. 6992–6997.

[37] ——, "H_∞-property of the discrete-time extended Kalman filter with uncertain measurements," in *to appear in the Proc. American Control Conf.*, 2016.

[38] F. Lewis and V. Syrmos, *Optimal Control*. New York: Wiley, 1995.

[39] R. Vaccaro, *Digital Control: A State-Space Approach*. New York: McGraw-Hill, 1995.

[40] E. Kreyszig, *Advanced Engineering Mathematics*, 12th ed. New Jersey: Wiley, 2011.

APPENDIX A

MATLAB CODE

The MATLAB code used for all of the simulations in this dissertation are contained in this Appendix.

A.1 Chapter 2 MATLAB Code

A.1.1 Convergence Study

```
close all
clear
%% Set initial values
tau  = .1;
runTime  = 100;
maxerror1 = 50;
stepsize = .1;
maxerror = maxerror1/stepsize;
errorRange = (2*maxerror+1);
n = 2;
p = 1;
%% set up the constant matrices and create the noise
Q = eye(n);
R = eye(p);
%% Set the initial state and run the original system
x(:,1) = [.2 ; .1];
for k=1:runTime;
```

```
% Set up the system
f(:,k)   = [x(1,k)+tau*x(2,k) ; x(2,k)-tau*sin(x(1,k))];
h(:,k)   = x(1,k);
x(:,k+1) = f(:,k);
y(:,k)   = h(:,k);
end
for i = 1:8
%% Initialize and clean up the signals
x_hat = zeros(n,runTime);
y_hat = zeros(p,runTime);
f_hat = zeros(n,runTime);
h_hat = zeros(p,runTime);
P = zeros(n,n,(runTime));
A = zeros(n,n,(runTime));
Ct= zeros(p,n,(runTime));
K = zeros(n,p,(runTime));
normx  = zeros(1,runTime);
normxhat   = zeros(1,runTime);
norme  = zeros(1,runTime);
norme2 = zeros(1,runTime);
min_eig_gamma1 = zeros(1,runTime);
%% Initialize the error in polar coordinates
rho = 5;
theta = [0 45 90 135 180 225 270 315];
initerror = [rho*cos(pi*theta(i)/180) ; rho*sin(pi*theta(i
   )/180)];
```

```
%% Set the initial estimate and apply the EKF
x_hat(:,1) = x(:,1) - initerror;
P(:,:,1) = eye(n);
for k = 1:runTime;
% Set up the system
A(:,:,k) = [1 , tau ; -tau*cos(x_hat(1,k)) , 1];
C(:,:,k) = [1 , 0];
f_hat(:,k) = [x_hat(1,k) + tau*x_hat(2,k) ; x_hat(2,k)-tau
   *sin(x_hat(1,k))];
h_hat(:,k) = x_hat(1,k);
y_hat(:,k) = h_hat(k);
% Kalman Gain
K(:,:,k) = (A(:,:,k)*P(:,:,k)*C(:,:,k)')*inv(C(:,:,k)*P
   (:,:,k)*C(:,:,k)'+R);
% State Estimate
x_hat(:,k+1) = f_hat(:,k)+K(:,:,k)*(y(:,k)-y_hat(:,k));
% Riccati Difference Equation
P(:,:,k+1) = (A(:,:,k)-K(:,:,k)*C(:,:,k))*P(:,:,k)*(A(:,:,
   k)-K(:,:,k)*C(:,:,k))' + Q + K(:,:,k)*R*K(:,:,k)';
end
%% Calculate Error and 2-Norm
e(:,:,i)=x-x_hat;
for j=1:runTime
norme(j)  = norm(e(:,j,i),2);
norme2(j) = norme(j)^2;
```

```
eig_gamma= eig(inv(P(:,:,j)) - (A(:,:,j)-K(:,:,j)*C(:,:,j)
   )'*inv(P(:,:,j+1))*(A(:,:,j)-K(:,:,j)*C(:,:,j)));
min_eig_gamma(j) = min(eig_gamma);
end
inf_gamma = min(min_eig_gamma);
H2_bound(i) = 1/inf_gamma;
%% Sum over simulation time
sum_e = sum(norme2);
V0 = e(:,1)'*P(:,:,1)*e(:,1);
H2(i) = sum_e/V0;
end
%% plots
e_0(:,:)   = e(:,:,1);
e_45(:,:)  = e(:,:,2);
e_90(:,:)  = e(:,:,3);
e_135(:,:) = e(:,:,4);
e_180(:,:) = e(:,:,5);
e_225(:,:) = e(:,:,6);
e_270(:,:) = e(:,:,7);
e_315(:,:) = e(:,:,8);
ratio_ST=H2./H2_bound;
deg_range = 0:45:360;
rad_range = 0:pi/4:2*pi;
t = 0:runTime;
figure(1)
```

```
plot(t,e_0(1,:),t,e_45(1,:),t,e_90(1,:),t,e_135(1,:),t,
   e_180(1,:),t,e_225(1,:),t,e_270(1,:),t,e_315(1,:))
xlabel('Time, k','FontSize',12)
ylabel('e_{1,k}','FontSize',12)
legend('e_0 = [5 0]^T','e_0 = [3.5355 3.5355]^T','e_0 = [0
    5]^T','e_0 = [-3.5355 3.5355]^T','e_0 = [-5 0]^T','e_0
    = [-3.5355 -3.5355]^T','e_0 = [0 -5]^T','e_0 = [3.5355
    -3.5355]^T','FontSize',12)
figure(2)
plot(t,e_0(2,:),t,e_45(2,:),t,e_90(2,:),t,e_135(2,:),t,
   e_180(2,:),t,e_225(2,:),t,e_270(2,:),t,e_315(2,:))
xlabel('Time, k','FontSize',12)
ylabel('e_{2,k}','FontSize',12)
legend('e_0 = [5 0]^T','e_0 = [3.5355 3.5355]^T','e_0 = [0
    5]^T','e_0 = [-3.5355 3.5355]^T','e_0 = [-5 0]^T','e_0
    = [-3.5355 -3.5355]^T','e_0 = [0 -5]^T','e_0 = [3.5355
    -3.5355]^T','FontSize',12)
```

A.1.2 H_2 Analysis for $f(y) = sin(y)$

NOTE: This is also modified for $f(y) = y^2$ and $f(y) = y^3$.

```
close all
clear
tau  = .1;
runTime  = 100;
maxerror1 = 50;
stepsize = .1;
```

```
maxerror = maxerror1/stepsize;
errorRange = (2*maxerror+1);
n = 2;
p = 1;
%% set up the constant matrices and create the noise
Q = eye(n);
R = eye(p);
%% Set the initial state and run the original system
x(:,1) = [.2 ; .1];
for k=1:runTime;
% Set up the system
f(:,k)   = [x(1,k)+tau*x(2,k) ; x(2,k)-tau*sin(x(1,k))];
h(:,k)   = x(1,k);
x(:,k+1) = f(:,k);
y(:,k)   = h(:,k);
end
% Sweep 360 degrees
for m = 1:361
%Increase the radius from stepsize to maxerror
for i = 1:3
%% Initialize and clean up the signals
x_hat = zeros(n,runTime);
y_hat = zeros(p,runTime);
f_hat = zeros(n,runTime);
h_hat = zeros(p,runTime);
P = zeros(n,n,(runTime));
```

```
A = zeros(n,n,(runTime));
Ct= zeros(p,n,(runTime));
K = zeros(n,p,(runTime));
normx  = zeros(1,runTime);
normxhat   = zeros(1,runTime);
norme  = zeros(1,runTime);
norme2 = zeros(1,runTime);
min_eig_gamma1 = zeros(1,runTime);
%% Initialize the error in polar coordinates
rho = [5 25 50];
theta = m-1;
initerror = [rho(i)*cos(pi*theta/180) ; rho(i)*sin(pi*
   theta/180)];
%% Set the initial estimate and apply the EKF
x_hat(:,1) = x(:,1) - initerror;
P(:,:,1) = eye(n);
for k = 1:runTime;
% Set up the system
A(:,:,k) = [1 , tau ; -tau*cos(x_hat(1,k)) , 1];
C(:,:,k) = [1 , 0];
f_hat(:,k) = [x_hat(1,k) + tau*x_hat(2,k) ; x_hat(2,k)-tau
   *sin(x_hat(1,k))];
h_hat(:,k) = x_hat(1,k);
y_hat(:,k) = h_hat(k);
% Kalman Gain
```

```
K(:,:,k) = (A(:,:,k)*P(:,:,k)*C(:,:,k)')*inv(C(:,:,k)*P
   (:,:,k)*C(:,:,k)'+R);
% State Estimate
x_hat(:,k+1) = f_hat(:,k)+K(:,:,k)*(y(:,k)-y_hat(:,k));
% Riccati Difference Equation
P(:,:,k+1) = (A(:,:,k)-K(:,:,k)*C(:,:,k))*P(:,:,k)*(A(:,:,
   k)-K(:,:,k)*C(:,:,k))' + Q + K(:,:,k)*R*K(:,:,k)';
end
%% Calculate Error and 2-Norm
e=x-x_hat;
for j=1:runTime
norme(j)  = norm(e(:,j),2);
norme2(j) = norme(j)^2;
eig_gamma= eig(inv(P(:,:,j)) - (A(:,:,j)-K(:,:,j)*C(:,:,j)
   )'*inv(P(:,:,j+1))*(A(:,:,j)-K(:,:,j)*C(:,:,j)));
min_eig_gamma(j) = min(eig_gamma);
end
inf_gamma = min(min_eig_gamma);
H2_bound(i,m) = 1/inf_gamma;
%% Sum over simulation time
sum_e = sum(norme2);
V0 = e(:,1)'*P(:,:,1)*e(:,1);
H2(i,m) = sum_e/V0;
end
end
%% plots
```

```
ratio_ST=H2./H2_bound;
deg_range = 0:360;
rad_range = 0:pi/180:2*pi;
figure(1)
polar(rad_range,ratio_ST(1,:),'--k')
hold on
polar(rad_range,ratio_ST(2,:),'-.b')
polar(rad_range,ratio_ST(3,:),'-r')
legend('||e_0|| = 5','||e_0|| = 25','||e_0|| = 50')
```

A.2 Chapter 3 MATLAB Code

A.2.1 Second Order System with Three Cases of Initial Conditions and Disturbance Magnitude

To use this code, change the run vector to have a 1 for the case number of interested, e.g. run = [0 1 0]; for case 2.

```
clear
global K
%% Select which cases to run
run = [0 0 1];
%% Case 1
tau   = .01;
runTime   = 1001;
F   = [10^(-3) , 0 ; 0 , 0];
H   = [0 , 10^(-1/2)];
caseNum   = 1*run(1);
x_hat0= [.5 ; .5];
```

```
dt_ekf_v3(tau,runTime,F,H,caseNum,x_hat0)
if run(1) == 1
for j=1:runTime
eig_FFt(j) = min(eig((F-K(1:2,j)*H)*(F-K(1:2,j)*H)'));
end
case1FFt = min(eig_FFt)
end
%% Case 2
tau  = 0.01;
runTime  = 2001;
F   = [10^-2 , 0 ; 0 , 0];
H   = [0 , 10^(1/2)];
caseNum  = 2*run(2);
x_hat0   = [.5 ; .5];
dt_ekf_v3(tau,runTime,F,H,caseNum,x_hat0)
if run(2) == 1
for j=1:runTime
eig_FFt(j) = min(eig((F-K(1:2,j)*H)*(F-K(1:2,j)*H)'));
end
case2FFt = min(eig_FFt)
end
%% Case 3
tau  = 0.01;
runTime  = 2001;
F   = [10^(-3) , 0 ; 0 , 0];
H   = [0 , 10^(-1/2)];
```

```
caseNum  = 3*run(3);
x_hat0   = [2.5 ; -2.7];
dt_ekf_v3(tau,runTime,F,H,caseNum,x_hat0)
if run(3) == 1
for j=1:runTime
eig_FFt(j) = min(eig((F-K(1:2,j)*H)*(F-K(1:2,j)*H)'));
end
case3FFt = min(eig_FFt)
end
```

This is the code for the function called in the above code:

```
function dt_ekf_v3(tau,runTime,F,H,caseNum,x_hat0)
%% If the case number is 0, just exit, else run the
   function through
if caseNum ~= 0
clear w x y x_hat y_hat P A At C Ct K
global K
%% Set the initial state and run the original system
x(1:2,1) = [.8;.2];
for k=1:runTime;
% Set up the system
w(:,k) = exp(-.001*k)*[randn;randn];
f(1:2,k)   = [x(1,k)+tau*x(2,k);
  x(2,k)+tau*(-x(1,k)+(x(1,k)^2+x(2,k)^2-1)*x(2,k))];
h(1:1,k)   = x(1,k);
x(1:2,k+1) = f(1:2,k)+F*w(:,k);
y(1:1,k)   = h(1:1,k)+H*w(:,k);
```

```
end
%% Set the initial estimate and apply the EKF
x_hat(1:2,1) = x_hat0;
P(:,:,1) = eye(2);
for k = 1:runTime;
% Set up the system
A(:,:,k)   = [1tau ;
  (-1+2*x_hat(1,k)*x_hat(2,k))*tau (1+(x_hat(1,k)^2+3*
     x_hat(2,k)^2-1)*tau)];
Ct(1:2,k)  = [1 0]';
f_hat(1:2,k)   = [x_hat(1,k)+tau*x_hat(2,k) ;
  x_hat(2,k)+tau*(-x_hat(1,k)+(x_hat(1,k)^2+x_hat(2,k)
     ^2-1)*x_hat(2,k))];
h_hat(1:1,k)   = x_hat(1,k);
y_hat(1:1,k)   = Ct(:,k)'*x_hat(1:2,k);
% Kalman Gain
K(1:2,k)   = (A(:,:,k)*P(:,:,k)*Ct(:,k)+F*H')*inv(Ct(:,k)
   '*P(:,:,k)*Ct(:,k)+H*H');
% State Estimate
x_hat(1:2,k+1) = f_hat(1:2,k)+K(1:2,k)*(y(1:1,k)-y_hat
   (1:1,k));
% Riccati Difference Equation
P(:,:,k+1) = (A(:,:,k)-K(1:2,k)*Ct(:,k)')*P(:,:,k)*(A(:,:,
   k)-K(1:2,k)*Ct(:,k)')'+(F-K(1:2,k)*H)*(F-K(1:2,k)*H)';
end
%% Calculate Error and 2-Norms
```

```
e(:,:)=x(:,:)-x_hat(:,:);
for j=1:runTime
normx(j)= norm(x(:,j),2);
normxhat(j) = norm(x_hat(:,j),2);
norme(j)= norm(e(:,j),2);
normw(j)= norm(w(:,j),2);
norme2(j)= norme(j)^2;
normw2(j)= normw(j)^2;
%% Sampled mean at each time step
norme2_bar(j) = (1/j)*sum(norme2(1:j));
normw2_bar(j) = (1/j)*sum(normw2(1:j));
end
%% Sum over simulation time
sum_e = sum(norme2_bar);
sum_w = sum(normw2_bar);
Hinf = sum_e/sum_w
% %% Create plots
 str=sprintf('Case Number %d:',caseNum);
t = [0:runTime-1];
% Figure 1
figure((caseNum-1)*3+1)
plot(t,x(1,1:runTime),'k',t,x_hat(1,1:runTime),'b--')
legend('x_{1,k}','x hat_{1,k}')
xlabel('Time Steps','Fontsize',12)
ylabel('State and Estimate Norm','Fontsize',12)
% Figure 2
```

```
figure((caseNum-1)*3+2)
plot(t,x(2,1:runTime),'k',t,x_hat(2,1:runTime),'b--')
legend('x_{2,k}','x hat_{2,k}')
xlabel('Time Steps','Fontsize',12)
ylabel('State and Estimate Norm','Fontsize',12)
% Figure 3
figure((caseNum-1)*3+3)
plot(t,norme,'k')
xlabel('Steps','Fontsize',12)
ylabel('\mid\mid e_k \mid\mid','Fontsize',12)
disp([str ' Completed'])
end
end
```

A.2.2 Scalar System with the Disturbance Magnitude Varied and Monte Carlo

```
clear all
tau    = .01;
numRuns    = 100;
runTime    = 1001;
initF    = 10^(1);
initH    = 10^(-1);
x_hat0= .2;
distRange = 501;
stepSize  = .2;
%% If the case number is 0, just exit, else run the
   function through
```

```
for m = 1:numRuns
for i = 1:distRange
dist_mag = (i-((distRange-1)/2)-1)*stepSize;
if dist_mag ~= 0
%% set up the constant matrices and create the noise
F  = dist_mag*initF;
H  = dist_mag*initH;
%% Set the initial state and run the original system
x(1) = .2;
for k=1:runTime;
% Set up the system
w(k)   = exp(-0.001*k)*randn;
f(k)   = x(k)+tau*sin(x(k));
h(k)   = x(k);
x(k+1) = f(k)+F*w(k);
y(k)   = h(k)+H*w(k);
end
%% Set the initial estimate and apply the EKF
x_hat(1) = x_hat0;
P(1) = 1;
for k = 1:runTime;
% Set up the system
A(k)   = 1+tau*cos(x_hat(k));
C(k)   = 1;
f_hat(k)   = x_hat(k)+tau*sin(x_hat(k));
h_hat(k)   = x_hat(k);
```

```
y_hat(k)  = h_hat(k);
% Kalman Gain
K(k)   = (A(k)*P(k)*C(k)+F*H)/(C(k)*P(k)*C(k)+H*H);
% State Estimate
x_hat(k+1) = f_hat(k)+K(k)*(y(k)-y_hat(k));
% Riccati Difference Equation
P(k+1) = (A(k)-K(k)*C(k))*P(k)*(A(k)-K(k)*C(k))+(F-K(k)*H)
   *(F-K(k)*H);
end
%% Calculate Error and 2-Norms
e=x-x_hat;
for j=1:runTime
normx(j)= norm(x(j),2);
normxhat(j) = norm(x_hat(j),2);
norme(j)= norm(e(j),2);
normw(j)= norm(w(j),2);
norme2(j)= norme(j)^2;
normw2(j)= normw(j)^2;
%% Sampled mean at each time step
norme2_bar(j) = (1/j)*sum(norme2(1:j));
normw2_bar(j) = (1/j)*sum(normw2(1:j));
eig_gamma1= eig(1/(P(j))-(A(j)-K(j)*C(j))*(A(j)-K(j)*C(j))
   /(P(j+1)));
min_eig_gamma1(j) = min(eig_gamma1);
eig_gamma2= eig((F-K(j)*H)*(F-K(j)*H)/(P(j+1)));
max_eig_gamma2(j) = max(eig_gamma2);
```

```
end
FFt = min(eig((F-K(j)*H)*(F-K(j)*H)));
inf_gamma1 = min(min_eig_gamma1);
sup_gamma2=max(max_eig_gamma2);
Hinf_bound(i,m) = sup_gamma2/inf_gamma1;
%% Sum over simulation time
sum_e = sum(norme2_bar);
sum_w = sum(normw2_bar);
Hinf(i,m) = sum_e/sum_w;
else
Hinf(i,m) = NaN;
Hinf_bound(i,m) = NaN;
end
end
end
HinfMC = mean(Hinf','omitnan');
Hinf_boundMC = mean(Hinf_bound','omitnan');
%% plots
t=-((distRange-1)/2)*stepSize:stepSize:((distRange-1)/2)*
   stepSize;
figure(24)
plot(t,HinfMC,'k',t,Hinf_boundMC,'--k')
xlabel('\delta','FontSize',14)
ylabel('Magnitude','FontSize',12)
legend('Actual H_\infty-gain','H_\infty-bound')
ratio_ST=HinfMC./Hinf_boundMC;
```

```
figure(25)
plot(t,ratio_ST,'k')
xlabel('\delta','FontSize',14)
ylabel('actual to theoretical ratio','FontSize',12)
```

A.2.3 H_∞ Analysis of Three Different Nonlinearities

```
clear all
index = 15;
tau   = .1;
numRuns   = 100;
runTime = 101;
initF   = [0.02 0.1 ; 0 0.01];
initH   = [0.1 0.1];
distRange = 201;
stepSize  = .01;
b=5;
%% If the case number is 0, just exit, else run the
   function through
for nonlinearity = 1:3;
nonlinearity
for m = 1:numRuns
for i = 1:distRange
dist_mag = -(i-((distRange-1)/2)-1)*stepSize;
if dist_mag ~= 0
%% set up the constant matrices and create the noise
F  = dist_mag*initF;
```

```
H  = dist_mag*initH;
%% Set the initial state and run the original system
x(:,1) = [.2;.5];
x_hat0 = x(:,1);
for k=1:runTime;
w(:,k) = [.9^k*randn ; .9^k*randn];
if nonlinearity == 1
f(:,k) = [x(1,k) + tau*x(2,k) ; (1-tau*b)*x(2,k)-tau*sin(x
   (1,k))];
elseif nonlinearity == 2
f(:,k) = [x(1,k) + tau*x(2,k) ; (1-tau*b)*x(2,k)-tau*x(1,k
   )^2];
else
f(:,k) = [x(1,k) + tau*x(2,k) ; (1-tau*b)*x(2,k)-tau*x(1,k
   )^3];
end
h(:,k) = [x(1,k)];
x(:,k+1)   = f(:,k)+F*w(:,k);
y(:,k) = h(:,k)+H*w(:,k);
end
%% Set the initial estimate and apply the EKF
x_hat(:,1) = x_hat0;
P(:,:,1)   = eye(2);
for k = 1:runTime;
% Set up the system
if nonlinearity == 1
```

```
A(:,:,k)= [1 , tau ; -tau*cos(x_hat(1,k)) , 1-tau*b];
f_hat(:,k)  = [x_hat(1,k) + tau*x_hat(2,k) ; (1-tau*b)*
   x_hat(2,k)-tau*sin(x_hat(1,k))];
elseif nonlinearity == 2
A(:,:,k)= [1 , tau ; -2*tau*x_hat(1,k) , 1-tau*b];
f_hat(:,k)  = [x_hat(1,k) + tau*x_hat(2,k) ; (1-tau*b)*
   x_hat(2,k)-tau*x_hat(1,k)^2];
else
A(:,:,k)= [1 , tau ; -3*tau*x_hat(1,k)^2 , 1-tau*b];
f_hat(:,k)  = [x_hat(1,k) + tau*x_hat(2,k) ; (1-tau*b)*
   x_hat(2,k)-tau*x_hat(1,k)^3];
end
Ct(:,:,k)= [1;0]; % I need to store it as a column vector
   so I am makeing C^T here
h_hat(:,k)  = [x_hat(1,k)];
y_hat(:,k)  = h_hat(:,k);
obsvCheck(k) = rank(obsv(A(:,:,k),Ct(:,:,k)'));
% Kalman Gain
K(:,:,k) = (A(:,:,k)*P(:,:,k)*Ct(:,:,k)+F*H')*inv(Ct(:,:,k
   )'*P(:,:,k)*Ct(:,:,k)+H*H');
% State Estimate
x_hat(:,k+1) = f_hat(:,k)+K(:,:,k)*(y(:,k)-y_hat(:,k));
% Riccati Difference Equation
P(:,:,k+1) = (A(:,:,k)-K(:,:,k)*Ct(:,:,k)')*P(:,:,k)*(A
   (:,:,k)-K(:,:,k)*Ct(:,:,k)')'+(F-K(:,:,k)*H)*(F-K(:,:,k
   )*H)';
```

```
end
if min(obsvCheck) ~= 2
min(obsvCheck)
end
%% Calculate Error and 2-Norms
e=x-x_hat;
for j=1:runTime
normx(j)= norm(x(:,j),2);
normxhat(j) = norm(x_hat(:,j),2);
norme(j)= norm(e(:,j),2);
normw(j)= norm(w(:,j),2);

norme2(j)= norme(j)^2;
normw2(j)= normw(j)^2;
%% Sampled mean at each time step
norme2_bar(j) = (1/j)*sum(norme2(1:j));
normw2_bar(j) = (1/j)*sum(normw2(1:j));
eig_phi1= eig(inv(P(:,:,j))-(A(:,:,j)-K(:,:,j)*Ct(:,:,j)')
   '*inv(P(:,:,j+1))*(A(:,:,j)-K(:,:,j)*Ct(:,:,j)'));
min_eig_phi1(j) = min(eig_phi1);
if min_eig_phi1(j) <= 0
sprintf('T = %d, dist = %d',runTime,dist_mag)
end
eig_phi2= eig((F-K(:,:,j)*H)'*inv(P(:,:,j+1))*(F-K(:,:,j)*
   H));
max_eig_phi2(j) = max(eig_phi2);
```

```
eig_FFt = eig((F-K(:,:,j)*H)*(F-K(:,:,j)*H)');
min_eig_FFt(j) = min(eig_FFt);
end
inf_FFt = min(eig_FFt);
inf_phi1 = min(min_eig_phi1);
sup_phi2=max(max_eig_phi2);
%% Sum over simulation time
sum_e = sum(norme2_bar);
sum_w = sum(normw2_bar);
Hinf_bound(i,m) = (sup_phi2/inf_phi1);
Hinf(i,m) = sum_e/sum_w;
ratio(i,m) = Hinf(i,m)/Hinf_bound(i,m);
else
Hinf(i,m) = NaN;
Hinf_bound(i,m) = NaN;
ratio(i,m) = NaN;
end
end
end
ratioMC = mean(ratio','omitnan');
%% plots
t=-((distRange-1)/2)*stepSize:stepSize:((distRange-1)/2)*
   stepSize;
str = sprintf('%d Monte Carlo',numRuns);
figure(index)
```

```
hold on
if nonlinearity == 1
plot(t,ratioMC,'k')
elseif nonlinearity == 2
plot(t,ratioMC,'b')
else
plot(t,ratioMC,'g')
end
xlabel('\delta','FontSize',14)
ylabel('H_\infty Ratio','FontSize',12)
title(str)
end
figure(index)
legend('f(y) = sin(y)','f(y) = y^2','f(y) = y^3')
```

A.3 Chapter 4 MATLAB Code

A.3.1 H_∞ Analysis of $f(y) = sin(y)$ with Three Different Run Times

NOTE: This is also modified for $f(y) = y^2$ and $f(y) = y^3$.

```
clear all
index = 12;
tau   = .01;
Gamma_bar = [0.90 0; 0 0.90];
upsilon   = Gamma_bar*(eye(2)-Gamma_bar);
numRuns   = 100;
runTime_all = [10;30;50];
```

```
initF    = [.02 .1;0 .01];
initH    = [0.1 0.1;0 0.001];
distRange = 401;
stepSize  = .1;
%% If the case number is 0, just exit, else run the
   function through
for runTime_index = 1:3;
runTime = runTime_all(runTime_index);
for m = 1:numRuns
for i = 1:distRange
dist_mag = (i-((distRange-1)/2)-1)*stepSize;
if dist_mag ~= 0
%% set up the constant matrices and create the noise
F   = dist_mag*initF;
H   = dist_mag*initH;
%% Set the initial state and run the original system
x(:,1) = [.2;.5];
x_hat0 = x(:,1);
g1 = 7;
g2 = 5;
for k=1:runTime;
% Set up the system
% Self generate bernoulli RVs
if g1 >9
gamma1(k) = 0;
g1 = 1;
```

```
else
gamma1(k) = 1;
g1 = g1+1;
end
if g2 >9
gamma2(k) = 0;
g2 = 1;
else
gamma2(k) = 1;
g2 = g2+1;
end
   % gamma(k) = binornd(1,lambda);
Gamma(:,:,k) = [gamma1(k) 0 ; 0 gamma2(k)];
w(:,k) = [exp(-0.001*k)*randn ; exp(-0.01*k)*randn];
f(:,k) = [x(1,k) + tau*x(2,k) ; x(2,k)-tau*sin(x(1,k))];
h(:,k) = [x(1,k) ; x(2,k)];
x(:,k+1)   = f(:,k)+F*w(:,k);
y(:,k) = Gamma(:,:,k)*h(:,k)+H*w(:,k);
end
%% Set the initial estimate and apply the EKF
x_hat(:,1) = x_hat0;
P(:,:,1)   = eye(2);
for k = 1:runTime;
% Set up the system
A(:,:,k)= [1 , tau ; -tau*cos(x_hat(1,k)) , 1];
C(:,:,k)= eye(2);
```

```
f_hat(:,k)  = [x_hat(1,k) + tau*x_hat(2,k) ; x_hat(2,k)-
   tau*sin(x_hat(1,k))];
h_hat(:,k)  = [x_hat(1,k);x_hat(2,k)];
y_hat(:,k)  = Gamma_bar*h_hat(:,k);
obsvCheck(k) = rank(obsv(A(:,:,k),C(:,:,k)));
% Kalman Gain
K(:,:,k) = (A(:,:,k)*P(:,:,k)*C(:,:,k)'*Gamma_bar'+F*H')*
   inv(upsilon.*(C(:,:,k)*P(:,:,k)*C(:,:,k)'+h_hat(:,k)*
   h_hat(:,k)')+Gamma_bar*C(:,:,k)*P(:,:,k)*C(:,:,k)'*
   Gamma_bar'+H*H');
% State Estimate
x_hat(:,k+1) = f_hat(:,k)+K(:,:,k)*(y(:,k)-y_hat(:,k));
% Riccati Difference Equation
P(:,:,k+1) = (A(:,:,k)-K(:,:,k)*Gamma_bar*C(:,:,k))*P(:,:,
   k)*(A(:,:,k)-K(:,:,k)*Gamma_bar*C(:,:,k))'+(F-K(:,:,k)*
   H)*(F-K(:,:,k)*H)'+K(:,:,k)*(upsilon.*(C(:,:,k)*P(:,:,k
   )*C(:,:,k)'+h_hat(:,k)*h_hat(:,k)'))*K(:,:,k)';
end
if min(obsvCheck) ~= 2
min(obsvCheck)
end
%% Calculate Error and 2-Norms
e=x-x_hat;
for j=1:runTime
normx(j)= norm(x(:,j),2);
normxhat(j) = norm(x_hat(:,j),2);
```

```
norme(j)= norm(e(:,j),2);
normw(j)= norm(w(:,j),2);
norme2(j)= norme(j)^2;
normw2(j)= normw(j)^2;
%% Sampled mean at each time step
norme2_bar(j) = (1/j)*sum(norme2(1:j));
normw2_bar(j) = (1/j)*sum(normw2(1:j));
eig_phi1= eig(inv(P(:,:,j))-(A(:,:,j)-K(:,:,j)*Gamma_bar*C
   (:,:,j))'*inv(P(:,:,j+1))*(A(:,:,j)-K(:,:,j)*Gamma_bar*
   C(:,:,j))-C(:,:,j)'*(upsilon.*(K(:,:,j)'*inv(P(:,:,j+1)
   )*K(:,:,j)))*C(:,:,j));
min_eig_phi1(j) = min(eig_phi1);
if min_eig_phi1(j) <= 0
sprintf('T = %d, dist = %d',runTime,dist_mag)
end
eig_phi2= eig((F-K(:,:,j)*H)'*inv(P(:,:,j+1))*(F-K(:,:,j)*
   H));
max_eig_phi2(j) = max(eig_phi2);
eig_phi3= eig(h_hat(:,j)'*(upsilon.*(K(:,:,j)'*inv(P(:,:,j
   +1))*K(:,:,j)))*h_hat(:,j));
max_eig_phi3(j) = max(eig_phi3);
eig_FFt = eig((F-K(:,:,j)*H)*(F-K(:,:,j)*H)');
min_eig_FFt(j) = min(eig_FFt);
end
inf_FFt = min(eig_FFt);
inf_phi1 = min(min_eig_phi1);
```

```
sup_phi2=max(max_eig_phi2);
sup_phi3=max(max_eig_phi3);
%% Sum over simulation time
sum_e = sum(norme2_bar);
sum_w = sum(normw2_bar);
Hinf_bound(i,m) = (sup_phi2/inf_phi1);
Hinf(i,m) = sum_e/sum_w;
ratio01(i,m) = inf_phi1*sum_e/(sup_phi2*sum_w+sup_phi3*(
   runTime+1+1));
else
Hinf(i,m) = NaN;
Hinf_bound(i,m) = NaN;
ratio01(i,m) = NaN;
end
end
end
HinfMC = mean(Hinf','omitnan');
Hinf_boundMC = mean(Hinf_bound','omitnan');
ratio01MC = mean(ratio01','omitnan');
ratioMC = HinfMC./Hinf_boundMC;
%% plots
t=-((distRange-1)/2)*stepSize:stepSize:((distRange-1)/2)*
   stepSize;
str = sprintf('%d Monte Carlo',numRuns);
figure(index+1)
hold on
```

```
if runTime_index == 1
plot(t,ratioMC,'k')
elseif runTime_index == 2
plot(t,ratioMC,'b')
else
plot(t,ratioMC,'g')
end
xlabel('\delta','FontSize',14)
ylabel('H_\infty Ratio','FontSize',12)
title(str)
end
figure(index+1)
legend('T=10','T=30','T=50')
```

A.3.2 H_∞ Analysis of Three Different Nonlinearities

```
clear all
index = 13;
tau   = .01;
Gamma_bar = [0.90 0; 0 0.90];
upsilon   = Gamma_bar*(eye(2)-Gamma_bar);
numRuns   = 100;
runTime = 30;
initF   = [.02 .1;0 .01];
initH   = [0.1 0.1;0 0.001];
distRange = 401;
stepSize  = .1;
```

```
for nonlinearity = 1:3;
for m = 1:numRuns
for i = 1:distRange
dist_mag = (i-((distRange-1)/2)-1)*stepSize;
if dist_mag ~= 0
%% set up the constant matrices and create the noise
F  = dist_mag*initF;
H  = dist_mag*initH;
%% Set the initial state and run the original system
x(:,1) = [.2;.5];
x_hat0 = x(:,1);
g1 = 7;
g2 = 5;
for k=1:runTime;
% Set up the system
% Self generate bernoulli RVs
if g1 >9
gamma1(k) = 0;
g1 = 1;
else
gamma1(k) = 1;
g1 = g1+1;
end
if g2 >9
gamma2(k) = 0;
g2 = 1;
```

```
else
gamma2(k) = 1;
g2 = g2+1;
end
   % gamma(k) = binornd(1,lambda);
Gamma(:,:,k) = [gamma1(k) 0 ; 0 gamma2(k)];
w(:,k) = [exp(-0.001*k)*randn ; exp(-0.01*k)*randn];
if nonlinearity == 1
f(:,k) = [x(1,k) + tau*x(2,k) ; x(2,k)-tau*sin(x(1,k))];
elseif nonlinearity == 2
f(:,k) = [x(1,k) + tau*x(2,k) ; x(2,k)-tau*x(1,k)^2];
else
f(:,k) = [x(1,k) + tau*x(2,k) ; x(2,k)-tau*x(1,k)^3];
end
h(:,k) = [x(1,k) ; x(2,k)];
x(:,k+1)    = f(:,k)+F*w(:,k);
y(:,k) = Gamma(:,:,k)*h(:,k)+H*w(:,k);
end
%% Set the initial estimate and apply the EKF
x_hat(:,1) = x_hat0;
P(:,:,1)    = eye(2);
for k = 1:runTime;
% Set up the system
if nonlinearity == 1
A(:,:,k)= [1 , tau ; -tau*cos(x_hat(1,k)) , 1];
```

```
f_hat(:,k)  = [x_hat(1,k) + tau*x_hat(2,k) ; x_hat(2,k)-
   tau*sin(x_hat(1,k))];
elseif nonlinearity == 2
A(:,:,k)= [1 , tau ; -2*tau*x_hat(1,k) , 1];
f_hat(:,k)  = [x_hat(1,k) + tau*x_hat(2,k) ; x_hat(2,k)-
   tau*x_hat(1,k)^2];
else
A(:,:,k)= [1 , tau ; -3*tau*x_hat(1,k)^2 , 1];
f_hat(:,k)  = [x_hat(1,k) + tau*x_hat(2,k) ; x_hat(2,k)-
   tau*x_hat(1,k)^3];
end
C(:,:,k)= eye(2);
h_hat(:,k)  = [x_hat(1,k);x_hat(2,k)];
y_hat(:,k)  = Gamma_bar*h_hat(:,k);
obsvCheck(k) = rank(obsv(A(:,:,k),C(:,:,k)));
% Kalman Gain
K(:,:,k) = (A(:,:,k)*P(:,:,k)*C(:,:,k)'*Gamma_bar'+F*H')*
   inv(upsilon.*(C(:,:,k)*P(:,:,k)*C(:,:,k)'+h_hat(:,k)*
   h_hat(:,k)')+Gamma_bar*C(:,:,k)*P(:,:,k)*C(:,:,k)'*
   Gamma_bar'+H*H');
% State Estimate
x_hat(:,k+1) = f_hat(:,k)+K(:,:,k)*(y(:,k)-y_hat(:,k));
% Riccati Difference Equation
P(:,:,k+1) = (A(:,:,k)-K(:,:,k)*Gamma_bar*C(:,:,k))*P(:,:,
   k)*(A(:,:,k)-K(:,:,k)*Gamma_bar*C(:,:,k))'+(F-K(:,:,k)*
```

```
   H)*(F-K(:,:,k)*H)'+K(:,:,k)*(upsilon.*(C(:,:,k)*P(:,:,k
   )*C(:,:,k)'+h_hat(:,k)*h_hat(:,k)'))*K(:,:,k)';
end
if min(obsvCheck) ~= 2
min(obsvCheck)
end
%% Calculate Error and 2-Norms
e=x-x_hat;
for j=1:runTime
normx(j)= norm(x(:,j),2);
normxhat(j) = norm(x_hat(:,j),2);
norme(j)= norm(e(:,j),2);
normw(j)= norm(w(:,j),2);
norme2(j)= norme(j)^2;
normw2(j)= normw(j)^2;
%% Sampled mean at each time step
norme2_bar(j) = (1/j)*sum(norme2(1:j));
normw2_bar(j) = (1/j)*sum(normw2(1:j));
eig_phi1= eig(inv(P(:,:,j))-(A(:,:,j)-K(:,:,j)*Gamma_bar*C
   (:,:,j))'*inv(P(:,:,j+1))*(A(:,:,j)-K(:,:,j)*Gamma_bar*
   C(:,:,j))-C(:,:,j)'*(upsilon.*(K(:,:,j)'*inv(P(:,:,j+1)
   )*K(:,:,j)))*C(:,:,j));
min_eig_phi1(j) = min(eig_phi1);
if min_eig_phi1(j) <= 0
sprintf('T = %d, dist = %d',runTime,dist_mag)
end
```

```
eig_phi2= eig((F-K(:,:,j)*H)'*inv(P(:,:,j+1))*(F-K(:,:,j)*
   H));
max_eig_phi2(j) = max(eig_phi2);
eig_phi3= eig(h_hat(:,j)'*(upsilon.*(K(:,:,j)'*inv(P(:,:,j
   +1))*K(:,:,j)))*h_hat(:,j));
max_eig_phi3(j) = max(eig_phi3);
eig_FFt = eig((F-K(:,:,j)*H)*(F-K(:,:,j)*H)');
min_eig_FFt(j) = min(eig_FFt);
end
inf_FFt = min(eig_FFt);
inf_phi1 = min(min_eig_phi1);
sup_phi2=max(max_eig_phi2);
sup_phi3=max(max_eig_phi3);
%% Sum over simulation time
sum_e = sum(norme2_bar);
sum_w = sum(normw2_bar);
Hinf_bound(i,m) = (sup_phi2/inf_phi1);
Hinf(i,m) = sum_e/sum_w;
ratio01(i,m) = inf_phi1*sum_e/(sup_phi2*sum_w+sup_phi3*(
   runTime+1+1));
else
Hinf(i,m) = NaN;
Hinf_bound(i,m) = NaN;
ratio01(i,m) = NaN;
end
end
```

```
end
ratio = Hinf./Hinf_bound;
ratioMC = mean(ratio','omitnan');
ratio01MC = mean(ratio01','omitnan');
%% plots
t=-((distRange-1)/2)*stepSize:stepSize:((distRange-1)/2)*
   stepSize;
str = sprintf('%d Monte Carlo',numRuns);
figure(index+1)
hold on
if nonlinearity == 1
plot(t,ratioMC,'k')
elseif nonlinearity == 2
plot(t,ratioMC,'b')
else
plot(t,ratioMC,'g')
end
xlabel('\delta','FontSize',14)
ylabel('H_\infty Ratio','FontSize',12)
title(str)
end
figure(index+1)
legend('f(y) = sin(y)','f(y) = y^2','f(y) = y^3')
```

A.4 Chapter 5 MATLAB Code

A.4.1 H_∞ Analysis of $f(y) = sin(y)$ with Three Different Run Times

NOTE: This is also modified for $f(y) = y^2$ and $f(y) = y^3$.

```
clear all
index = 6;
tau   = .01;
Gamma_bar = 0.90;
upsilon   = Gamma_bar*(1-Gamma_bar);
numRuns   = 100;
runTime_all = [10;30;50];
initF   = [.02 0.1 ; 0 .01];
initH   = [0.1 0.1];
distRange = 301;
stepSize  = .1;
for runTime_index = 1:3;
runTime = runTime_all(runTime_index);
for m = 1:numRuns
for i = 1:distRange
dist_mag = (i-((distRange-1)/2)-1)*stepSize;
if dist_mag ~= 0
%% set up the constant matrices and create the noise
F  = dist_mag*initF;
H  = dist_mag*initH;
%% Set the initial state and run the original system
x(:,1) = [.2;.5];
```

```
x_hat0 = x(:,1);
g1 = 4;
for k=1:runTime;
% Set up the system
% Self generate bernoulli RVs
if g1 >9
gamma1(k) = 0;
g1 = 1;
else
gamma1(k) = 1;
g1 = g1+1;
end
   % gamma(k) = binornd(1,lambda);
w(:,k) = [exp(-0.001*k)*randn ; exp(-0.01*k)*randn];
f(:,k) = [x(1,k) + tau*x(2,k) ; x(2,k)-tau*sin(x(1,k))];
h(:,k) = x(1,k);
x(:,k+1)    = f(:,k)+F*w(:,k);
y(:,k) = gamma1(k)*h(:,k)+H*w(:,k);
end
%% Set the initial estimate and apply the EKF
x_hat(:,1) = x_hat0;
P(:,:,1)    = eye(2);
for k = 1:runTime;
% Set up the system
A(:,:,k)= [1 , tau ; -tau*cos(x_hat(1,k)) , 1];
Ct(:,:,k)    = [1;0];
```

```
f_hat(:,k)  = [x_hat(1,k) + tau*x_hat(2,k) ; x_hat(2,k)-
   tau*sin(x_hat(1,k))];
h_hat(:,k)  = x_hat(1,k);
y_hat(:,k)  = Gamma_bar*h_hat(:,k);
obsvCheck(k) = rank(obsv(A(:,:,k),Ct(:,:,k)'));
% Kalman Gain
K(:,:,k) = (Gamma_bar*A(:,:,k)*P(:,:,k)*Ct(:,:,k)+F*H')*
   inv(upsilon*(Ct(:,:,k)'*P(:,:,k)*Ct(:,:,k)+h_hat(:,k)*
   h_hat(:,k)')+(Gamma_bar^2)*Ct(:,:,k)'*P(:,:,k)*Ct(:,:,k
   )+H*H');
% State Estimate
x_hat(:,k+1) = f_hat(:,k)+K(:,:,k)*(y(:,k)-y_hat(:,k));
% Riccati Difference Equation
P(:,:,k+1) = (A(:,:,k)-Gamma_bar*K(:,:,k)*Ct(:,:,k)')*P
   (:,:,k)*(A(:,:,k)-Gamma_bar*K(:,:,k)*Ct(:,:,k)')'+(F-K
   (:,:,k)*H)*(F-K(:,:,k)*H)'+upsilon*K(:,:,k)*(Ct(:,:,k)
   '*P(:,:,k)*Ct(:,:,k)+h_hat(:,k)*h_hat(:,k)')*K(:,:,k)';
end
if min(obsvCheck) ~= 2
min(obsvCheck)
end
%% Calculate Error and 2-Norms
e=x-x_hat;
for j=1:runTime
normx(j)= norm(x(:,j),2);
normxhat(j) = norm(x_hat(:,j),2);
```

```
norme(j)= norm(e(:,j),2);
normw(j)= norm(w(:,j),2);
norme2(j)= norme(j)^2;
normw2(j)= normw(j)^2;
%% Sampled mean at each time step
norme2_bar(j) = (1/j)*sum(norme2(1:j));
normw2_bar(j) = (1/j)*sum(normw2(1:j));
eig_phi1= eig(inv(P(:,:,j))-(A(:,:,j)-Gamma_bar*K(:,:,j)*
   Ct(:,:,j)')'*inv(P(:,:,j+1))*(A(:,:,j)-Gamma_bar*K(:,:,
   j)*Ct(:,:,j)')-upsilon*Ct(:,:,j)*K(:,:,j)'*inv(P(:,:,j
   +1))*K(:,:,j)*Ct(:,:,j)');
min_eig_phi1(j) = min(eig_phi1);
if min_eig_phi1(j) <= 0
sprintf('T = %d, dist = %d',runTime,dist_mag)
end
eig_phi2= eig((F-K(:,:,j)*H)'*inv(P(:,:,j+1))*(F-K(:,:,j)*
   H));
max_eig_phi2(j) = max(eig_phi2);
eig_phi3= eig(h_hat(:,j)'*(upsilon.*(K(:,:,j)'*inv(P(:,:,j
   +1))*K(:,:,j)))*h_hat(:,j));
max_eig_phi3(j) = max(eig_phi3);
eig_FFt = eig((F-K(:,:,j)*H)*(F-K(:,:,j)*H)');
min_eig_FFt(j) = min(eig_FFt);
end
inf_FFt(i,m) = min(eig_FFt);
inf_phi1(i,m) = min(min_eig_phi1);
```

```
sup_phi2(i,m)=max(max_eig_phi2);
sup_phi3(i,m)=max(max_eig_phi3);
%% Sum over simulation time
sum_e(i,m) = sum(norme2_bar);
sum_w(i,m) = sum(normw2_bar);
Hinf_bound(i,m) = (sup_phi2(i,m)/inf_phi1(i,m));
Hinf(i,m) = sum_e(i,m)/sum_w(i,m);
ratio01(i,m) = inf_phi1(i,m)*sum_e(i,m)/(sup_phi2(i,m)*
   sum_w(i,m)+sup_phi3(i,m)*(runTime+1+1));
else
Hinf(i,m) = NaN;
Hinf_bound(i,m) = NaN;
ratio01(i,m) = NaN;
end
end
end
ratio = Hinf./Hinf_bound;
ratioMC = mean(ratio','omitnan');
ratio01MC = mean(ratio01','omitnan');
%% plots
t=-((distRange-1)/2)*stepSize:stepSize:((distRange-1)/2)*
   stepSize;
str = sprintf('%d Monte Carlo',numRuns);
figure(index+1)
hold on
if runTime_index == 1
```

```
plot(t,ratioMC,'k')
elseif runTime_index == 2
plot(t,ratioMC,'b')
else
plot(t,ratioMC,'g')
end
xlabel('\delta','FontSize',14)
ylabel('H_\infty Ratio','FontSize',12)
title(str)
end
figure(index+1)
legend('T=10','T=30','T=50')
```

A.4.2 H_∞ Analysis of Three Different Nonlinearities

```
clear all
index = 1;
tau   = .01;
Gamma_bar = 0.90;
upsilon   = Gamma_bar*(1-Gamma_bar);
numRuns   = 100;
runTime = 30;
initF   = [.02 0.1 ; 0 .01];
initH   = [0.1 0.1];
distRange = 301;
stepSize  = .1;
for nonlinearity = 1:3;
```

```
for m = 1:numRuns
for i = 1:distRange
dist_mag = (i-((distRange-1)/2)-1)*stepSize;
if dist_mag ~= 0
%% set up the constant matrices and create the noise
F  = dist_mag*initF;
H  = dist_mag*initH;
%% Set the initial state and run the original system
x(:,1) = [.2;.5];
x_hat0 = x(:,1);
g1 = 4;
for k=1:runTime;
% Set up the system
% Self generate bernoulli RVs
if g1 >9
gamma1(k) = 0;
g1 = 1;
else
gamma1(k) = 1;
g1 = g1+1;
end
   % gamma(k) = binornd(1,lambda);
w(:,k) = [exp(-0.001*k)*randn ; exp(-0.01*k)*randn];
if nonlinearity == 1
f(:,k) = [x(1,k) + tau*x(2,k) ; x(2,k)-tau*sin(x(1,k))];
elseif nonlinearity == 2
```

```
f(:,k) = [x(1,k) + tau*x(2,k) ; x(2,k)-tau*x(1,k)^2];
else
f(:,k) = [x(1,k) + tau*x(2,k) ; x(2,k)-tau*x(1,k)^3];
end
h(:,k) = x(1,k);
x(:,k+1)    = f(:,k)+F*w(:,k);
y(:,k) = gamma1(k)*h(:,k)+H*w(:,k);
end
%% Set the initial estimate and apply the EKF
x_hat(:,1) = x_hat0;
P(:,:,1)    = eye(2);
for k = 1:runTime;
% Set up the system
if nonlinearity == 1
A(:,:,k)= [1 , tau ; -tau*cos(x_hat(1,k)) , 1];
f_hat(:,k)  = [x_hat(1,k) + tau*x_hat(2,k) ; x_hat(2,k)-
   tau*sin(x_hat(1,k))];
elseif nonlinearity == 2
A(:,:,k)= [1 , tau ; -2*tau*x_hat(1,k) , 1];
f_hat(:,k)  = [x_hat(1,k) + tau*x_hat(2,k) ; x_hat(2,k)-
   tau*x_hat(1,k)^2];
else
A(:,:,k)= [1 , tau ; -3*tau*x_hat(1,k)^2 , 1];
f_hat(:,k)  = [x_hat(1,k) + tau*x_hat(2,k) ; x_hat(2,k)-
   tau*x_hat(1,k)^3];
end
```

```
Ct(:,:,k)    = [1;0];
h_hat(:,k)   = x_hat(1,k);
y_hat(:,k)   = Gamma_bar*h_hat(:,k);
obsvCheck(k) = rank(obsv(A(:,:,k),Ct(:,:,k)'));
% Kalman Gain
K(:,:,k) = (Gamma_bar*A(:,:,k)*P(:,:,k)*Ct(:,:,k)+F*H')*
   inv(upsilon*(Ct(:,:,k)'*P(:,:,k)*Ct(:,:,k)+h_hat(:,k)*
   h_hat(:,k)')+(Gamma_bar^2)*Ct(:,:,k)'*P(:,:,k)*Ct(:,:,k
   )+H*H');
% State Estimate
x_hat(:,k+1) = f_hat(:,k)+K(:,:,k)*(y(:,k)-y_hat(:,k));
% Riccati Difference Equation
P(:,:,k+1) = (A(:,:,k)-Gamma_bar*K(:,:,k)*Ct(:,:,k)')*P
   (:,:,k)*(A(:,:,k)-Gamma_bar*K(:,:,k)*Ct(:,:,k)')'+(F-K
   (:,:,k)*H)*(F-K(:,:,k)*H)'+upsilon*K(:,:,k)*(Ct(:,:,k)
   '*P(:,:,k)*Ct(:,:,k)+h_hat(:,k)*h_hat(:,k)')*K(:,:,k)';
end
if min(obsvCheck) ~= 2
min(obsvCheck)
end
%% Calculate Error and 2-Norms
e=x-x_hat;
for j=1:runTime
normx(j)= norm(x(:,j),2);
normxhat(j) = norm(x_hat(:,j),2);
norme(j)= norm(e(:,j),2);
```

```
normw(j)= norm(w(:,j),2);
norme2(j)= norme(j)^2;
normw2(j)= normw(j)^2;
%% Sampled mean at each time step
norme2_bar(j) = (1/j)*sum(norme2(1:j));
normw2_bar(j) = (1/j)*sum(normw2(1:j));
eig_phi1= eig(inv(P(:,:,j))-(A(:,:,j)-Gamma_bar*K(:,:,j)*
   Ct(:,:,j)')'*inv(P(:,:,j+1))*(A(:,:,j)-Gamma_bar*K(:,:,
   j)*Ct(:,:,j)')-upsilon*Ct(:,:,j)*K(:,:,j)'*inv(P(:,:,j
   +1))*K(:,:,j)*Ct(:,:,j)');
min_eig_phi1(j) = min(eig_phi1);
if min_eig_phi1(j) <= 0
sprintf('T = %d, dist = %d',runTime,dist_mag)
end
eig_phi2= eig((F-K(:,:,j)*H)'*inv(P(:,:,j+1))*(F-K(:,:,j)*
   H));
max_eig_phi2(j) = max(eig_phi2);
eig_phi3= eig(h_hat(:,j)'*(upsilon.*(K(:,:,j)'*inv(P(:,:,j
   +1))*K(:,:,j)))*h_hat(:,j));
max_eig_phi3(j) = max(eig_phi3);
eig_FFt = eig((F-K(:,:,j)*H)*(F-K(:,:,j)*H)');
min_eig_FFt(j) = min(eig_FFt);
end
inf_FFt = min(eig_FFt);
inf_phi1 = min(min_eig_phi1);
sup_phi2=max(max_eig_phi2);
```

```
sup_phi3=max(max_eig_phi3);
%% Sum over simulation time
sum_e = sum(norme2_bar);
sum_w = sum(normw2_bar);
Hinf_bound(i,m) = (sup_phi2/inf_phi1);
Hinf(i,m) = sum_e/sum_w;
ratio01(i,m) = inf_phi1*sum_e/(sup_phi2*sum_w+sup_phi3*(
   runTime+1+1));
else
Hinf(i,m) = NaN;
Hinf_bound(i,m) = NaN;
ratio01(i,m) = NaN;
end
end
end
ratio = Hinf./Hinf_bound;
ratioMC   = mean(ratio','omitnan');
ratio01MC = mean(ratio01','omitnan');
%% plots
t=-((distRange-1)/2)*stepSize:stepSize:((distRange-1)/2)*
   stepSize;
str = sprintf('%d Monte Carlo',numRuns);
figure(index+1)
hold on
if nonlinearity == 1
plot(t,ratioMC,'k')
```

```
elseif nonlinearity == 2
plot(t,ratioMC,'b')
else
plot(t,ratioMC,'g')
end
xlabel('\delta','FontSize',14)
ylabel('H_\infty Ratio','FontSize',12)
title(str)
end
figure(index+1)
legend('f(y) = sin(y)','f(y) = y^2','f(y) = y^3')
```

A.5 Chapter 6 MATLAB Code

A.5.1 Second Order System

NOTE: This is modified for the various examples in Chapter 6 of the dissertation.

```
clear all
close all
fntsz = 12;
%% Global Variables
global F H Q Rinv dist_mag dist_tc1 dist_tc2 dist_freq b
%% Set up disturbance parameters
 dist_tc1   = 0.5;
 dist_tc2   = 1;
 dist_freq = 2;
 b=5;
```

```
%% Debug Flag
debug = 1;
%% Begin loop for different parameters
for i = 1:3
clear Xs t X0 txs txtemp normx normxhat w e C P mat eigMat
    maxeig supeig
%% DEBUG Mode Printout
if debug == 1
disp(['i = ', num2str(i)]);
end;
%% Define time span and initial state condition
t  = 0:.01:30;
x0 = [0.8;0.2];
%%% Determine distrubance magnitude and initial estimate
   %%%%%%%%%%%%%%
if i == 1
dist_mag = .1;
xhat0 = x0+[-.1;-.1];
elseif i == 2
dist_mag = 5;
xhat0 = x0+[-.1;-.1];
else
dist_mag = .1;
xhat0 = x0+[-2;-2];
end
F = [.2 1;0 .1];
```

```
H = [.1 .1];
%% Set up the EKF around eq point [0;0]
Q= eye(2);
R= 1;
Rinv = 1/R;
P0  = [1 0;0 1];
beta = .1;
%% Calcualte the norm of the estimate of the inital
   condition
est_error_norm = norm(xhat0-x0,2);
%% Form the initial condition for the ODE solver
X0 = [P0(1,1);P0(1,2);P0(2,2);x0;xhat0];
%% DEBUG Mode Printout
if debug == 1
disp('The EKF is set up');
end;
%% Set up ODE
%  Set the tolerance and run two ODEs: the first ODE is
   for the state
%  as standalone (Xtemp) - this is done to obtain a more
   accurate
%  result for x(t) when xhat becomes unstable, the second
   ODE solves x,
%  xhat and P to obtain the error dynamics
tol = 1e-9;% <= default is 1e-3
options = odeset('RelTol',tol);
```

```
[txtemp,Xtemp] = ode45('ct_sys_eq',t,x0,options);
[txs,Xs]   = ode45('ctekf_ric_eq',t,X0,options);
maxTC=length(txs);
for j=1:maxTC
P = [Xs(j,1),Xs(j,2);Xs(j,2),Xs(j,3)];
C = [1,0];
QT  = inv(P)*(Q-F*H'*Rinv*H*F')*inv(P)+C'*Rinv*C;
eigQT   = eig(QT);
mineigQT(j) = min(eigQT);
gam2=[F',H']*[inv(P);-Rinv*(C+H*F'*inv(P))]*[inv(P),-(C'+
   inv(P)*F*H')*Rinv]*[F;H];
eigGam2=eig(gam2);
maxeigGam2(j)=max(eigGam2);
end
gamma2(i) = (1/beta)*max(maxeigGam2)
gamma1(i) = min(mineigQT)-beta
Hinf_bound = gamma2(i)/gamma1(i)
%% DEBUG Mode Printout
if debug == 1
disp('The EKF was computed');
end;
sizetx = size(txtemp);
maxt = sizetx(1)
for j=1:maxt
normx(j) = norm(Xtemp(j,1:2),2);
end
```

```
sizetxhat = size(txs);
maxt = sizetxhat(1)
for j=1:maxt
normxhat(j) = norm(Xs(j,6:7),2);
end
%% Plots of x(t) and xhat(t)
%  Use a subplot to show x(t) and the estimate
%  Use the standalone solution for x(t) to ensure a
   numerically stable
%  solution
figure('color', 'w')
plot(txs,Xs(:,4),'b-',txs,Xs(:,6),'m--','LineWidth',2)
legend('x_1','x hat_1')
xlabel('Time','FontSize',fntsz)
ylabel('Magnitude','FontSize',fntsz)
figure('color', 'w')
plot(txs,Xs(:,5),'b-',txs,Xs(:,7),'m--','LineWidth',2)
legend('x_2','x hat_2')
xlabel('Time','FontSize',fntsz)
ylabel('Magnitude','FontSize',fntsz)
%% DEBUG Mode Printout
if debug == 1
disp('The state and estimates plot was created');
end;
%% Plots of the error
%  Calculate the error
```

```
e = Xs(:,4:5)-Xs(:,6:7);
%  Plot the error
figure('color', 'w')
plot(txs,e(:,1),'b-',txs,e(:,2),'m--','LineWidth',2)
xlabel('Time','FontSize',fntsz)
ylabel('Error','FontSize',fntsz)
legend('x_1 error','x_2 error')
%% Calculate the Hinf gain 03/23/2015
% First Error energy (integral of norm^2), then
   disturbance energy
% Then find ratio
% 03/23/2015
disturbanceT=zeros(2,maxt)';
for j=1:maxt
disturbanceT(j,:) = dist_mag*[exp(-dist_tc1*txs(j));exp(-
   dist_tc2*txs(j))]'; %dist_mag*exp(-dist_tc*txs(j))*sin
   (2*pi*dist_freq*txs(j));
end
eEnergy=0;
wEnergy=0;
for j=1:maxt-1
  delt=txs(j+1)-txs(j);
  eEnergy=eEnergy + [norm(e(j,:))^2]*delt;
  wEnergy=wEnergy + [norm(disturbanceT(j,:))^2]*delt;
end
eEnergy
```

```
wEnergy
Hinf=eEnergy/wEnergy
%% DEBUG Mode Printout
if debug == 1
disp('The error plot was created');
end
end
```

This is the code for the system model function:

```
function xdot=ct_sys_eq(t,y)
global F H Q Rinv dist_mag dist_tc1 dist_tc2 dist_freq b
xdot= zeros(2,1);
x    = [y(1);y(2)];
w= dist_mag*[exp(-dist_tc1*t);exp(-dist_tc2*t)]; %dist_mag
   *exp(-dist_tc*t).*sin(2*pi*dist_freq*t);
xdot = [x(2);-x(1)+(x(1)^2+x(2)^2-1)*x(2)]+F*w;
```

This is the code for the Riccati differential equation function:

```
function xdotv=ctekf_ric_eq(t,y)
global F H Q Rinv dist_mag dist_tc1 dist_tc2 dist_freq b
xdotv= zeros(7,1);
P= [y(1) y(2);y(2) y(3)];
x= [y(4);y(5)];
xhat = [y(6);y(7)];
A= [0 , 1 ; -1+2*xhat(1)*xhat(2) , xhat(1)^2+3*xhat(2)
   ^2-1];
C= [1 0];
```

```
w= dist_mag*[exp(-dist_tc1*t);exp(-dist_tc2*t)]; %dist_mag
   *exp(-dist_tc*t).*sin(2*pi*dist_freq*t);
Pdot = (A-F*H'*Rinv*C)*P+P*(A-F*H'*Rinv*C)'+Q-P*C'*Rinv*C*
   P-F*H'*Rinv*H*F';
xdotv(1) = Pdot(1,1);
xdotv(2) = Pdot(1,2);
xdotv(3) = Pdot(2,2);
xdot = [x(2);-x(1)+(x(1)^2+x(2)^2-1)*x(2)]+F*w;
xdotv(4) = xdot(1);
xdotv(5) = xdot(2);
K= (P*C'+F*H')*Rinv;
xhatdot  = [xhat(2);-xhat(1)+(xhat(1)^2+xhat(2)^2-1)*xhat
   (2)]+K*(C*x+H*w-C*xhat);
xdotv(6) = xhatdot(1);
xdotv(7) = xhatdot(2);
```